Functional characterization of recombinant K_v1 channel subtypes in HEK-293 cells for screening of selective inhibitors

Thesis submitted to Dublin City University for the award of Ph.D.

By

Seshu Kumar Kaza, M.Sc.

Supervised by Prof. J. Oliver Dolly

Co-Supervisors

Dr. Jiafu Wang
Dr. Gary Lawrence

School of Biotechnology
International Centre for Neurotherapeutics
Dublin City University
Ireland

July, 2016

Declaration

I hereby certify that this material, which I now submit for assessment on the programme of study leading to the award of Doctor of Philosophy, is my own work, and that I have exercised reasonable care to ensure the work is original, and does not to the best of my knowledge breach any law of copyright, and has not been taken from the work of others save and to the extent that such work has been cited and acknowledged within the text of my work.

Signed _____ ID number: 10109455

Seshu Kumar Kaza Date:

Acknowledgements

I am proud to have Prof. J. Oliver Dolly as my mentor. He has always motivated me to develop critical thinking, learn many valuable techniques and writing skills without which this Ph.D. would not have been possible. I pay my gratitude to Dr. Jiafu Wang and Dr. Ahmed Al-Sabi for their kind guidance throughout this research project that enabled me to overcome difficult problems, especially in molecular biology and electrophysiology, respectively.

I sincerely thank Dublin City University for awarding me with a three year DCU President Scholarship and the Science Foundation Ireland for the fund provided to me from Principal Investigator Grant of Prof. J. Oliver Dolly.

I want to acknowledge with a million thanks the Post-doctoral research scientists at ICNT, Dr. Gary Lawrence, Dr. Tom Zurawski, and Dr. Jianghui Meng, who contributed with their helpful discussions, ideas and advice. A special thanks to Sharon Whyte for her kindness and helping with manuscript editing.

I also thank Dr. Om Prakash Edupuganti for his immense support inside and outside the lab to build my career. I am grateful to my fellow researchers for their assistance and maintaining a friendly environment.

With great respect, I thank my beloved parents for their constant support, encouragement and guidance.

Heartfelt thanks to my lovely wife Prakani in helping me finish this thesis. All my blessings and wishes to my son Gowtham who has brought immeasurable happiness to our family.

Publications

Al-Sabi, A., Daly, D., Hofer, P., Kinsella, G. K., **Kaza, S. K.,** Nolan, K. and Dolly, J. O. A rational design of a selective inhibitor for K_v1.1 channels prevalent in demyelinated nerves that improves their impaired axonal conduction (Manuscript submitted)

Bagchi, B., Al-Sabi, A., **Kaza, S.,** Scholz, D., O'Leary, V. B., Dolly, J. O. and Ovsepian, S. V. (2014) Disruption of myelin leads to ectopic expression of K_v1.1 channels with abnormal conductivity of optic nerve axons in a cuprizone-induced model of demyelination. *PLoS ONE*. 9(2): e87736.

Al-Sabi, A*., **Kaza, S. K*.,** Dolly, J. O. and Wang, J. (2013) Pharmacological characteristics of K_v1.1- and K_v1.2-containing channels are influenced by the stoichiometry and positioning of their α subunits. *Biochem J.* 454(1):101-8.

Al-Sabi, A., **Kaza, S.,** Le Berre, M., O'Hara, L., Bodeker, M., Wang, J. and Dolly, J. O. (2011) Position-dependent attenuation by K_v1.6 of N-type inactivation of K_v1.4-containing channels. *Biochem J. Cell.* 48(2):389-396.

* These authors made an equal contribution to this work

Table of Contents

List of Figures

List of Tables

Abbreviations

4-AP, 4-aminopyridine

1P, 1 pore

Ab, antibody

AIS, axonal initial segment

AP, action potential

BCA, bicinchoninic acid

BCT, basket cell terminals

Ca^{2+}, calcium ion

CAMs, cell adhesion molecules

CAPs, compound action potentials

Caspr2, contactin-associated protein 2

cDNA, complementary DNA

CNS, central nervous system

C-terminus, carboxyl terminal domain of proteins

Dlg1, *Drosophila* disc large tumor suppressor 1

DMEM, Dulbecco´s modified Eagle's medium

DMSO, dimethyl sulfoxide

DNA, deoxyribonucleic acid

***DPM*,** dipyrromethane

***DPM I - III*,** dipyrromethane I - III compounds

DTX_k, dendrotoxin-K

DTT, dithiothreitol

EDTA, ethylenediaminetetracetic acid

EGFP, enhanced green fluorescent protein

FBS, fetal bovine serum

fc, fractional current

GI number, a simple series of digits that are assigned consecutively to each sequence record processed by NCBI

g_k-V, K^+ conductance–voltage relationships

HEK-293, human embryonic kidney cells; 293, cell clone of 293rd experiment of Frank Graham

HGNC, HUGO Gene Nomenclature Committee

HRP, horse radish peroxidase

HUGO, Human Genome Organization

IC_{50}, median inhibition concentration

IgG, immunoglobulin G

***I_K*,** delayed rectifying outward potassium current

IRES, internal ribosomal entry site

IUPHAR, International Union of Pharmacology

IV, current voltage relationship

K^+, potassium ion

K_v, voltage-gated potassium channel

K_v1.X, K_v1 channel subtypes (K_v1-8, Shaker-related)

$K_v\beta$, ancillary β-subunit of voltage-gated potassium channels

LDS, lithium dodecyl sulfate

MAGUKs, membrane-associated guanylate kinases

MCS, multiple cloning site

Mg^{2+}, magnesium ion

mRNA, messenger ribonucleic acid

MS multiple sclerosis

Na^{+}, sodium ion

Nav, voltage gated Na^{+} channel

NCBI, National Centre for Biotechnology Information

NIB, N-terminal inactivation ball

NIP, N-type inactivation prevention

N-terminus, amino-terminal domain of proteins

ORF, open reading frame

ON, optic nerve

PBS, phosphate buffer saline (0.02 M sodium phosphate, 0.15 M sodium chloride, pH 7.4)

PCR, polymerase chain reaction

PDZ, [post synaptic density protein 95 (PSD95), *Drosophila* disc large tumor suppressor 1 (Dlg1), and zonula occluden-1 (ZO-1)] -binding motif

PNS, peripheral nervous system

PSD-93, postsynaptic density protein-93

PSD-95, post synaptic density protein-95

RCK, rat cortex K^{+} channel

RES, restriction enzyme sites

SDS-PAGE, sodium dodecyl sulphate polyacrylamide gel electrophoresis

S.E.M. standard error of the mean

SF, selectivity filter

τ, tau (time constant)

TAE, tris-acetate-EDTA

TAG-1, transient axonal glycoprotein-1

TBST, tris-buffered saline Tween 20

TEA, tetraethyl ammonium

TM, transmembrane

TsTX-K, tityustoxin-K

TX-100, triton X-100

UTR, untranslated region

VSD, voltage-sensing domain

WB, Western blotting

ZO-1, zonula occluden-1

Units

µM, micromolar

µg, microgram

bp, base pair

Kb, kilo-base pair

K, kilo-Dalton

mA, milliampere

ml, milliliter

mM, millimolar

ms, milliseconds

mV, millivolt

Abstract

Seshu Kumar Kaza

Functional characterization of recombinant K_v1 channel subtypes in HEK-293 cells for screening of selective inhibitors

Shaker-related voltage activated K^+ channels or K_v1 channels occur in neurons as homo- and hetero-tetramers of α subunits ($K_v1.1$-1.7), associated with auxiliary β subunits, and control their excitability. The aim of this project was to create recombinantly homo- and hetero-meric K_v1 channel constructs resembling those in neurons, using a novel concatenation strategy, and to evaluate their expression and function in HEK-293 cells. This involved either altering the number and arrangement of each subunit or mutating their genes to change the sensitivities to tetraethylammonium (TEA) or other blockers. α subunit genes encoding $K_v1.1$, 1.2, 1.4 and 1.6 were amplified and concatenated with unique restriction enzymes for cassette cloning and sub-cloned in different combinations, generating homo- and hetero-tetramers of known composition to facilitate their expression as single proteins. Restriction enzyme digestion and DNA sequencing of extracted plasmid from *E. coli* transformed with the concatenated genes established that the tetramers have the correct integrity and composition. Biotinylation and Western blotting confirmed the expression of intact tetrameric channels on the surface of transfected HEK-293 cells. Repositioning of α $K_v1.6$ subunit in a hetero-tetramer revealed that N-type rapid inactivation, a characteristic feature of $K_v1.4$-containing channels, can be over-ridden by an adjacent $K_v1.6$ via the latter's N-type inactivation prevention (NIP) domain. Mutation of critical residues in the NIP restored the fast inactivation in Kv1.4-containing channels. In another objective to understand and raise the TEA sensitivity of $K_v1.1/1.2$-containing hetero-tetrameric channels, increasing the ratio of $K_v1.1$ to 1.2 in a $K_v1.2$-1.2-1.1-1.2 or mutagenesis of the critical residue in the first $K_v1.2$, placed adjacent or in close proximity to a $K_v1.1$ subunit in $K_v1.2$-1.2-1.2-1.1, made the channels more sensitive to TEA. Additionally, increasing the number of $K_v1.1$ subunits in a tetrameric channel decreases the voltage threshold and accelerates the activation kinetics. Overall, these findings assessed the possible consequences of α subunits being precisely arranged in K_v1 channels, by examining recombinantly created variants with known composition, an important criterion in designing drugs selective for K_v1 oligomeric subtypes. Screening of small inhibitor compounds for $K_v1.1$ allowed us to identify 2,2'-((5,5'-(di-p-topyldipyrromethane)bis(2,2'-carbonyl)bis(azanediyl))diethaneamine.2HCl as a potential therapeutic drug for use in the treatment of multiple sclerosis (MS). It potently (IC_{50} = ~15 μM) and selectively blocks $K_v1.1$ channels recombinantly expressed in mammalian cells. This novel inhibitor also induces a positive shift in the voltage-dependency of K^+ current activation and slows the activation kinetics. Importantly, this new non-photo-toxic compound inhibited K_v1 heteromeric channels containing 2 or more $K_v1.1$ subunits, regardless of their positioning in concatenated tetramers, though $K_v1.3$-mediated K^+ current was reduced to a lesser extent.

CHAPTER 1

GENERAL INTRODUCTION

1.1 Ion channels

The cell membrane, a bilayer of phospholipids containing hydrophobic fatty acid tails facing each other in the middle of the bilayer, is normally impermeable to all but small, uncharged molecules. In order to allow important physiological ions to cross this barrier, ion channels serve as highly selective filters through which ions can pass into and out of cells. These are integral membrane proteins present in both excitable and non-excitable cells. In response to alterations in intracellular pH, concentration of ions, or membrane voltage some parts of the ion channel proteins change their conformation, thereby, opening or closing their conduction pore (Hille, 2001). With over 400 members of ion channels identified in the human genome, voltage- and ligand-gated ion channels are widely studied functional groups of proteins in heterologous expression systems (Klassen et al., 2011). Propelled by electrochemical gradients, these channels allow passive passage of small ions across the lipid membrane. Membrane excitability is a characteristic of many cell types in all animals. For example, channels can gate open and close an ion conduction pathway in response to the changes in membrane potential, neurotransmitter or other chemical stimulus, so as to modulate neuron excitability (Hille, 2001). The movement of ions, mainly, potassium ion (K^+), sodium ion (Na^+), calcium ions (Ca^{2+}) and chloride ion (Cl^-), through their respective ion channels are responsible for the shaping of action potential (AP) (Lockery and Goodman 2009). K^+ channels are the primary determinants of the

resting membrane potential of the cell and the major modulators of the shape, duration, frequency and repolarization phase of APs in excitable cells (Kuo et al., 2005; Stein and Litman, 2015).

1.2 K^+ channels

K^+ channels are the most diverse group of proteins that have been observed, being present in virtually all cell types from a wide phylogenetic range of species, including prokaryotes (Milkman, 1994). The first K^+ channel gene was cloned from the *Drosophila* Shaker locus (Papazian et al., 1987). Based on the structural and functional diversity, observed from molecular cloning and functional expression studies, K^+ channel genes were grouped into several conserved families. However, all K^+ channel genes share a universal feature of having a hyper-conserved signature sequence that forms a part of a K^+-selective pore (Heginbotham, et al. 1992, 1994) and have three basic properties: 1) high conduction rates upto 10^7 - 10^8 ions per second, 2) selectivity for K^+ and 3) their conduction is gated (Doyle et al., 1998). They are involved in performing basic and specific cellular functions, such as setting of resting potentials and defining the inter-spike intervals of endogenously beating cells, respectively (Bezanilla, 2008). K^+ channels are encoded by 30-100 different K^+ genes in humans, *Drosophila*, and *Caenorhabditis elegans* (Miller, 2000; Heitzmann and Warth, 2008).

1.3 Classification of K^+ channels into families based on the structure of their transmembrane segments

Cloning followed by physiological, functional and structural analysis of K^+ channels has allowed their classification into different families characterized by the number of

transmembrane (TM) segments and pore (P) domains (Fig 1.1). Inward rectified channels (Kir channels) have 2TM segments with 1P domain; tandem two pore-domain (K_{2P}) channels comprise 4TM segments and 2P domains; voltage-gated channels contain 6TM segments plus 1P domain. The yeast Tok1 K^+ channel has 8TM segments (Pongs, 1992; Wei et al., 1996; Jan and Jan, 1997; Talley et al., 2003; Buckingham et al., 2005).

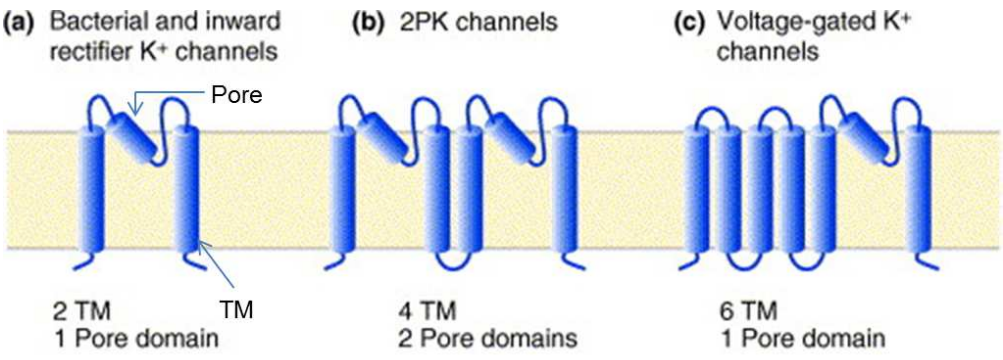

Fig. 1.1 Schematic of transmembrane (TM) segments and pore-forming (P) domains of the three main classes of K^+ channels.

(a) Inward rectifier channels, which contain two TM domains and one P domain; (b) Two-pore-domain channels, which contain four TM domains and two P domains and (c) Voltage-gated K^+ channels, which contain six TM domains and one P domain (adapted from Buckingham et al., 2005).

The ancestor of the K^+ channel types is thought to be the 2TM K^+ channel based on its wide distribution in both prokaryotes and eukaryotes. Addition of other transmembrane segments to the N-terminus of a 2TM precursor could have yielded other families of K^+ channel proteins such as 4TM and 6TM K^+ subtypes, with distinguished features from the primitive ones (2TM channels). For instance, 6TM channels have intrinsic gating structures as opposed to the Kir inward rectifiers, which are gated by extrinsic cytoplasmic factors, Mg^{2+} and/or polyamines (Lopatin et al., 1994). Voltage-gated Ca^{2+} and Na^{2+} channels, which

belong to 6TM channels, probably originated from their ancestral tetrameric 6TM K^+ channel (Gutman et al., 2003, 2005).

1.4 Nomenclature and families of voltage-gated potassium (K_v) channels

The voltage-gated K^+ channels (K_v) play an important role in determining the electrical properties of excitable cells. In response to membrane depolarization, K_v channels allow increased K^+ efflux from cells and attain resting potential when hyperpolarized (Huang and Jan, 2014). Studies revealed the involvement of multiple K_v channels in controlling the process of falling phase of the AP in excitable cells (Jan and Jan, 1990). In addition to their vital role in excitable cells, K_v channels expressed in non-excitable cell types also have an essential role in various functions including electrolyte transport, cell volume regulation, cell migration, wound healing, proliferation, apoptosis, carcinogenesis, and oxygen sensing (O'Grady et al, 2005) in tissues such as renal (Hebert et al, 2005), gastro-intestinal (Hietzmann and Warth, 2008) and respiratory epithelia (Bardou et al, 2009). Voltage-sensitivity of K_v channels is provided by positively charged amino acids (lysine or arginine) in S4 transmembrane region and a tripeptide sequence motif located in P-loop of the S5-S6 linker represents the K^+ selectivity filter of the pore (Shieh et al., 2000).

Alignment and analysis of amino acid sequence in hydrophobic cores (S1–S6) of human K_v channels revealed the phylogeny tree of K_v channels (K_v1-9 families) comprising of K_v1-6 and K_v8-9 families. Gutman et al. updated the existing tree by incorporating the sequences of K_v7.1–7.5, K_v6.4, and K_v8.2 to the existing alignment, by use of a combination of maximum parsimony and neighbor-joining analysis (Gutman et al., 2005; Stein and Litman, 2015).

Table 1.1 Classification and nomenclature of 6TM 1P K^+ channels

Structural Class	Families	Subfamilies	Members	
			IUPHAR	HGNC
6TM 1P	Voltage-gated	Shaker-related	$K_v1.1$	KCNA1
			$K_v1.2$	KCNA2
			$K_v1.3$	KCNA3
			$K_v1.4$	KCNA4
			$K_v1.5$	KCNA5
			$K_v1.6$	KCNA6
			$K_v1.7$	KCNA7
			$K_v1.8$	KCNA10
		Shab-related	$K_v2.1$	KCNB1
			$K_v2.2$	KCNB2
		Shaw-related	$K_v3.1$	KCNC1
			$K_v3.2$	KCNC2
			$K_v3.3$	KCNC3
			$K_v3.4$	KCNC4
		Shal-related	$K_v4.1$	KCND1
			$K_v4.2$	KCND2
			$K_v4.3$	KCND3
		Modifier	$K_v5.1$	KCNF1
		Modifiers	$K_v6.1$	KCNG1
			$K_v6.2$	KCNG2
			$K_v6.3$	KCNG3
			$K_v6.4$	KCNG4
	KQT	KVLQT	$K_v7.1$	KCNQ1
		KQT2	$K_v7.2$	KCNQ2
			$K_v7.3$	KCNQ3
			$K_v7.4$	KCNQ4
			$K_v7.5$	KCNQ5
		Modifiers	$K_v8.1$	KCNV1
			$K_v8.2$	KCNV2
		Modifiers	$K_v9.1$	KCNS1
			$K_v9.2$	KCNS2
			$K_v9.3$	KCNS3
	Eag	eag1	$K_v10.1$	KCNH1
		eag2	$K_v10.2$	KCNH5
		erg1	$K_v11.1$	KCNH2
		erg2	$K_v11.2$	KCNH6
		erg3	$K_v11.3$	KCNH7
		elk1, elk3	$K_v12.1$	KCNH8
		elk2	$K_v12.2$	KCNH3
		elk1	$K_v12.3$	KCNH4

IUPHAR: International Union of Pharmacology; HGNC: Human Genome Organization (HUGO) Gene Nomenclature Committee (Gutman et al., 2005).

Four conserved subfamilies, first cloned from *Drosophila*, comprise the K_v family of channels: Shaker (Papazian et al., 1987; Kamb et al., 1987; Pongs et al, 1988), Shab, Shaw and Shal (Wei et al., 1990) (Table 1.1). Extensive numbers of vertebrate homologies for each subfamily have been isolated (Chandy and Gutman, 1995). Only after the expression of Shaker in *Xenopus* oocytes and physiological studies was it possible to confirm that these proteins were really K^+ channels (Tempel et al. 1987, 1988; Iverson et al., 1988; Papazian et al., 1988; Timpe et al., 1988). The Shaker locus has a large open reading frame of 21 exons that can produce several transcripts by alternative splicing (Papazian et al., 1987; Tempel et al., 1987; Iverson et al., 1988). Using Shaker cDNA as a probe, it was possible to identify a K^+ channel from rat brain, RCK1 (Baumann et al., 1988) and RBK1 (Christie et al., 1989), and some inward rectifying channels (Kubo et al., 1993). Subsequently, the RCK1 sequence was used to probe cDNA libraries and led to the isolation of several more neuronal voltage-dependent K^+ channel clones (Stuhmer et al., 1988). At the same time, 3 additional voltage-dependent K^+ channel members (Shab, Shal and Shaw) were identified in *Drosophila* by cross-hybridisation with the Shaker sequence (Covarrubias et al., 1991). As for Shaker, equivalents of these channels were also found in mammalian cDNA libraries; their K^+ channel subunits are encoded by multiple separate genes whereas in *Drosophila* alternative splicing of a large transcriptional unit occurs.

1.5 Shaker subfamily of K_v channels (K_v1)

Shaker-related K_v1 subfamily is the most intensely studied among the diverse family of membrane-spanning proteins, K_v channels (Pongs and Schwarz, 2010). Involvement in controlling cell excitability and synaptic transmission make them potential targets for neurotherapeutics. Malfunctioning of Shaker subfamily members is involved in certain

human diseases (Kullmann, 2002) where they are altered by mutation (e.g. certain forms of epilepsy) or truncation (e.g. Episodic ataxia type I). In the healthy nervous system, K_v1 channels are clustered in high density at, for example (1) the basket cell terminals (BCTs) of cerebellar pinceau where they regulate GABAergic inhibition of the Purkinje neuron efferent axon (McNamara et al., 1993), (2) juxta-paranodes of myelinated axons where they modulate AP propagation and dampen repetitive firing of injured and developing myelinated axons, and (3) axon initial segments (AIS) where they regulate AP waveform, synaptic efficacy, and threshold of cortical inter-neurons (Wang et al., 1993; Devaux et al., 2002; Kole et al., 2007; Goldberg et al., 2008).

1.6 α and β subunits of K_v1 channels

The cloning and functional characterization of K^+ channels from animals has revealed that K^+ channels are formed by a hetero-oligomeric assembly of α- and β-subunits (Fig. 1.2) (Rehm and Lazdunski, 1988; Parcej and Dolly, 1989; Parcej et al., 1992; Rettig et al., 1994; Scott et al., 1994a; Orlova et al., 2003), of which α-subunits form the K^+ channel (Jan and Jan, 1994). Although α subunits can form functional K_v channels alone, crystallographic and functional studies of β subunits conferred additional properties that match natural preparations. Auxiliary β subunits further contribute to the diversity of K_v channels as they co-assemble with α subunits and regulate both biophysical properties and channel trafficking to the membrane. In K_v1 channels, the structure of the highly conserved cytoplasmic N-terminal tetramerization domain or T1 domain (Fig. 1.2) of α subunit plays an important role in restricting K_v channel subunit hetero-multimerization in complex with an auxiliary β-subunit protein (Gulbis et al., 2000; Strang et al., 2001).

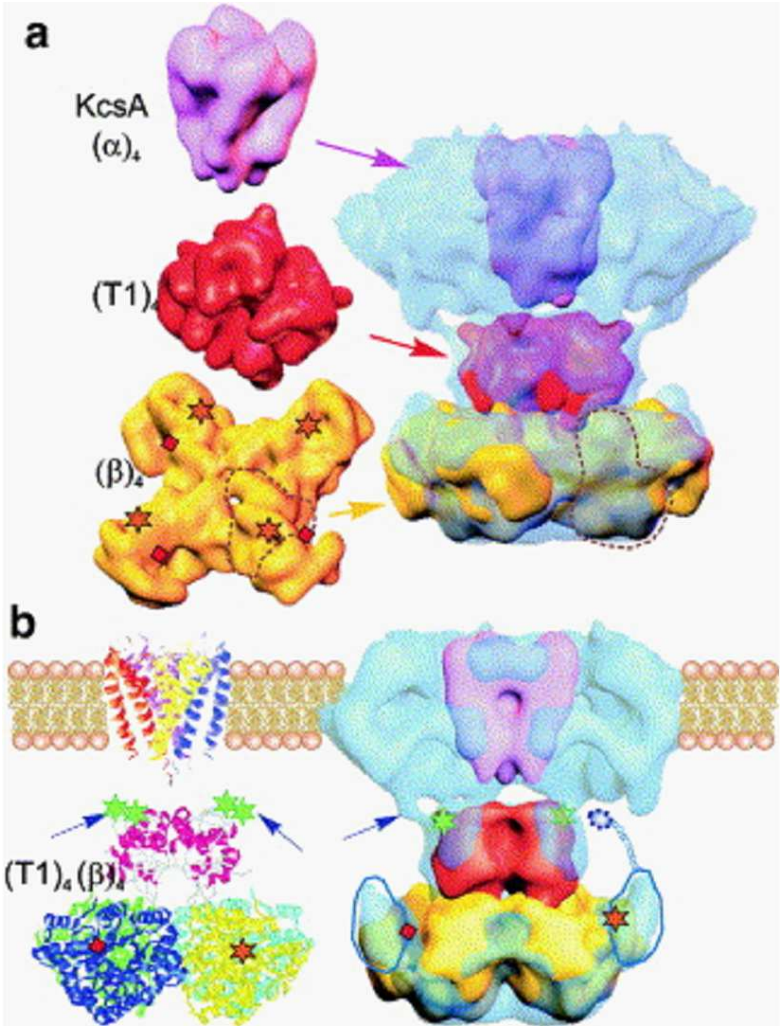

Fig. 1.2 Schematic of octomer K_v1 channel 3D structure.

(a) Super-imposed semi-transparent K^+ channel picture resulting from a X-ray structures of recombinant truncated KcsA (pink), T1 (red) and $t\beta_2$ tetramers (gold) before and after fitting into the electron microscopy (EM) map (blue); putative position of the triosephosphate isomerase (TIM) barrels are indicated with broken lines; approximate positions of N termini in $t\beta_2$ protein is depicted with stars along with red diamonds placed at its active sites. (b) K_v1 channel incorporated into a membrane, green stars identify the C termini of the $(T1)_4$, adjacent to the connectors (blue arrows). The blue contours outline the extra mass visualized by EM near the N termini but absent from the X-ray map of $(t\beta2)_4$. The blue broken line (in figure on right, above the star) indicates the postulated position for the N-terminal extension in β1, containing the inactivation ball and chain, with a possible pathway to reach the inner mouth of the channel (adapted from Orlova et al., 2003).

In addition, the gating of the K^+ channel is affected by the conformational changes in the buried polar interface between T1 subunits. The β2-subunit (or rather the truncated β2-subunit, tβ2, with residues 1–35 omitted) showing a tetramer of oxidoreductase proteins with 4-fold symmetry (Fig. 1.2). Each of these subunits contains an active site with catalytic residues and a nicotinamide adenine dinucleotide phosphate cofactor. The complex of tβ2 with T1 demonstrated that T1 provides a docking platform for the auxiliary β-subunit whose activity is coupled to the channel's function (Orlova et al., 2003).

Cloned K_vβ subunit genes from brain (Rettig et al., 1994; Scott et al., 1994b; Heinemann et al., 1995; Coleman et al., 1999) and heart (England et al., 1995; Majumder et al., 1995; Morales et al., 1995) encode cytoplasmic proteins that form stable complexes with K_v1α subunits and exert multiple effects on K_v1α currents. The K_vβ isoforms (three K_vβ1 isoforms and K_vβ3) affects the inactivation kinetics to K_v1α subunits but with variable potency (Rettig et al., 1994; Heinemann et al., 1995; Wang et al., 1996). Complexes between K_v1α and K_vβ subunits have been found to form in the endoplasmic reticulum to assist the folding and assembly of the K_v1α subunits. The association of K_v1.2 with K_vβ subunits produces more efficient glycosylation of K_v1.2, by increasing the stability of K_v1.2 through K_v1.2-K_vβ complex formation and results in an increase in cell surface expression (Shi et al., 1996; Nagaya and Papazian, 1997). Members of the same K_v family co-assemble in a homo- or hetero-terameric manner to form functional channels (Shamotienko et al., 1997; Coleman et al., 1999). K_v1.4 co-localizes with K_v1.2 at juxta-paranodes and axon initial segments (Rasband et al., 2001; Ogawa et al., 2008), has the same PDZ [post synaptic density protein 95 (PSD95), *Drosophila* disc large tumor suppressor 1 (Dlg1), and zonula occluden-1 (ZO-1)] -binding motif as K_v1.2, and express more efficiently on the cell

surface than $K_v1.2$ because of the variation in a cytoplasmic C-terminal endoplasmic reticulum-export motif (Manganas et al., 2001a).

In addition to the effect of co-assembled β subunits, the localization, expression and function of K_v1 channels is also influenced by other scaffolding proteins and enzymes (Schulte et al., 2006). K_v1 channels form macromolecular protein complexes with the cell adhesion molecules (CAMs) Caspr2 and TAG-1, the membrane-associated guanylate kinases (MAGUKs) PSD-93 and PSD-95, and the cytoskeletal scaffold (Poliak et al., 1999, 2001; Traka et al., 2002; Horresh et al., 2008) though at BCTs neither Caspr2 nor PSD-95 is needed for channel clustering (Rasband et al., 2002). Juxta-paranodal K_v1 channel clustering depends on CAMs, but not MAGUKs (Rasband et al., 2002; Poliak et al., 2003; Traka et al., 2003; Horresh et al., 2008). In contrast, K_v1 channel clustering at the AIS was reported to depend on MAGUKs rather than CAMs (Ogawa et al., 2008). Thus, although these different axonal domains share a similar molecular organization, their mechanisms of assembly are distinct.

1.7 The pore-forming region of K_v channels

A bacterial K^+ channel from *Streptomyces lividans*, KcsA, was the first ion channel whose structure was determined (Doyle et al., 1998). It was identified as one of the channels of the inward rectified channels (Kir channels), although the pore region is more homologous to mammalian voltage-dependent channels. The crystallographic structure (Fig. 1.3) revealed considerable information on the pore region, selectivity filter (Doyle et al., 1998; Zhou et al., 2001) and ion conduction (MacKinnon, 2004). Studies based on molecular cloning and mutagenesis experiments have revealed that all K^+ channels contain a conserved amino acid

region, called the pore region, composed of the sequence GYG. Mutation of single amino acid alters the channel activity, which is no longer able to discriminate between K^+ and Na^+ (Doyle et al., 1998).

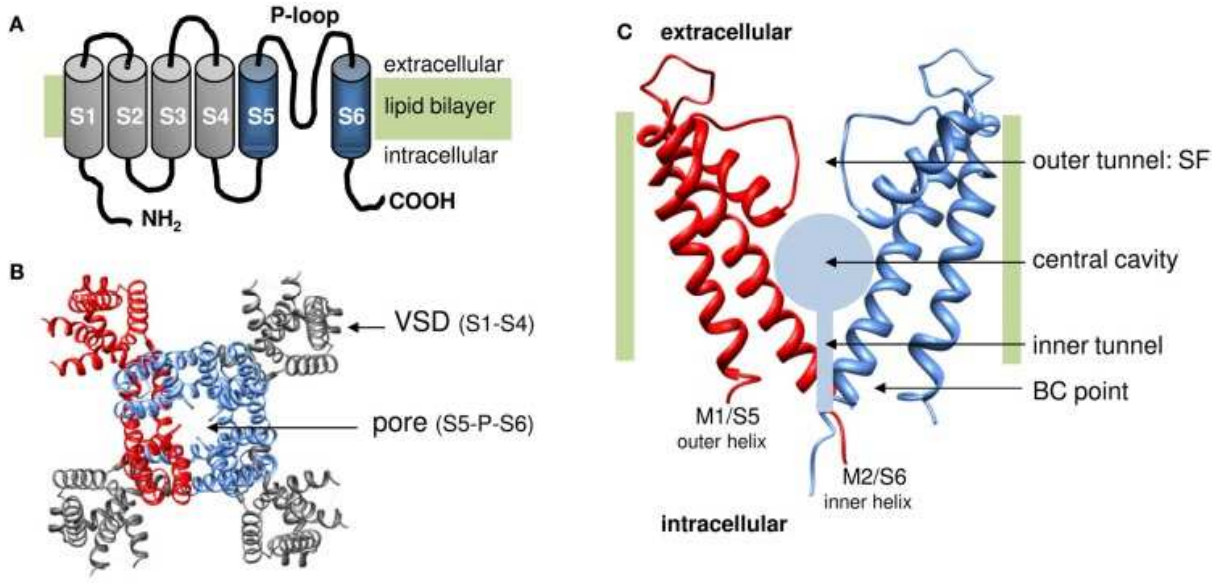

Fig. 1.3 Topology of K_v channels.

(A) Schematic of the 6TM-1P topology of a K_v channel α-subunit with both amino (NH_2) and carboxyl (COOH) terminus located intracellular. The S1–S4 segments form the voltage-sensing domain (VSD) (represented in gray) and the S5-P-loop-S6 region assembles with three other pore domains into the K^+ permeation pathway. (B) Top view (from the extracellular side) of the 3D structure of the $K_v1.2$ channel (protein data bank accession code 2A79; Long et al., 2005). To illustrate the four-fold symmetrical assembly of the α-subunits into a functional channel, one α-subunit is represented in red. In the other subunits the pore region (S5-P-loop-S6) is colored blue and the VSD (S1–S4) is represented in gray. Note that the pore regions form a centrally located K^+ pore that is surrounded by four independent VSDs. (C) Side view of the pore module of the 2TM-1P K channel KcsA that was crystallized in the closed state (protein data bank accession code 1BL8; adapted from Doyle et al., 1998).

The first TM segment (Fig. 1.3a), M1 resembles S5 in K_v channels is located at the periphery and faces the lipid bilayer whereas the second (M2 corresponding to S6) forms the inner pore helix. The front and back α-subunit are omitted to illustrate the layout of the

K^+ permeation pathway that - from the intracellular to the extracellular side - can be divided in three recognizable sections (Fig.1.3C); (1) a water filled inner tunnel, (2) a wider 12Å diameter water filled cavity, and (3) a narrower outer tunnel that forms the ion selectivity filter (SF) that dictates K^+ selectivity. Both the inner tunnel and the central cavity are formed by the inner pore helices that cross the membrane at an angle of ∼25° resembling an inverted teepee (Doyle et al., 1998). The K^+ pathway contains two energy barriers for K^+ that function as a gate: (1) at the bundle crossing (BC) of the M2/S6 helices (BC gate) that forms a barrier for hydrated K^+ and (2) the SF that allows passage of K^+ which have shed their hydration shell (Labro and Snyders, 2012).

1.8 Molecular determinants of K_v channel function

Besides being divided into subfamilies based on sequence homologies, K_v channels can be classified according to their biophysical behavior (Hille, 2001). K_v channels are all activated by depolarization, but present with wide diversity of activation and inactivation kinetics.

1.8.1 Gating of K_v channels. As each α subunit contributes distinct properties, the resultant channels reaching the plasmalemma vary considerably in their pharmacological and biophysical properties. K_v1.4 is the only K_v1 member that shows both N- and C-type inactivation, yielding a distinctive A-type transient outward current (Stuhmer et al., 1989).

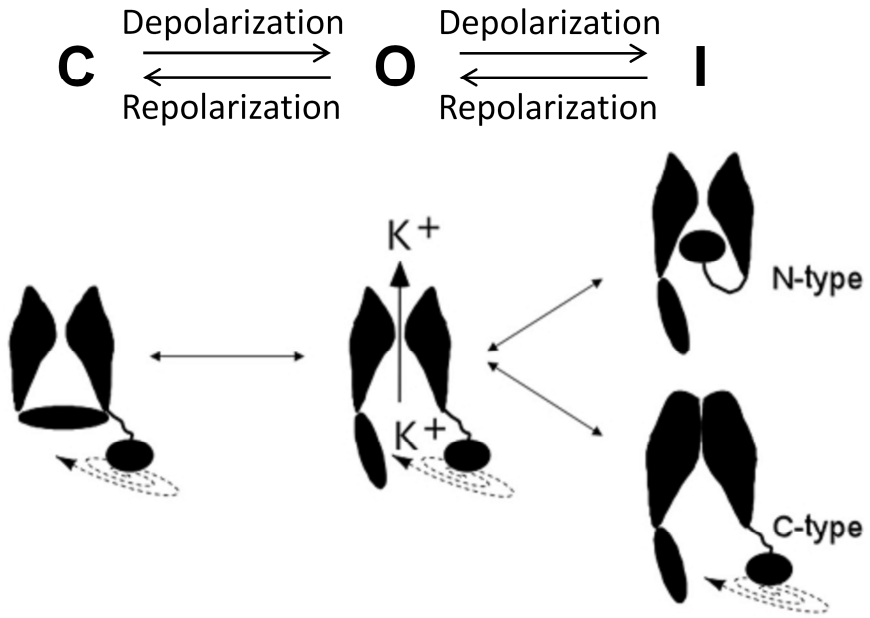

Fig. 1.4 Gating modes and models.

Schematic cartoon of the conformational states and voltage-driven gating modifications of K_v channels. The drawings at the bottom represent two α-subunits and a symbolic cytoplasmic gate, with one diffusible ball-and-chain structure attached to their cytoplasmic face. N-type inactivation is a consequence of plugging of the pore after opening the cytoplasmic activation gate, and C-type inactivation by collapsing of the selectivity filter gate, are represented on the right (adapted from Barros et al., 2012).

After opening of these K_v1 channels by membrane depolarization, inactivation follows via two mechanisms. N-type inactivation mediated through the N-terminal inactivation ball (NIB) occurs by a 'ball and chain' process in which NIB occludes the inner mouth of the ion pore (Hoshi et al., 1990; Zagotta et al., 1990) (Fig. 1.4). Mutations which affect N-type inactivation (Isacoff et al., 1991) and co-expression of $K_v1.6$ containing N-type inactivation prevention (NIP) influence channel conductance (Roeper et al., 1998). In addition, $K_v\beta1$ subunits provide alternative N-terminal domains that confer rapid inactivation on non- or slow-inactivating K_v1 channels. This is because $K_v\beta1$ subunits contain an inactivation ball in the amino-terminal sequence that blocks the internal mouth of associated slow-inactivating α subunits upon depolarization and leads to the formation of A-type K_v

channels (Rettig et al., 1994; Heinemann et al., 1996; Morales et al., 1996). On the other hand, C-type inactivation arises from prolonged depolarization which leads to a local rearrangement and constriction of the channel at the outer mouth (Yellen et al., 1994; Liu et al., 1996; Kiss and Korn, 1998).

1.9 Native combinations of K_v1 channels in brain

The extensive diversity in K_v currents is matched by the multiplicity of genes encoding the pore-forming or α-subunit of K_v channels (Jan and Jan, 1990). Each K^+ channel α subunit gene encodes a single polypeptide, and functional channels are formed by the tetrameric association of individual subunits apparently mediated by specific binding between the N-terminal domains of subunits within individual subfamilies (Li et al., 1992; Xu et al., 1995). Multiple copies of different K_v1 channel α subunit genes may co-assemble as heteromeric complexes (Wang et al., 1993; Shamotienko et al., 1997; Coleman et al., 1999) that are thought to form functionally distinct K^+ channels.

K_v1 channels in the brain, purified using the selective blockers α DTX (α dendrotoxin) or DTX_k, are large (molecular mass ~400 K) sialoglycoprotein (a combination of sialic acid and glycoprotein) complexes (Parcej et al., 1992) consisting of four pore-forming α subunits and four cytoplasmically-associated auxiliary β proteins (Scott et al., 1994a, b). When heterologously expressed alone, each of the major genes encoding α subunits [K_v1.1–1.6 (Stuhmer et al., 1989; Grupe et al., 1990; Swanson et al., 1990) and K_v1.7 (Kalman et al., 1998)] yields a homo-tetrameric channel with distinct biophysical and pharmacological profiles. Heteromerized K_vl.4 and l.2 subunits have been localized in axons and nerve terminals, which may form the molecular basis of a presynaptic A-type K^+

channel involved in the regulation of neurotransmitter release (Sheng et al., 1993). Further diversity *in vivo* results from hetero-polymerization, but only a subset of the possible oligomeric combinations has been found in mammalian brain (Covarrubias et al., 1991; Shamotienko et al., 1997; Coleman et al., 1999; Sokolov et al., 2007), suggesting that their synthesis and/or assembly are restricted to members of the same family but not between subunits among different subfamilies (K_v1, 2, 3, or 4).

K_v1.2 is the most prevalent in neuronal membranes where some occur as a homo-tetramer and the majority is heteromerized with other K_v1α subunits (Shamotienko et al., 1997; Coleman et al., 1999; Sokolov et al., 2007); interestingly, there is preponderance in these preparations of the less abundant K_v1.1 subunit in oligomers with K_v1.2. Following depolarization, the voltage-dependent delayed rectifier members of the K_v1 channel family play an important role in rapidly restoring the neuronal resting membrane potential. Both K_v1.1 and K_v1.2 heteromeric channels are considered low-voltage activated channels that open with small depolarizations below the resting potential (Brew et al., 2003 and 2007). Notably, the homomeric K_v1.1 channel activates at more negative potentials compared with its K_v1.2 counterpart when expressed in mammalian (Grissmer et al., 1994) or *Xenopus* (Akhtar et al., 2002) systems. This difference in their voltage-dependence of activation would confer rapid conduction of high-frequency APs (Wang et al., 1993; Wang et al., 1995).

1.10 K_v1 channelopathies

Mutations or diseases that disrupt the clustering, localization, or composition of K_v1 channels severely compromise nervous system function and lead to conduction block,

episodic ataxia, and/or epilepsies (Rasband et al., 1998; Eunson et al., 2000; Nashmi et al., 2000; Manganas et al., 2001b). Fergestad et al. reported that mutations affecting K^+ and Na^+ channel genes either by increase in membrane excitability or those that decrease membrane excitability can cause neuro-degeneration to varying degrees (Fergestad et al., 2006). Abnormal $K_v1.1$ activity, originating in the distal motor axons, results in muscle hyperactivity, indicative for myokymia (da Silva et al., 1977; Newsom-Davis and Mills, 1993). In addition to the classical description of this disorder, phenotypic variants include EA1 with partial epilepsy, isolated neuromyotonia (Zuberi et al., 1999; Eunson et al., 2000) and EA1 without myokymia (Lee et al., 2004). An electrophysiological study also revealed that a mutation ($K_v1.1$ N255D) in wild-type $K_v1.1$ results in a non-functional $K_v1.1$ channel (Glaudemans et al., 2009).

*1.10.1 K_v1 channels in multiple sclerosis (MS)***.** Multiple Sclerosis (MS) is on the increase, being more common in young adults but also found in children. Prevalence of the disease ranges between 2–2.5 million worldwide (Milo and Kahana, 2010). According to the national incidence study in Ireland, there are over 8000 MS sufferers (The Multiple Sclerosis Society of Ireland, website listed in references). It is an inflammatory, neuronal demyelinating disease, with phenotypic neurological signs and symptoms ranging from vision impairment to movement disabilities (Pugliatti et al., 2006). The pathophysiology of demyelinated axons depends mainly on the re-distribution of K_v channels along the axon (Waxman, 1992), and the expression of unique subfamily member (K_v1) on demyelinated axons in patients suffering from MS contributes to abnormal propagation of nerve signals with resultant debilitating muscle weakness (Judge and Bever Jr., 2006). Selective inhibitors for this particular K_v1 channel associated with MS might well restore the

excitability of demyelinated axons, which appears to underlie clinical remissions in MS patients. Two K^+ channel blockers, 4-aminopyridine (4-AP) and 3,4-diaminopyridine, are of some benefit in the symptomatic treatment of patients with MS (Bever, 1994; Solari et al., 2002) by overcoming conduction block in demyelinated axons in MS lesions. Because of poor selectivity and indiscriminate blockade of other K^+ channels present in neurons, these exert toxic side-effects. Thus, it is essential to identify new blockers which would have the potency and specificity to inhibit only the MS-associated $K_v1$channel subtype.

1.11 Pharmacology of K_v1 channels

*1.11.1 Small blockers of Kv1 channels***.** The two primary criteria for delayed rectifier K_v channel classification are that they are both 4-AP sensitive or insensitive and tetraethylammonium (TEA) insensitive or sensitive (Thorneloe and Nelson, 2005). TEA is a classical K_v channel blocker, from the external or internal side of the pore region (Stanfield, 1983; Kirsch et al., 1991; Taglialatela et al., 1991; Yellen et al., 1991; Pascual et al., 1995). It is noteworthy herein, that mutations which affect N-type inactivation also influence the binding of intracellular channel blocker like TEA (Yellen et al., 1991). In the case of external TEA, neuronal K_v1 channels are either sensitive (IC_{50} = 0.3–10 mM; $K_v1.1$, 1.3 and 1.6) or insensitive (IC_{50} > 100 mM; $K_v1.2$, 1.4, 1.5 and 1.7) (Gutman et al., 2005).

*1.11.2 K_v1 channel inhibition by toxins***.** In the last few decades, venomous animals provided pharmacological tools that can block a variety of Ca^{2+} activated (e.g. apamin, iberiotoxin, charybdotoxin, scyllatoxin), voltage-gated (K_v) (e.g. dendrotoxins (DTX), kaliotoxin, conotoxins, hanatoxins, phrixotoxins), and inward-rectifier (tertiapin) K^+ channels. These toxins have been isolated from scorpion, snake, cone-shell, spider, bee or

sea anemone venoms (Mehraban et al., 1984; Breeze and Dolly, 1989; Parcej et al., 1992; Smith et al., 1993; Swartz and MacKinnon, 1995; Kauferstein et al., 2003). Due to their high specificity and affinity for K^+ channels, these toxins have facilitated the purification of K^+ channels, determination of their subunit stoichiometry and sub-cellular localization and tissue distribution (Parcej and Dolly, 1989; Scott et al., 1990; Awan and Dolly, 1991; Reid et al., 1992; Aiyar et al., 1995; Wang et al., 1999b; Legros et al., 2000). They have served as crucial tools for determining the involvement of particular K_v channels in patho-physiological pathways. For example, DTX_k, mast cell degranulating (MCD) peptide, kaliotoxin and ShK peptide, isolated from snake, bee, scorpion and sea anemone venoms, respectively, were of primary importance in characterizing the function of $K_v1.1$ channels in epilepsy and the contribution of $K_v1.3$ channels in inflammatory processes (Bagetta et al., 1997; Mourre et al., 1997; Wang et al., 1999a; Beeton et al., 2001, 2003).

1.12 Aims of this study

The group of Prof. Oliver Dolly has been focusing on characterizing the biophysical profiles of K_v1 oligomers (Shamotienko et al., 1997; Shamotienko et al., 1999; Wang et al., 1999) in order to establish their pharmacological criteria (Al-Sabi et al., 2010) with the aim of enhancing the effectiveness of selective inhibitors in treating neurological disorders (such as MS). This study was intended to assess the functional significance of K_v subunit compositions and their stoichiometry in K_v1 channel subtypes. In addition, the biophysical and pharmacological profiles of K_v1 channels expressed in mammalian cell were determined. Main objectives of this research were: (1) Re-creating 'native-like' neuronal K_v1 oligomers, using an established tandem-linked strategy (Al-Sabi et al., 2010), and evaluating their structural/functional characteristics as well as surface expression as intact

multimers in human embryonic kidney (HEK)-293 cells; (2) Exploiting the functioning of the NIP domain of $K_v1.6$ α subunit on rapid inactivation of $K_v1.4$-containing channels, mediated through a NIB to prove the effectiveness of the concatenation; (3) Exploring how positioning of K_v1α subunit genes in tandem-linked constructs influence the assembly and biophysical/pharmacological properties of hetero-tetrameric K^+ channels when expressed in HEK-293 cells; (4) Investigating the biophysical changes in K^+ currents by incorporating one or more mutations into $K_v1.2$ of $K_v1.1/1.2$-containing tetramers; and (5) Utilizing the proprietary recombinant K_v1 subtypes, representative of those in neurons, for screening K_v1 channel selective inhibitors to normalize aberrant K^+ channel function to ameliorate disease symptoms.

CHAPTER 2

MATERIALS AND METHODS

2.1 Materials

Molecular biology*:* K_v1.X genes in pAKS plasmid were a gift from Prof. Olaf Pongs (University of Hamburg, Germany). The vector, pβUT2, was a gift from Dr. Adam Rodaway (Kings College, London, UK), pIRES2-EGFP vector were purchased from Clontech, Ireland. PCR-blunt plasmid, Platinum® *Pfx* DNA Polymerase, TOP10 competent cells, and SOC medium were from Invitrogen, Ireland. HiSpeed plasmid purification kits were from Qiagen, UK. Restriction enzymes and 1 Kb DNA ladder were purchased from New England Biolabs, UK. Sigma–Aldrich (Ireland) supplied DNA gel loading solution.

Cell culture reagents*:* Dulbecco's Modified Eagle's Medium (DMEM, D6429), 0.25% (w/v) trypsin/EDTA, antibiotic/antimycotic (anti/anti) solution, glutathione and poly-D-lysine were bought from Sigma-Aldrich, Ireland. GIBCO (Ireland) supplied Accutase, Geneticin and B-27 supplement. Polyfect and *Trans*IT®-2020 transfection reagents were purchased from Qiagen, UK and Mirus Bio LLC, Ireland, respectively. Bio-Sciences supplied Hank's balanced salt solution (HBSS). EXCELL® animal-component-free medium was purchased from SAFC Biosciences, UK.

Protein Biochemistry*:* EZ-Link Sulfo-NHS-LC-Biotin, Pierce® Streptavidin–agarose beads and Pierce® BCA protein assay kit were purchased from Thermo Scientific, Ireland.

Calbiochem protease inhibitor cocktail set III was purchased from Merck Millipore. Details of all the primary antibodies used are given as follows.

Table 2.1 List of primary antibodies used for Western blotting

Name of the antibody	Dilution used	Supplier
Mouse monoclonal anti-K_v1.1, clone K20/78	1:10 (WB)	NeuroMab, USA
Mouse monoclonal anti-K_v1.2, clone K14/16	1:10 (WB)	NeuroMab
Mouse monoclonal anti-K_v1.4, clone K13/31	1:10 (WB)	NeuroMab
Rabbit polyclonal anti-K_v1.6, ab65792	1:500 (WB)	Abcam, UK

Western blotting secondary antibodies*:* donkey anti-mouse antibody (1:10,000) and anti-rabbit antibody (1:10,000) were purchased from Jackson ImmunoResearch laboratories Inc., UK. Bio-Rad (Ireland) supplied protein molecular weight markers. 4-AP was purchased from Lancaster Synthesis, UK and TEA from Sigma-Aldrich, Ireland. All other chemicals were from Sigma-Aldrich, Ireland.

2.2 Methods

2.2.1 PCR amplification of K_v1 channel genes with flanking half-linkers and unique restriction enzyme sites

Concatenation of four K_v subunits as a single open reading frame (ORF) was accomplished using an inter-subunit linker derived from the untranslated regions (UTRs) of the *Xenopus* β-globin gene (GeneBank® accession number J00978) (Sokolov et al., 2007). When

sequenced, the K_v1.1, 1.2, 1.4 and 1.6 constructs corresponded to those previously published GI number (see list of abbreviations for full form): 148356232, GI: 148298857, GI: 205042, GI: 253970438, GI: 467797 and GI: 499327, respectively. Amplification of K_v channel genes was carried out using K_v sequence-specific primers which incorporated flanking XbaI/XhoI sites (Table 2.2A), allowing their individual cloning into a previously modified UTR-containing intermediate pβUT plasmid, at XbaI/XhoI cloning sites (Al-Sabi et al., 2010). A second round of PCR, using primers specific to the UTRs themselves, allowed amplification of α subunit ORF contiguous with the flanking UTRs and paired restriction sites for NheI/BglII, BglII/EcoRI, EcoRI/SalI and SalI/BamHI (Table 2.2B). To insert a gene into position IV of a tetramer, K_v gene subunits were engineered with stop codon(s). Thus, UTR-specific primers for positions I, II, III and IV differed only by position-specific flanking restriction sites. A bank of monomeric α K_v1.1, 1.2 and 1.6 gene subunits were generated and cloned into the multiple cloning site (MCS) of expression vector pIRES2-EGFP. To construct K_v1.4-containing tetramers, K_v1.4 gene was amplified using specific primers for NheI and BglII sites without inter-subunit linker (Table 2.2C).

Table 2.2 PCR primers used to amplify K_v α subunits and insert restriction sites

A

Rat K_v1 α subunit	Forward primer (with XbaI site underlined)	Reverse primer (with XhoI site underlined)
1.1	GTCTAGAATGACGGTGATGTCAGGGGAGAATGC	GCTCGAGAACATCGGTCAGGAGCTTGCTCTTATTAAC (-); GCTCGAG*TTATC*AAACATCGGTCAGGAGCTTGCTCTTATTAAC (+)
1.2	GTCTAGAATGACAGTGGCTACCGGAGACCCAGTGG	GCTCGAGGACATCAGTTAACATTTTGGTAATATTCAC (-); GCTCGAG*TTATC*AGACATCAGTTAACATTTTGGTAATATTCAC (+)
1.6	GTCTAGAATGAGATCGGAGAAATCCCTTACGC	GCTCGAGAACCTCGGTGAGCATCCTTTTCTCTGC (-); GCTCGAG*TTA* AACCTCGGTGAGCATCCTTTTCTCTGC (+)

B

Subunit position in pIRES	Forward primer (restriction site underlined)	Reverse primer (restriction site underlined)
I (NheI-BglII)	AGCTAGCAGAATAAACGCTCAACTTTGGCAGATC	GAGATCTCCAGATCCGGTACCAGATCGATCTCGAC
II (BglII-EcoRI)	GAGATCTAGAATAAACGCTCAACTTTGGCAGATC	CGAATTCCCAGATCCGGTACCAGATCGATCTCGAC
III (EcoRI-SalI)	CGAATTCAGAATAAACGCTCAACTTTGGCAGATC	AGTCGACCCAGATCCGGTACCAGATCGATCTCGAC
IV (SalI-BamHI)	AGTCGACAGAATAAACGCTCAACTTTGGCAGATC	AGGATCCCCAGATCCGGTACCAGATCGATCTCGAC

C

Rat K_v1.4 in position I	Forward primer (restriction site underlined)	Reverse primer (restriction site underlined)
NheI-BglII	GAATCAGCTAGCATGGAGGTGGCAATGGTGAG	GAATCAAGATCTCACATCAGTCTCCACAGCCTTTG

2.2.2 Site-directed mutagenesis of K_v1 channel constructs

Selected mutations R354A, V381Y, R354A/V381Y, Q357H/V381Y or Q357H/P359S/V381Y in the pore region of K_v1.2 (Table 2.3, and cf. Fig. 3.1 later), were sequentially introduced by using inverse PCR with suitable primers, *Pfx* high-fidelity polymerase and K_v1.2 monomer as a template, followed by self-ligation. The NIP function of K_v1.6 was abolished by carrying out amino acid substitutions identified by others (Roeper et al., 1998). Briefly, K_v1.6 was mutated using *Pfx* polymerase in the presence of primers to substitute NIP residues, glutamic acid 27, 30 and 32, with alanines, thereby, yielding the mutant (K_v1.6 E27/30/32A) (Table 2.3). After verification of the resultant mutants by DNA sequencing, each gene was subsequently cloned into the desired position of selected tetrameric constructs (cf. Fig. 3.6 and 4.7 later).

Table 2.3 List of mutations created in K_v genes

Rat K_v gene	Position of mutation in protein	Amino acid conversion	Mutated K_v gene created
1.2	354*	Arginine (CGA) to Alanine (GCA)	$1.2^{(R354A)}$
1.2	381	Valine (GTT) to Tyrosine (TAT)	$1.2^{(V381Y)}$
1.2	354 and 381	Arginine (CGA) to Alanine (GCA) and Valine (GTT) to Tyrosine (TAT)	$1.2^{(R354A/V381Y)}$
1.2	357 and 381	Glutamine (CAG) to Histidine (CAC) and Valine (GTT) to Tyrosine (TAT)	$1.2^{(Q357H/V381Y)}$
1.2	357, 359 and 381	Glutamine (CAG) to Histidine (CAC), Proline (CCC) to Serine (TCC) and Valine (GTT) to Tyrosine (TAT)	$1.2^{(Q357H/P359S/V381Y)}$
1.6	27, 30 and 32	Glutamic acid (GAG) to Alanine (GCG)	$1.6^{(E27/30/32A)}$

* = amino acid residue number

Conditions for amplification using *Pfx* high-fidelity polymerase were: initial denaturation, 95^{o}C for 2 minutes, 22 cycles of amplification, each cycle comprising denaturation at 94^{o}C for 30 seconds, annealing T_m of primers for 45 seconds and elongation at 68^{o}C for 2 minutes. PCR products were purified by gel electrophoresis followed by band recovery, and cloned into subsequent vectors.

2.2.3 Assembly of monomeric K_v1 gene cassettes to generate pre-defined tetrameric constructs

A bank of $K_v1\alpha$ gene(s) cassettes generated after insertion of inter-subunit half-linkers (5' – end linker amino acid sequence: R I N A Q L W Q I D S R; 3' – end linker amino acid sequence: L E T S R S I W Y R I W) and position-specific restriction enzyme sites (Fig. 2.1), were trimmed with chosen pair(s) of position-dependent restriction enzymes (NheI/BglII, BglII/EcoRI, EcoRI/SalI or SalI/BamHI) and sequentially

sub-cloned into each of the four position(s) (I–IV) of pIRES2-EGFP to generate multimeric construct(s) (Al-Sabi et al., 2010). Each single α subunit encoding gene fragment in K_v1.1/1.2-containing tetramers was separated by a combined 78 bp linker including restriction enzyme sites. In K_v1.4-containing concatemers, K_v1.4 gene inserted into position I was separated from the second subunit by a 42 bp linker including a BglII restriction site. In all the constructs, a subunit gene followed by a stop codon was sub-cloned in position IV. The DNA constructs generated were transformed in TOP10 chemically competent *E.coli* and selected on the antibiotic resistant Luria-Bertani (LB) agar containing the appropriate antibiotic, kanamycin sulphate (30 µg/ml). Selected bacterial clones were grown in large volumes (500 ml) and DNA was isolated using HiSpeed plasmid purification kits from Qiagen, UK.

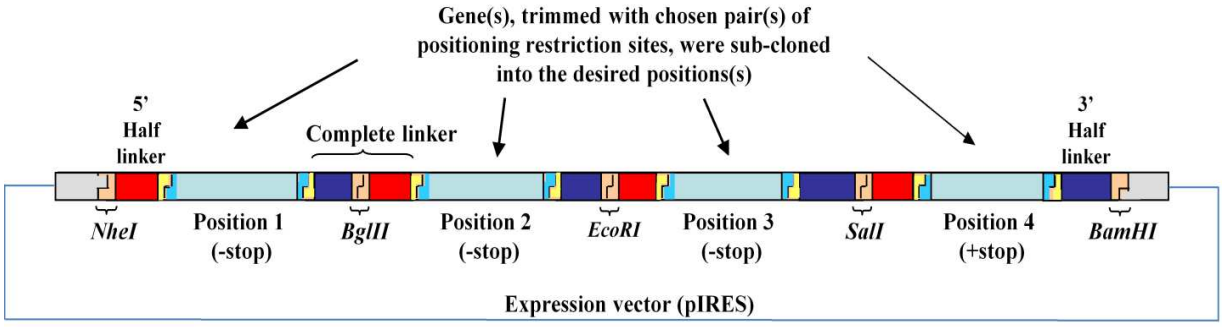

Fig. 2.1 Representation of the positional arrangement of genes sub-cloned into an expression vector (pIRES) to generate multimeric constructs.

Four α subunit genes were trimmed on both ends with restriction enzymes and such cassette(s) were sub-cloned into an expression plasmid containing a reporter gene, to generate multimeric construct(s) into desired positions. The postions I- IV in a multimeric construct were linked by a 78 bp linker (complete recombinant linker), including restriction enzyme sites (BglII, EcoRI or SalI) in K_v1.1/1.2-containing tetramers, whereas a 42 bp linker, including the enzyme site (BglII), joined position I and II subunits in K_v1.4 -containing tetramers. The gene(s) inserted in I, II and III were devoid of a stop codon, whereas the gene in the fourth position is carrying stop codon(s) at the 3'end.

2.2.4 DNA mapping

All recombinant DNA constructs were analysed by digestion with various restriction enzymes and sequenced to confirm their identities.

2.2.4.1 Restriction enzyme digestion analysis of recombinant DNA constructs**.** Purified maxi DNA preparations of desired recombinant K_v gene constructs (monomers and tetramers) were analysed by restriction enzyme digestion, throughout the cloning process, for their correct orientation and positioning in cloning and expression vectors. Monomeric K_v1.1, 1.2 and 1.6 in pIRES2-EGFP vector with stop codon(s) were digested with SalI/BamHI. Tetrameric constructs are digested with NheI/BglII, BglII/EcoRI, EcoRI/SalI and SalI/BamHI to release the genes sub-cloned in position I-IV, respectively. Enzymes that were used to identify the genes incorporated in the vectors are listed in the Table 2.4.

Table 2.4 List of restriction enzymes used to confirm the chosen cloning site in a vector and the identity of respective K_v genes cloned

Construct	Vector	Gene(s)	Restriction enzymes used to confirm	
			Position in the MCS of vector	Gene incorporated
Tetrameric α K_v1.1-pIRES	pIRES2-EGFP	K_v1.1	NheI/BglII, BglII/EcoRI, EcoRI/SalI & SalI/BamHI	SphI
Tetrameric α K_v1.2-pIRES	pIRES2-EGFP	K_v1.2	NheI/BglII, BglII/EcoRI, EcoRI/SalI & SalI/BamHI	EcoRV
Tetrameric α K_v1.1/1.2-pIRES	pIRES2-EGFP	K_v1.1 and 1.2	NheI/BglII, BglII/EcoRI, EcoRI/SalI & SalI/BamHI	EcoRV, SphI
Tetrameric α K_v1.4/1.6/1.2-pIRES	pIRES2-EGFP	K_v1.4, 1.6 and 1.2	NheI/BglII, BglII/EcoRI, EcoRI/SalI & SalI/BamHI	EcoRV, SphI and KpnI

All the enzyme digestions were kept at 37 ^{o}C for 2 h, mixed with DNA gel loading solution followed by electrophoresis through 0.85 % agarose gel. 1 Kb DNA ladder was used as a reference marker.

2.2.4.2 Confirmation of recombinant K_v channel genes by DNA sequencing. In addition to the restriction analysis, all the wild-type and mutated forms of the monomeric and tetrameric constructs built herein were subjected to DNA sequencing (Eurofins MWG, Germany), to verify correct nucleotide sequence of the genes. For sequencing monomeric K_v1 channel genes in a vector, primers were designed corresponding to the nucleotide sequence of the respective genes and to the sequence of vector near to the 5' end and 3' end of the incorporated gene. DNA samples were prepared without restriction digestion. However, to sequence concatenated multimeric constructs, each subunit was isolated from a tetramer by digestion with position-specific restriction enzymes (NheI/BglII, BglII/EcoRI, EcoRI/SalI and SalI/BamHI), if more than one copy of the same K_v gene was present. To sequence the linker region in a tetramer, a set of two genes was isolated by restriction digestion while preserving the linker region, gel extracted, followed by DNA sequencing using primers designed to complement sites near to the linker sequence (Fig. 2.2). Primers complementary to the pIRES vector sequence near to the 5' (pIRES forward) or 3' (pIRES reverse) end of complete tetrameric construct were used to sequence position I or position IV subunit when left intact with vector after isolation of remaining subunits. When isolated, each subunit was sequenced with the gene-specific primers (Fig. 2.2).

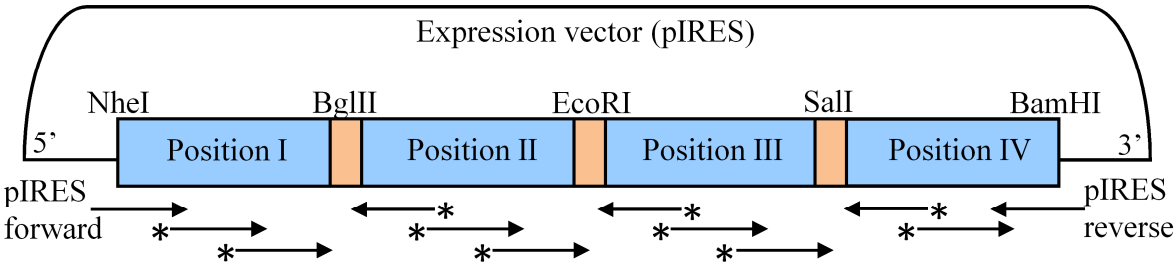

Fig. 2.2 Strategy applied to sequence a tetrameric construct.

The pattern of primers designed to sequence each individual subunit encoding fragment of gene(s) of a complete tetramer is depicted. The pIRES forward and reverse primers were used to sequence subunits in position I and IV, respectively, along with gene-specific primers (arrows with asterisk). Total sequencing of tetrameric DNA was performed by releasing desired subunits with restriction digestion, gel (0.85% agarose) electrophoresis and extraction followed by nucleotide sequencing.

2.3 Cell culture

2.3.1 Culturing of mammalian cells

Mammalian cell lines, Human Embryonic Kidney (HEK)-293 (ATCC, UK), were maintained in DMEM supplemented with 10 % fetal (v/v) bovine serum (FBS), 100 IU/ml of Penicillin and 100 µg/ml of Streptomycin, as adherent cultures in a 5% CO_2 incubator at 37 °C. Cells were trypsinised (0.25% (v/v) Trypsin-EDTA solution, Cat no. T4049 Sigma-Aldrich Ireland) and re-plated once they reached 80 % confluency. For long-term storage in liquid nitrogen, cells were kept in FBS containing 10 % (v/v) dimethyl sulfoxide (DMSO). Cells were then processed as required.

For electrophysiology experiments, coverslips were washed thoroughly with concentrated nitric acid, followed by rinsing with deionised water, sterilized by autoclaving and dried in culture dishes before using. One coverslip (9 mm diameter) per well was placed in a 24 well plate or an appropriate culture dish. For coating, poly-D-lysine solution (500 µl of 0.1

mg/ml, dissolved in sterilized double distilled water) was added to the wells/culture dishes with or without coverslips. After 30 min of incubation at room temperature, wells/culture dishes were washed twice with sterile water and dried. Coated dishes were stored at room temperature until use.

2.3.2 Transfection of HEK-293 cells using Polyfect or TransIT-2020

Approximately 18–24 h before transfection, HEK-293 cells at a density of 3.0×10^5 cells/ml were plated in 2.5 ml complete growth medium per well in a 6-well plate. After overnight incubation, cells ≥ 60% confluence were transfected. Plasmid DNA (2.5 µg) was added to 250 µl of DMEM without antibiotics and serum. Polyfect or Mirus *Trans*IT®-2020 reagent was added to the diluted DNA according to the manufacturer's recommendations. After gentle pipetting, the mixture was incubated at room temperature for 15 minutes to allow DNA/reagent complex to form. Serum supplemented DMEM was added to the DNA/reagent mixture and the total volume transferred to the cells with gentle swirling to ensure even distribution of the complexes. Cells were then incubated at 37 °C, in a 5 % CO_2 atmosphere for 48 h to allow gene expression.

2.3.3 Generation of monoclonal and polyclonal stable cell lines expressing K_v1 channels

Post transfection HEK-293 cells were allowed to grow for 48 hrs in culture medium. Adherent cells were trypsinised, washed with PBS and allowed to grow for ~2-3 weeks in culture medium at a final concentration of 500 µg/ml of geneticin (Life Technologies). Culture supernatant was replaced with fresh medium (containing geneticin) as the non-transfected cells started to die and float during incubation. Surviving cells (referred as polyclonal) expressing enhanced green fluorescent protein (EGFP) marker were detached

and plated at a density of 1 cell/well in a 24-well plate. Clones stably expressing K_v1.X gene with EGFP (referred as monoclonal) were selected and analysed by microscopy, before further analysis by surface biotinylation and electrophysiology.

2.4 Characterization of recombinant gene expression in HEK-293 cells

2.4.1 Biotinylation and isolation of cell surface expressed proteins in HEK-293 cells

Biotinylation of cells was performed as depicted in Fig. 2.3. Briefly, cells were washed twice with ice-cold PBS. EZ-Link Sulfo-NHS-LC-Biotin at 1 mg/ml in ice-cold PBS was added to each flask and placed for 30 minutes at 4°C with gentle agitation for every 5 min. The reaction was quenched by adding glycine to a final concentration of 100 mM in PBS to each flask. Cells were scraped off the surface and centrifuged at 500 × *g* for 3 min after rinsing the flask with 1xTris-buffered saline (TBS). Supernatant was discarded and cells were washed twice with PBS at 500 × *g* for 3 minutes. Cell lysis was performed by suspending the cells in 500 µl of 1 x lysis buffer containing protease inhibitors cocktail (1:200 dilution, Cat. no. P8340 Sigma-Aldrich Ireland) and incubated for 60 minutes on an end-over-end rotator at 4°C. Lysate was centrifuged at 10,000 × *g* for 10 minutes at 4°C and clarified supernatant was collected. Meanwhile, Streptavidin agarose beads (total volume of 150 µl of slurry) were sedimented for 1 min at 1,000 × *g*. After the supernatant was discarded, the resin was washed twice with 500 µl of cell lysis buffer, centrifuged for 1 minute at 1,000 × *g* and the supernatant discarded. The clarified cell lysate was applied to the washed resin and incubated for 60 minutes at 4°C on a rotator. Then, the resin with cell lysate was centrifuged for 1 minute at 1,000 × *g* and the flow-through retained. The resin was washed three times; 1 minute at 1,000 × *g*, with 500 µl wash buffer supplemented with protease inhibitors cocktail. 1 x Lithium dodecyl sulfate (LDS) sample buffer (100 µl)

containing a final concentration of 50 mM DTT was added to the resin and heated for 5 minutes at 95°C. The samples were centrifuged for 5 min at 10,000 × *g*, the supernatant collected and stored at -20°C for further analysis.

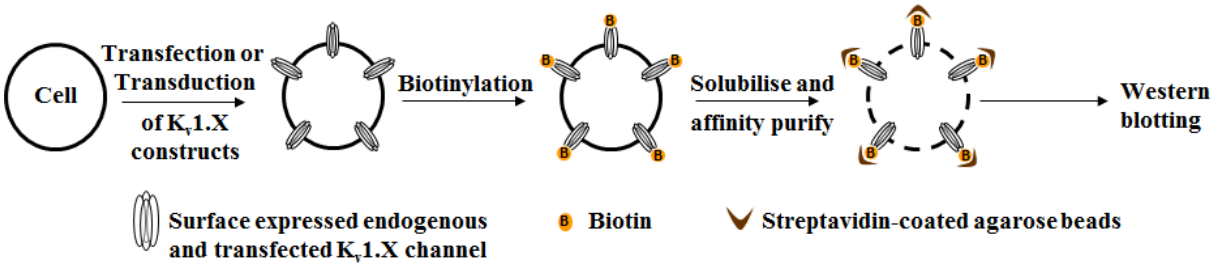

Fig. 2.3 Schematic of experimental steps to characterize cell-surface expressed K_v proteins using EZ-Link Sulfo-NHS-LC-Biotin.

Cells were labelled with EZ-Link Sulfo-NHS-LC-Biotin, subsequently lysed with a mild detergent and the labelled proteins then isolated with agarose beads. The bound proteins released by incubating with SDS-PAGE sample buffer were analysed by Western blotting.

2.5 Electrophysiological recordings

Whole-cell voltage clamp was performed as outlined previously (Al-Sabi et al., 2010), except where specified. In the conventional patch-clamp system (EPC10 amplifier; HEKA Elektronik, Germany), the recording pipette was filled with an internal solution of the following composition: 95 mM KF, 30 mM KCl, 1 mM $CaCl_2$, 1mM $MgCl_2$, 11 mM EGTA, 10 mM Hepes and 2 mM Na_2ATP (pH 7.2 with KOH), with fire-polished tips having resistances between 1.5 and 3.0 MΩ. To ensure functionality of the NIB moiety, 2 mM glutathione was introduced as a reducing agent to the internal solution (Ruppersberg et al., 1991; Roeper et al., 1998). The external (bath) medium contained: 135 mM NaCl, 5 mM KCl, 2 mM $CaCl_2$, 2 mM $MgCl_2$, 5 mM Hepes and 10 mM sucrose (pH 7.4 with NaOH). Correction was made for liquid junction potential (+7 mV). Only cells with an I_K

of >1 nA were chosen for experimentation to avoid interference from endogenous outward currents (< 200 pA at +20 mV potential). Likewise, only cells with series resistances <10 MΩ throughout the experiments were included in the present study. Leakage and capacitive currents were subtracted online using the P/4 subtraction protocol. Currents were filtered at 1 kHz, and sampled at 10 kHz (with the exception of 10 seconds pulses, which were sampled at 50 Hz). Whole-cell currents were measured at a holding potential of −90 mV, and then depolarized to +20 mV for 300 ms or stepped from the holding potential in +10 mV increments from −80 mV to 80 mV. gK–V (K^+ conductance–voltage relationships) were determined from averaged steady-state currents after 200 ms of activation and normalized relative to the K^+ driving force, by assuming a reversal potential of −82 mV. Time constants for activation were determined by fitting the I_K amplitudes corresponding to 40–90 % of the maximum with a single exponential function. Time-dependent inactivation constants were measured during 10 seconds depolarization steps from −10 to 10 mV, in 10 mV increments, and the currents fitted with double exponential functions (Sokolov et al., 2007). For experiments on the recovery from inactivation, a variable interval-gapped pulse protocol was used; from a −90 mV holding potential, depolarization to +10 mV for 300 ms in an initial step was followed by a second identical pulse with gap intervals of 0–20 seconds. The ratios of the normalized peak currents at time intervals were plotted and fitted with a single exponential function to obtain time courses of recovery from inactivation. Measurement of steady-state inactivation involved a 10 seconds conditioning pulse applied in 10 mV increments from −100 to +10 mV, followed by a 500 ms test pulse at +10 mV (at −90 mV holding potential). Steady-state inactivation constants were calculated from the peak currents of the test pulses. Normalized inactivation curves were fitted to the

Boltzmann function ($I = \{1+\exp[(V - V_{1/2})/k]\}^{-1}$), where V is the membrane (pre-pulse) potential, $V_{1/2}$ is the potential at half-maximal inactivation and k is the slope factor.

An automated whole-cell voltage clamp system (QPatch 16, Sophion Bioscience) was utilized as outlined previously (Al-Sabi etal., 2010), using the same internal and external solutions as in the conventional system, and with Qplate pin-holes having resistances 2–3 MΩ. TEA chloride was substituted for an equivalent amount of NaCl. HEK-293 cells expressing the desired K_v1 channel were detached from culture plates with Accutase and suspended in EXCELL® animal-component-free medium, 25 mM Hepes and 5 mM L-glutamine (pH 7.4)] and washed twice with external solution before being applied to the pipetting wells in the Qplate. Giga-seals were formed following execution of a combined suction/voltage protocol; gradually increasing suction leads to the whole-cell configuration. Compounds were applied, via a four-way pipetting robot, through integrated glass-coated microfluidic flow channels. Data analysis was performed using an integrated database (Oracle) within QPatch software (Sophion Bioscience). TEA inhibition was determined by the Hill equation fitted to six to eight concentrations. A Dynaflow-16 perfusion system (Cellectricon) in the conventional patch-clamp rig, where test solutions were exchanged by continuous microfluidic flow, was used to confirm the results made by the QPatch 16. In the Dynaflow-16 system, data were taken from one to six TEA concentrations to quantify the inhibition, according to the relationship $IC_{50} = fc/(1-fc)[TEA]$, where fc is the fractional current and [TEA] is the TEA concentration.

2.6 Data analysis

Electrophysiological results were analysed using FitMaster (HEKA Electronik), re-plotted and fitted using IGOR Pro 6 (WaveMetrics, USA). Data are reported as means $\pm$ S.E.M.

and *n* values refer to the number of individual cells tested. Statistical significance was evaluated by an unpaired two-tailed Student's *t* test or, where indicated in the text, a Mann–Whitney *U* test, using data obtained from at least four independent experiments.

$P < 0.01$ was considered significant.

CHAPTER 3

RESULTS

Position-dependent attenuation by $K_v1.6$ of N-type inactivation of $K_v1.4$-containing channels

3.1 Overview

Biochemical studies on brain membranes have revealed that $K_v1.4$ α subunit is a constituent of K^+ channel oligomers containing $K_v1.2$ and 1.6 subunits (Shamotienko et al., 1997, Coleman et al., 1999). The fast N-type inactivation endowed by $K_v1.4$ can be prevented by the presence of $K_v1.6$ through its NIP domain (Roeper et al., 1998), giving rise to a much slower inactivating/sustained K^+ current. As tetramerization of K_v channel subunits occurs in the endoplasmic reticulum (Pfaffinger and DeRubeis, 1995**)**, pinpointing their ordering *in vivo* has thus far eluded researchers because of an inability to pre-determine the arrangement of their assembled constituents in the oligomers delivered to the cell surface. Therefore, it was warranted to focus efforts on gaining a clearer understanding of the influences on channel properties of subunit ordering, particularly as the resultant data could give insights into the modulation of neurotransmission by K_v1 channels. Furthermore, such information is medically relevant given that delayed rectifier K_v1 subunits, but not $K_v1.4$, are down-regulated in the hippocampus of animal models prone to seizures (Lee et al.,

2009), whereas K_v1.4 is up-regulated following chronic injury of the spinal cord (Edwards et al., 2002).

The present study addressed whether subunit ordering influences the biophysical profiles of K_v1 channels. For this, advantage was taken of the NIP in K_v1.6 (Roeper et al., 1998) being able to prevent fast inactivation of K_v1.4-containing channels. If NIP competes directly for the binding site of NIB on K_v1.4, displacing it and giving rise to slow inactivation, no differences ought to be expected when these two α subunits are placed adjacently or distally in concatenated heteromers, with both of their currents inactivating slowly. On the other hand, if NIP function relies on it directly interacting with the NIB, dissimilarities in inactivation rates may occur with a slow-inactivating current only occurring when both domains are optimally placed. Suboptimal placement might result in a fast-inactivating channel when NIP is positioned away from NIB and unable to modulate it. To address this important question, inactivation, voltage-dependence of inactivation and recovery from inactivation were measured in three recombinantly-expressed tetramers having identical subunit composition, but distinct subunit positioning. A fourth tetramer, K_v1.4-1.2-1.2-1.2 was constructed as a control, having one copy of K_v1.4 within the tetramer. The novel outcome of this approach questions the wisdom of predicting channel properties based on subunit content alone because their positioning greatly influences the channels' characteristics. Also, the data reaffirm convincingly that this concatenation of genes pre-determines the positions of α subunits in the assembled functional channels on the cell surface.

3.2 Channel concatemers of defined α subunit composition expressed following domain-specific assembly of gene cassettes into the pIRES2-EGFP plasmid

In this study, two subunits having opposite roles on inactivation kinetics were selected to obtain proof of principle for retaining their functionalities depending on their positioning within the concatemer (Fig. 3.1). K_v1.4, which mediates N-type inactivation of mammalian K_v1 channels through its NIB domain (Ruppersberg et al., 1991; Tseng-Crank et al., 1993) together with K_v1.6, which overrides this rapid inactivation via its NIP domain (Roeper et al., 1998), were expressed in different positions with respect to each other. Two or three copies of K_v1.2 formed the other constituent of these hetero-tetramers. In one concatenated gene construct, K_v1.4 was separated from K_v1.6 with a single copy of K_v1.2 (K_v1.4–1.2–1.6–1.2), in another case K_v1.6 was placed immediately adjacent to K_v1.4 followed by two copies of K_v1.2 (K_v1.4–1.6–1.2–1.2), and the third tetramer had two copies of K_v1.2 between K_v1.4 and K_v1.6 (K_v1.4–1.2–1.2–1.6), giving three tetramers with identical composition of subunit, but different ordering. A fourth construct was assembled containing one copy of K_v1.4 along with three copies of K_v1.2 (K_v1.4–1.2–1.2–1.2); this was expected to show a rapid inactivating K^+ current due to lack of the K_v1.6-containing NIP domain (Fig. 3.1).

All tetramer construction employed an inter-subunit linker derived from the *Xenopus* β-globin gene shown previously to be suitable (Al-Sabi et al., 2010). Initial PCR of cDNA encoding K_v1.4, 1.6 or 1.2, yielded single bands on electrophoresis with the expected sizes of ~2.0, 1.6 and 1.5 Kb, respectively. Flanking inter-subunit linkers and paired restriction sites, allowing cloning into the pIRES2-EGFP expression vector, were added to the amplified products of K_v1.2 and/or K_v1.6 as described (Al-Sabi et al., 2010).

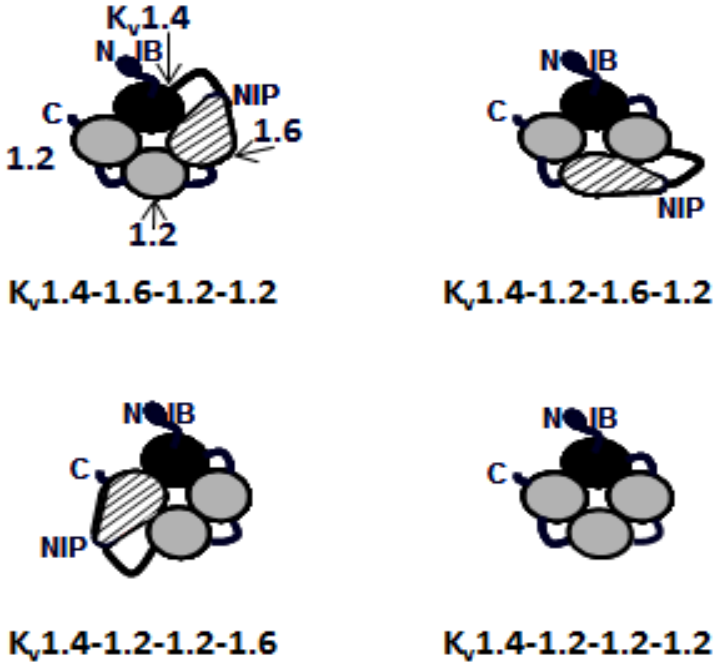

Fig. 3.1 Schematics showing predicted arrangement of concatenated channels based on order of K_v1 genes in recombinant constructs.

NIB and NIP refer to the $K_v1.4$ N-terminal inactivation ball and its prevention domain in $K_v1.6$, respectively.

The resultant hetero-tetramers, $K_v1.4$–1.6–1.2–1.2, $K_v1.4$–1.2–1.6–1.2, $K_v1.4$–1.2–1.2–1.6 and $K_v1.4$–1.2–1.2–1.2 were assembled into pIRES2-EGFP with the $K_v1.4$ gene introduced at the start (position I) to conserve functionality of its NIB. $K_v1.6$, when present, was placed either adjacently (position II or position IV) or distally (position III) to the $K_v1.4$ sequence (Fig. 3.2). Each K_v1 gene incorporated in a tetramer was analysed for their positioning (I-IV) by restriction digestion with position-specific enzymes NheI/BglII, BglII/EcoRI, EcoRI/SalI and SalI/BamHI, respectively. EcoRV, SphI and KpnI are gene specific enzymes used to verify the presence of $K_v1.2$, 1.4 or 1.6 (Fig. 3.2). Complete DNA sequencing analysis of the tetramers in Fig. 3.2 confirmed the presence of desired subunits with correct nucleotide sequence.

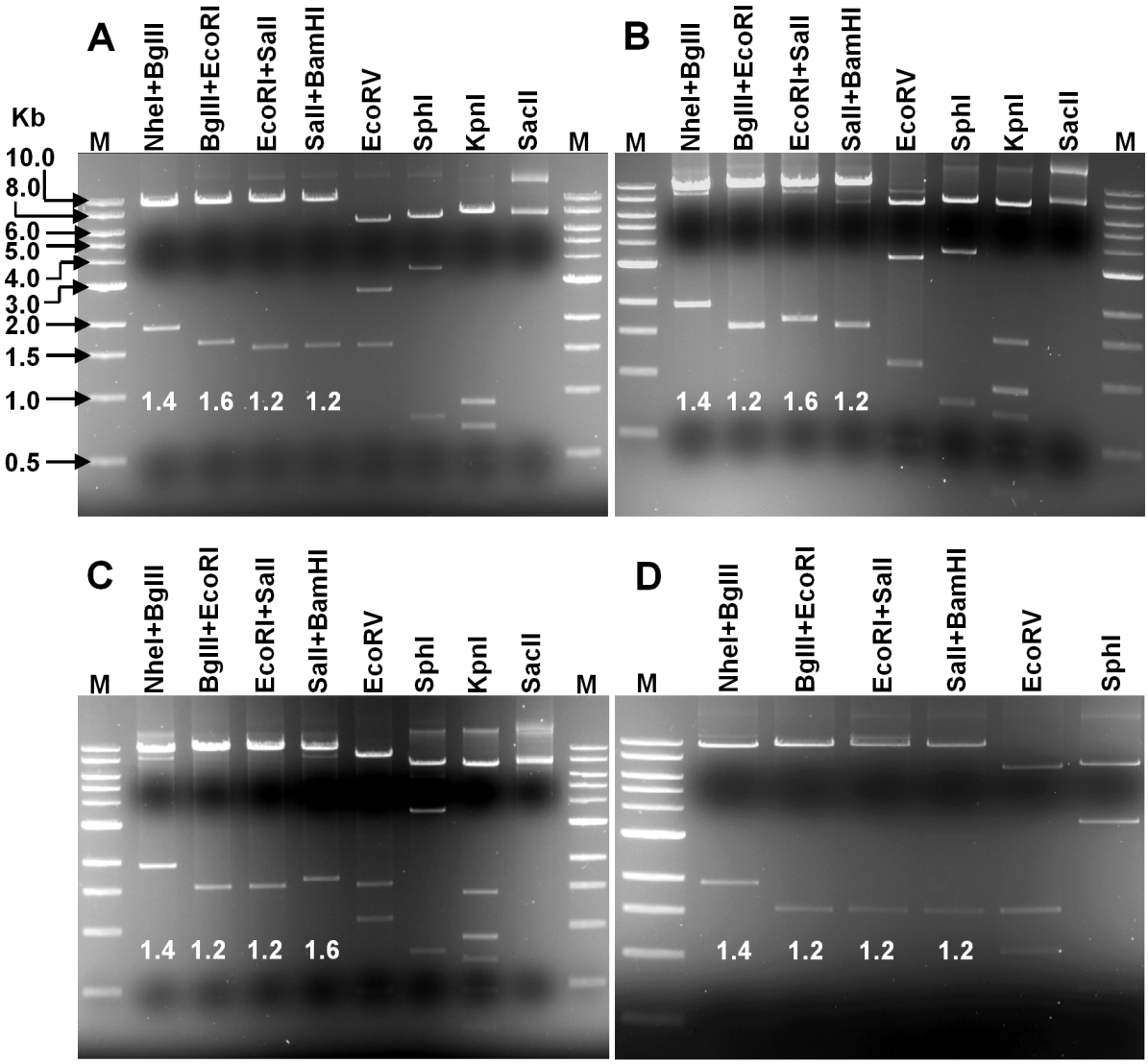

Fig. 3.2 Restriction maps of K_v1.X tetramers.

Agarose (0.85%) gel electrophoretograms showing the sequential release of each subunit (K_v1.4, K_v1.6 or K_v1.2) from tetrameric constructs K_v1.4–1.6–1.2–1.2 (A), K_v1.4–1.2–1.6–1.2 (B), K_v1.4–1.2–1.2–1.6 (C) and K_v1.4–1.2–1.2–1.2 (D) by digestion with NheI/BglII, BglII/EcoRI, EcoRI/SalI and SalI/BamHI respectively. EcoRV, SphI and KpnI are gene-specific restriction enzymes used to verify the presence of K_v1.2, 1.4 or 1.6 subunits in desired positions. M, 1 Kb DNA ladder.

3.3 Concatenated K_v1.4-containing channel expressed on the surface of HEK-293 cells as a single intact protein

All of the concatenated constructs, upon transfection into HEK-293 cells and following surface biotinylation analysis, yielded an expressed protein band on SDS/PAGE at Mr ~280 K, when probed with antibodies specific to K_v1.4, 1.6 or 1.2 (Figure 3.3). This band represents full-length intact tetrameric protein with a smeared appearance possibly due to the highly glycosylated nature of K_v1.4 (Watanabe et al., 2015). A number of faint non-specific bands were observed with the K_v1.4 antibody at Mr ~140, 50 and 40 K, whereas a lower molecular weight non-specific band was also visible with the K_v1.2 antibody (clone 14/16, NeuroMab), but have no effect on the K_v1 channel activity when tested electrophysiologically.

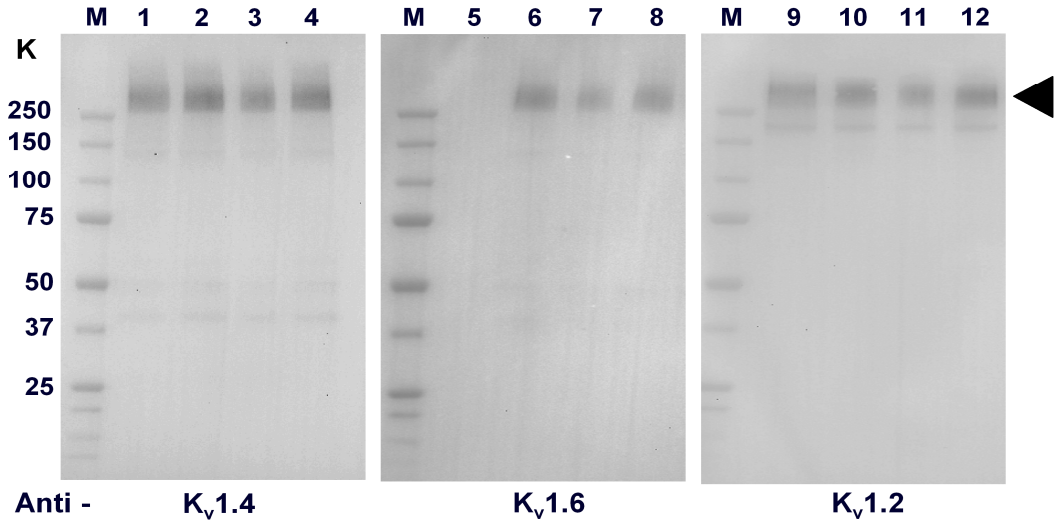

Fig. 3.3 Surface expression of complete hetero-tetrameric K_v1.4-containing channels on plasmalemma of HEK-293 cells.

Transiently transfected HEK-293 cells expressing Kv1.4–1.2–1.2–1.2 (lanes 1, 5 and 9), Kv1.4–1.6–1.2–1.2 (lanes 2, 6 and 10), Kv1.4–1.2–1.6–1.2 (lanes 3, 7 and 11) or Kv1.4–1.2–1.2–1.6 (lanes 4, 8 and 12). Intact cells were biotinylated, detergent solubilized, precipitated with streptavidin–agarose beads and analysed by Western blotting, using antibodies specific for Kv1.4 (lanes 1–4), Kv1.6 (lanes 5–8) or Kv1.2 (lanes 9–12); M, denotes a molecular weight marker (K).

3.4 K_v1.6 subunit prevents fast inactivation of K^+ currents only when positioned adjacent to K_v1.4 in heteromeric channel proteins

When subjected to a 10-s depolarization step to +10 mV or −10 mV, the expressed K_v1.4–1.2–1.6–1.2 channel displayed a rapidly inactivating A-type K^+ current (Fig. 3.4A), which is notable as this heteromer contains a NIP domain known to disallow N-type fast inactivation (Roeper et al., 1998). Such rapid decay suggests that distal positioning of the NIP-containing K_v1.6 relative to K_v1.4 in this heteromer attenuates NIP functionality. This fast inactivation profile of K_v1.4–1.2–1.6–1.2 channel is similar to that of K_v1.4–1.2–1.2–1.2 (Fig. 3.4B). In stark contrast, heteromers K_v1.4–1.6–1.2–1.2 and K_v1.4–1.2–1.2–1.6 yielded slow-inactivating currents (Fig. 3.4C, D) as expected, due to the dominant-negative effect of the NIP domain in K_v1.6 (Roeper et al., 1998).

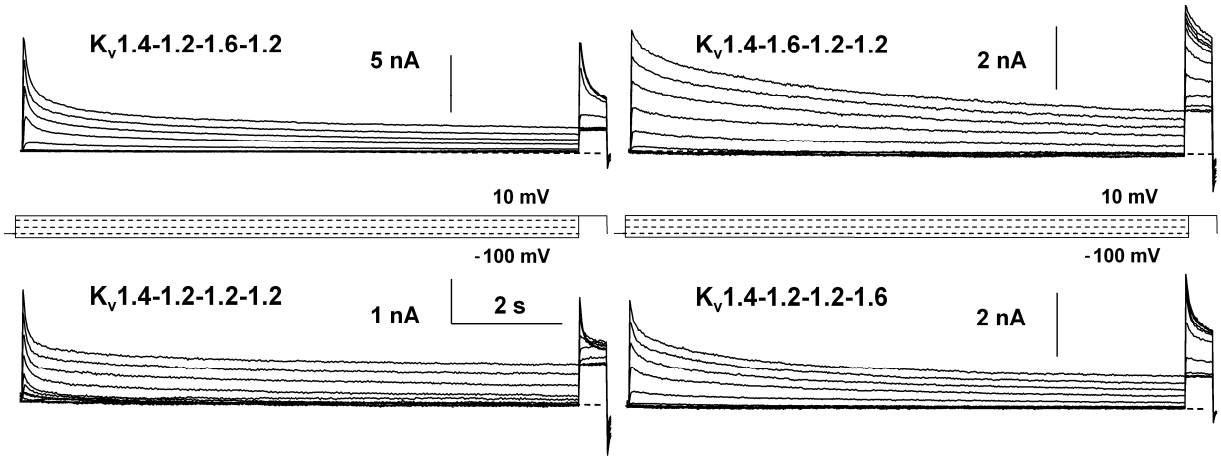

Fig. 3.4 Representative current traces, in response to a two-pulse steady-state inactivation protocol, for each depicted channel showing fast inactivation only when K_v1.6 subunit is absent or in a distal position from K_v1.4.

Currents obtained with Kv1.4–1.6–1.2–1.2 and Kv1.4–1.2–1.2–1.6 channels are slow-inactivating; while Kv1.4–1.2–1.6–1.2 and Kv1.4–1.2–1.2–1.2 showed fast decay. (n = 4-7).

Current traces from the three heteromeric (K_v1.4/1.6/1.2-containing) channels were best fitted with a double exponential function, which revealed significant differences in

inactivation rates (Fig. 3.5A). Accordingly, the K^+ current resulting from heteromers where K_v1.4 and 1.6 were placed adjacently (K_v1.4–1.6–1.2–1.2 and K_v1.4–1.2–1.2–1.6) showed slower τ_{1inact} and τ_{2inact} values than those of K_v1.4–1.2–1.6–1.2 and K_v1.4–1.2–1.2–1.2, especially at more negative potentials (Fig. 3.5A, Table 3.1). The fast-inactivating channels (K_v1.4–1.2–1.6–1.2 and K_v1.4–1.2–1.2–1.2) gave fairly constant τ_{1inact} and τ_{2inact} values at different potentials, while the slow-inactivating channel counter-parts revealed variable τ_{1inact}, but not τ_{2inact}, values, corresponding to optimal or suboptimal positioning of K_v1.4 to 1.6 subunits. Among the two slow-inactivating channels, differences in τ_{1inact} values at more positive potentials can be correlated with shifting the K_v1.6 subunit from the second to the fourth position, which might affect the NIP functionality. A steady-state inactivation protocol demonstrated the influence of NIP positioning in the concatemers on the voltage dependence of inactivation. The ensuing results, fitted by a single Boltzmann function (Fig. 3.5B, Table 3.1), unveiled a difference in the midpoints for voltage-dependent inactivation. Hetero-tetramers where K_v1.6 and 1.4 subunits are in adjacent positions showed $V_{1/2}$ values of −32 mV for K_v1.4–1.6–1.2–1.2, and −31 mV for K_v1.4–1.2–1.2–1.6 with a significant shift ($P < 0.05$) compared with −40 mV for K_v1.4–1.2–1.6–1.2 and −49 mV for K_v1.4–1.2–1.2–1.2. Also, membrane potentials more negative than −70 mV were required to remove inactivation from all heteromers tested (Fig. 3.5B).

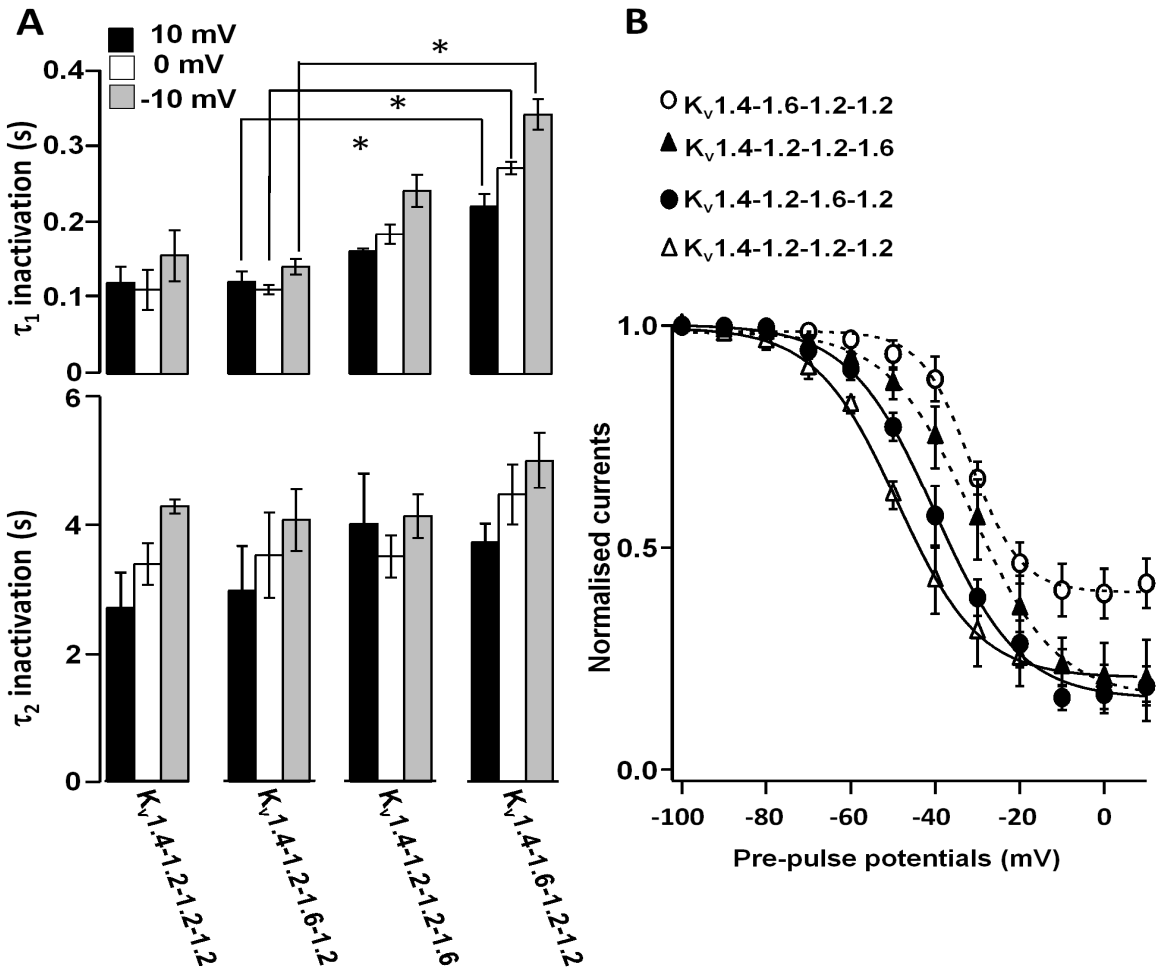

Fig. 3.5 Inactivation kinetics of K^+ currents are strongly dependent on the position of K_v1.6 relative to K_v1.4 in the concatemers.

(A) The histograms display the mean time constant of inactivation (τ1 and τ2) for the representative channels at different potentials. *, P < 0.05, Mann-Whitney *U* test. (B) The steady-state inactivation relationship, taken from normalized peak currents triggered by pre-pulse potentials and fitted with a single Boltzmann function. This plot shows a significant (P < 0.05, Mann-Whitney *U* test) voltage shift for Kv1.4-1.6-1.2-1.2 (○, broken line) and K_v1.4-1.2-1.2-1.6 (▲, broken line) to more positive potentials compared to Kv1.4-1.2-1.6-1.2 channels (●, straight line) or K_v1.4-1.2-1.2-1.2 (Δ, straight line) channels, as a result of K_v1.6 NIP functionality. Error bars represent means ± S.E.M. in panel A and B. (n = 4-7).

Table 3.1 Summary of inactivation parameters for K_v1.4-containing heteromers expressed in HEK-293 cells

	Inactivation time constants				Steady state inactivation		Recovery from inactivation
Channels	τ_{1inact} at 10 mV (ms)	τ_{2inact} at 10 mV (ms)	τ_{1inact} at −10 mV (ms)	τ_{2inact} at −10 mV (ms)	$V_{1/2}$ (mV)	Slope (k)	τ at −90 mV (s)
Kv1.4–1.6–1.2–1.2	220 ± 16 (5)*	3720 ± 280	340 ± 20 (5)*	4990 ± 430	−32 ± 1 (5)*	6 ± 1	3.1 ± 0.1(4)*
Kv1.4–1.2–1.2–1.6	160 ± 4 (7)*	4000 ± 790	240 ± 21 (7)*	4120 ± 340	−31 ± 1 (7)*	10 ± 1	2.6 ± 0.04 (6)*
Kv1.4–1.2–1.2–1.2	119 ± 21 (4)	2700 ± 550	155 ± 34 (4)	4270 ± 110	−49 ± 0.5 (4)	10 ± 1	2.7 ± 0.01 (4)
Kv1.4–1.6(mut)–1.2–1.2	112 ± 15 (5)	2040 ± 360	190 ± 20 (5)	3090 ± 570	−37 ± 1 (5)	9 ± 1	2.6 ± 0.02 (4)
Kv1.4–1.2–1.6–1.2	120 ± 14 (7)*	2970 ± 690	140 ± 10 (7)*	4060 ± 480	−40 ± 1 (5)*	10 ± 1	2.2 ± 0.1 (7)*
Kv1.4–1.2–1.6(mut)–1.2	110 ± 14 (4)	2610 ± 180	210 ± 40 (4)	3990 ± 650	−37 ± 1 (5)	7 ± 1	2.0 ± 0.1 (4)

Results recorded are presented as means ± S.E.M., *n*-values (same for τ_{1inact} and τ_{2inact}) are in brackets *, values are significant when compared to K_v1.4–1.2–1.6–1.2, $P < 0.05$ (Mann-Whitney *U* test).

The recovery from inactivation was studied with a step from −90 to 10 mV, using a variable interval-gapped pulse protocol (Fig. 3.6A). Analysis of the time dependence of recovery from inactivation (Fig. 3.6B, Table 3.1) revealed that this is significantly faster for K_v1.4–1.6–1.2–1.2 followed by K_v1.4–1.2–1.2–1.6, than that observed for K_v1.4–1.2–1.6–1.2 (Fig. 3.6B, Table 3.1), as a result of the removal of K_v1.4 N-type inactivation by the adjacently-placed K_v1.6 NIP. Likewise, the time dependence of recovery from inactivation for K_v1.4–1.6–1.2–1.2 was faster than that recorded for K_v1.4–1.2–1.2–1.2. On the other hand, the presence of a residual fast component in the K^+ current of K_v1.4–1.2–1.2–1.6 might be affecting the τ value for recovery due to the suboptimal adjacent positioning of K_v1.4 subunit to K_v1.6.

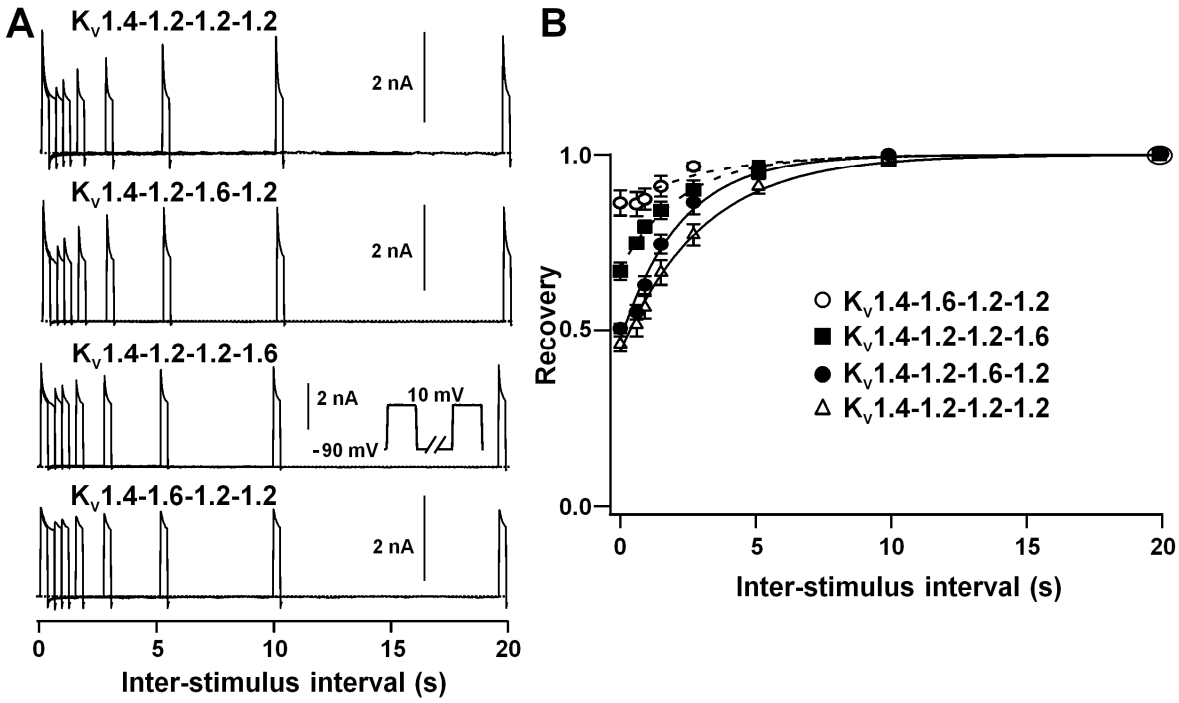

Fig. 3.6 Recovery from inactivation is faster when K_v1.6 is adjacent to K_v1.4 in the concatemers.

(A) Recovery from inactivation measured for K_v1.4-1.2-1.2-1.2, K_v1.4-1.2-1.6-1.2, K_v1.4-1.6-1.2-1.2 and K_v1.4-1.2-1.2-1.6, using variable interval-gapped pulse protocol (inset). (B) The resultant curves, fitted with a single exponential function show a significantly faster ($P < 0.05$, Mann-Whitney *U* test) recovery from inactivation for K_v1.4-1.6-1.2-1.2 (○, broken line) and Kv1.4-1.2-1.2-1.6 (■, broken line) than observed for the K_v1.4-1.2-1.6-1.2 channel (●,unbroken line). This is due to the removal of K_v1.4 N-type inactivation by the K_v1.6 NIP domain. Notice the slow recovery from inactivation for K_v1.4-1.2-1.2-1.2 (Δ, unbroken line) channel compared to K_v1.4-1.6-1.2-1.2. Some error bars fall within the data symbols; dotted lines indicate zero current. Data are summarized in Table 3.1. (n = 4-7).

3.5 Mutagenesis proved that attenuation of N-type inactivation by K_v1.6 is mediated by NIP

Having demonstrated modulation of the K_v1.4 NIB by K_v1.6 within concatenated hetero-tetramers of pre-determined ordering, it was necessary to ascertain if these observed effects are entirely attributable to the NIP domain. Mutagenesis of residues in the K_v1.6 α subunit identified previously as crucial for NIP function (Roeper et al., 1998), and replacing the

wild-type with mutated subunit (E27/30/32A), yielded $K_v1.4–1.2–1.6^{(E27/30/32A)}–1.2$ and $K_v1.4–1.6^{(E27/30/32A)}–1.2–1.2$ channels (Fig. 3.7).

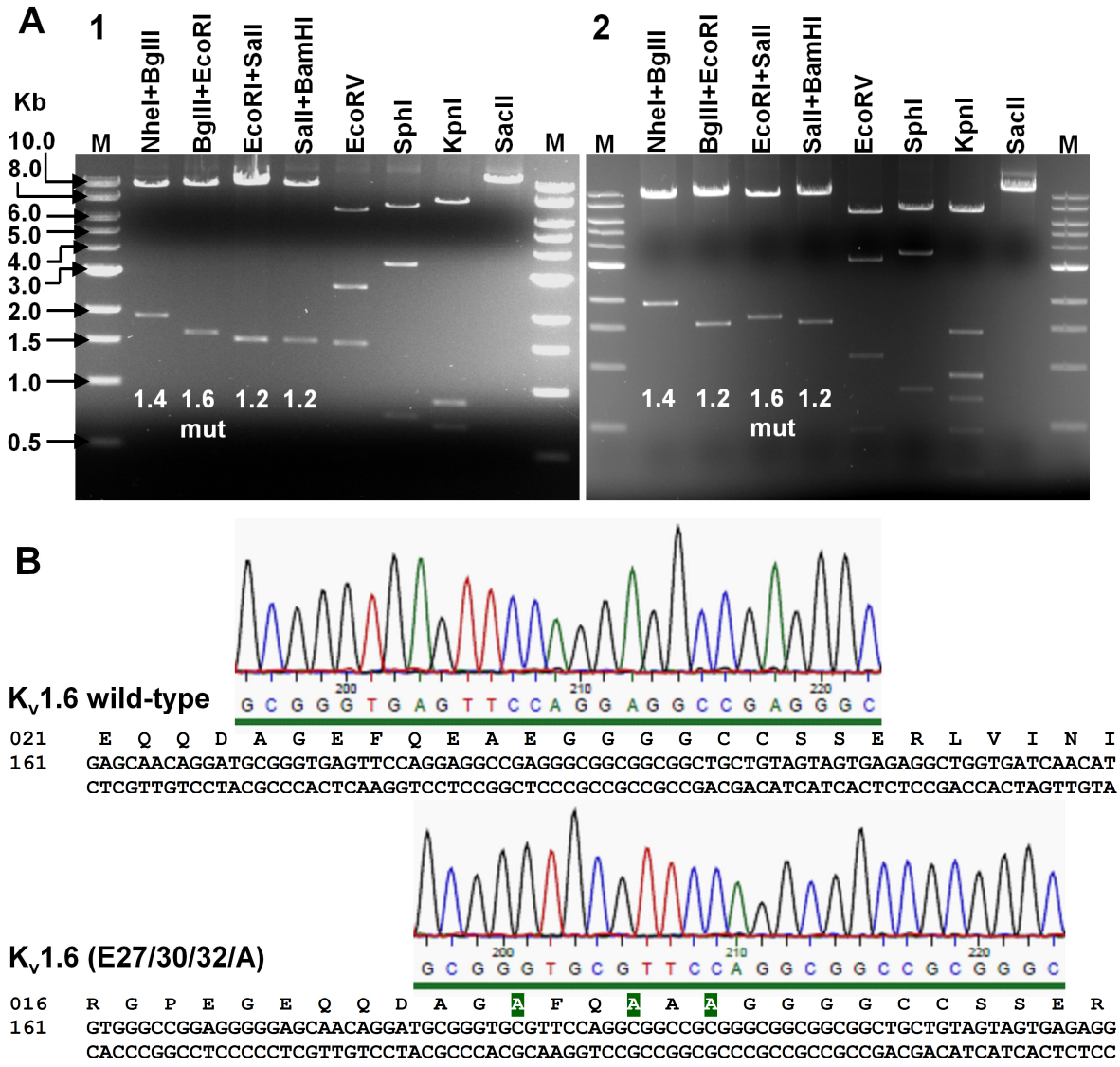

Fig. 3.7 Gene mapping of mutations created in $K_v1.6$ subunit of $K_v1.4$-containing hetero-tetramers.
(A) Position-specific restriction enzyme (NheI/BglII, BglII/EcoRI, EcoRI/SalI and SalI/BamHI) digestion of $K_v1.4–1.6mut–1.2–1.2$ (A1) and $K_v1.4–1.2–1.6mut–1.2$ (A2) released each subunit ($K_v1.4$, 1.6 or 1.2) in tetrameric constructs. EcoRV, SphI and KpnI are gene-specific restriction enzymes used to verify the presence of $K_v1.4$, 1.6 or 1.2 subunits in desired positions. A SacII site was deliberately introduced into mutant $K_v1.6$ gene which is absent from $K_v1.4$, 1.2 subunits and the pIRES2-EGFP vector (after digestion with NheI/BamHI). As expected, SacII linearized the tetramers containing the $K_v1.6$ mutant (A1 and A2). M, 1 Kb DNA ladder. (B) Analysis of $K_v1.6$

NIP mutant nucleotide sequence by DNA sequencing confirmed conversion of the codons for three glutamic acids at 27, 30 and 32, to alanine within the NIP domain. Sequences: Top line is amino acid sequence (numbering was given according to the published mRNA sequence). Middle (sense strand) and bottom (anti-sense strand) lines are of nucleotide sequences (numbering was generated by the sequencer during sequencing). A distinct colour was assigned to each nucleotide to identify their representative traces during sequencing.

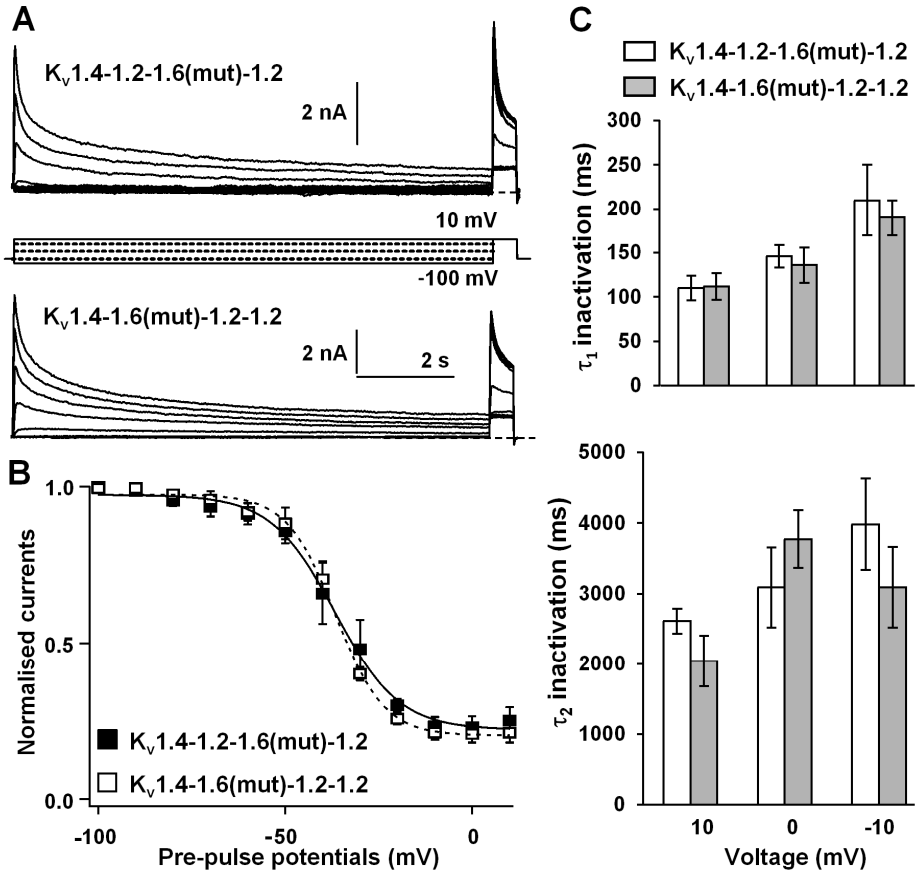

Fig. 3.8 Position-dependent functioning (K_v1.4 NIB attenuation) of K_v1.6 is NIP-mediated: replacement of K_v1.6 with a mutant form abolished NIP activity, thereby restoring rapid inactivation.

(A) Representative current traces for channels with mutated K_v1.6 (E27/30/32A) incorporated (K_v1.4-1.6-1.2-1.2 and K_v1.4-1.2-1.6-1.2) and expressed in HEK-293 cells. (B) Steady-state inactivation relationships obtained for these channels, fitted by a Boltzmann function [broken line for K_v1.4-1.6-1.2-1.2 (□) and unbroken line for K_v1.4-1.2-1.6-1.2 (■)], revealed near-identical profiles. (C) The bar diagrams summarize the τ_1 and τ_2 rates of inactivation of both channels observed at different potentials. Error bars represent means ± S.E.M. (n = 4-5).

Both tetrameric channels containing K_v1.6 NIP mutant decayed rapidly (Fig. 3.8A). These inactivation time courses are similar to those observed with heteromers containing distally arranged wild-type K_v1.6 (Fig. 3.8A, Table 3.1), confirming a complete loss of NIP function from K_v1.6 can be achieved either by mutation or distal positioning of the wild-type, each permitting fast inactivation of the K^+ current. Both mutated channels showed similar values of inactivation for τ_{1inact} and τ_{2inact} at the different potentials tested (Fig. 3.8C, Table 3.1) and similar to those observed for the fast inactivating channel, K_v1.4-1.2-1.6-1.2. This is attributable to the fast inactivation mediated by K_v1.4 subunit in each heteromer where NIP function is attenuated and has no discernible effect on the NIB moiety.

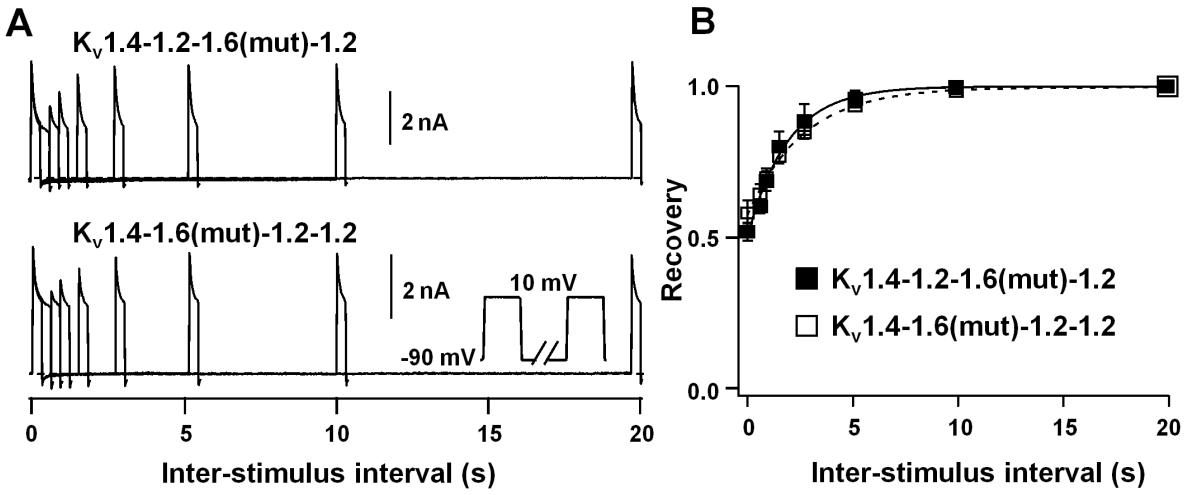

Fig. 3.9 Mutating residues critical for NIP interacting with NIB domain creates fast-inactivating channels, regardless of K_v1.4 and 1.6 subunit positioning in the concatemer.

(A) Typical currents showing recovery from inactivation of each hetero-tetramer fitted to a single exponential function. (B) When plotted, the average data for each channel, from at least four cells gave superimposable curves; some error bars fall within the data points. Error bars represent means ± S.E.M. (n = 4-5).

These results were supported by the observed restoration of voltage dependence for inactivation ($V_{1/2}$ −37 mV for both channels) and recovery from inactivation for either

channel containing the mutated K_v1.6 subunit (Fig. 3.8B, Fig. 3.9A and Fig. 3.9B) to values similar to that of K_v1.4–1.2–1.6–1.2 or K_v1.4–1.2–1.2–1.2 (Fig. 3.9B).These corroborative data highlight that only the NIP domain in K_v1.6 prevents fast inactivation, whose function is dependent on its position relative to the K_v1.4 subunit.

3.6 Discussion

3.6.1 Arrangements of K_v1α genes in constructs determine subunit positions in the expressed channels

The concatenation cloning platform was employed herein for expressing four α subunits as a single protein, with pre-determined subunit ordering relative to each other in the functional channels which were examined on the plasmalemma. Importantly, and in contrast with previous systems (Gagnon and Bezanilla, 2009), the use of inter-subunit linkers appears to have ensured retention of the behaviour of pre-positioned subunits as illustrated by NIP function observed for K_v1.6. Three such pre-assembled hetero-oligomers are presented, all with identical α subunit composition, but in different arrangements, containing a single K_v1.4 and 1.6 subunit plus two copies of K_v1.2. This offered the advantage over previous studies (Roeper et al., 1998) in allowing the effects of their positioning to be examined. Hetero-tetramers (K_v1.4–1.2–1.6–1.2, K_v1.4–1.6–1.2–1.2 and K_v1.4–1.2–1.2–1.6) elicited K^+ currents, with the first displaying significantly different inactivation properties to the other two. Such dissimilarity, together with the uniform nature of the currents produced by each concatenated tetramer, established that the gene arrangements in the constructs dictate subunit ordering. A fourth heteromer (K_v1.4–1.2–1.2–1.2) possessing a single K_v1.4 subunit with three copies of K_v1.2 was used as a control

for a fast-inactivating hetero-tetramer; its lack of $K_v1.6$ subunit results in the fastest inactivation kinetics in comparison with the other heteromers tested.

3.6.2 Subunit ordering reveals position dependency of NIP function

In this study, the subunit ordering and delivery of intact hetero-tetramers to the plasmalemma allowed the generation of channels that exhibit different types of inactivation by incorporating just one copy of $K_v1.4$ and 1.6, rather than two as examined previously (Roeper et al., 1998). Moreover, the concatenation of these subunits along with $K_v1.2$, combinations reported to coexist in the brain (Shamotienko et al., 1997), permitted elucidation of the importance of their ordering. The NIP in $K_v1.6$ proved functional only if placed immediately next to (position II or IV) its target $K_v1.4$ (position I) in the formed channel, yielding a slow-inactivating K^+ current. Positioning $K_v1.6$ distal to $K_v1.4$ (position III) led to N-type fast inactivation, presumably because NIP is not optimally positioned to appropriately antagonize the activity of NIB. Furthermore, the same fast inactivation kinetics were observed with NIP mutated forms of these channels, confirming that only the NIP domain is responsible for counteracting the function of NIB. Such position dependency of NIP activity could accord with a previous suggestion (Roeper et al., 1998) that this domain does not act by occupying the acceptor site for NIB, instead, interacting directly with the latter.

3.6.3 NIP, NIB and inactivation outcomes

It was of interest to consider the observed inactivation profiles in relation to occupancy (or not) by NIB of its receptor site on the S6 segment of the channel, because this mechanism is the basis of N-type inactivation (Hoshi et al., 1990; Zagotta et al., 1990; Tseng-Crank et

al., 1993). A reported inability of expressed homo-tetrameric $K_v1.6$ channel (Stuhmer et al., 1989; Roeper et al., 1998) to produce a fast-inactivating K^+ current implies that its NIP moiety is unable to bind to the inner pore, at least in a blocking fashion. It is noteworthy that the observed rates of fast inactivation for the mutated adjacent and distal concatemers are similar, indicative of the positioning of a non-functional NIP domain not impacting on their fast inactivation. Moreover, the fast inactivation behaviour of $K_v1.4–1.6^{(E27/30/32A)}–1.2–1.2$ channels showed clearly that NIP and NIB domains are directly interacting upon depolarization, mainly by probable electrostatic interactions before the NIB reaches its receptor, by an undefined mechanism (Roeper et al., 1998). One can speculate that conformational changes, initiated by the activation process, would be sensed by both charged motifs of the NIP and NIB domains facilitating their interaction. Positioning of both domains away from each other would prevent such interaction, as seen with both $K_v1.4–1.2–1.6^{(E27/30/32A)}–1.2$ and $K_v1.4–1.2–1.6–1.2$ channels. In situ hybridization and immuno-histochemical localization studies have suggested that $K_v1.2$, 1.4 and 1.6 proteins may coexist on the membranes of several types of central neurons in mammals (Veh et al., 1995; Shamotienko et al., 1997; Chung et al., 2005; Kim et al., 2007; Lee et al., 2009). In rat brain membranes, hetero-multimeric K_v1 channels of $K_v1.4$ and 1.6 subunits were co-immunoprecipitated using subunit-specific antibodies in immuno-affinity experiments (Shamotienko et al., 1997; Roeper et al., 1998). Collectively, these findings suggest that the gating contributions of $K_v1.4$ subunits can be modified by differential positioning of the NIP domain of $K_v1.6$ subunit in neuronal K_v1 channels. In co-expression studies, recombinant $K_v\beta1$ has been shown to confer rapid inactivation, via its distinct NIB domain, on all tested members of $K_v1\alpha$ subunits except $K_v1.6$, suggesting that $K_v\beta1$ subunit could also be an important modulator of K^+ channel complexes (Rettig et al., 1994; Heinemann et

al., 1996). In fact, the K_v1.2, 1.4, and 1.6 α subunits in rat brain membranes can be co-immuno-precipitated with K_vβ1 (Rhodes et al., 1997). These findings indicate that, in neurons, the gating of K_v1 heteromers can be modified by NIB/NIP domain(s) and/or auxiliary β1 subunits. In either case, the K_v1.6 subunit position in the heteromeric K_v1 channel could play a key role in tuning the inactivation process and, thus, shaping the firing pattern of the neuron. It is tempting to speculate on the functional relevance of NIP action in diseased states. Seizure activity in an animal model has been linked to the spatio-temporal changes in the expression of the K_v1 subfamily within the hippocampus (Lee et al., 2009), where the levels of delayed rectifier K_v1 channels (including K_v1.2 and K_v1.6) are reduced with minor changes in K_v1.4. This curious alteration might be a physiological response to seizure events in which K_v1.4 inactivation by NIP gets diminished, thereby dampening unwanted depolarizations during attacks. Extensive investigations would have to be performed to assess the *in vivo* functional implications of NIP and its placement within native hetero-tetramers.

It is clear from the results presented herein that: (a) concatenation of K_v1 subunits results in the predicted assembly of functional channels at the plasmalemma; (b) subunit ordering crucially influences channel properties; (c) stoichiometry alone is not sufficient for predicting the characteristics of native channels and (d) NIP–NIB interaction(s) occur at a site distinct from that of the NIB-binding site in the inner portion of the ion pore.

CHAPTER 4

RESULTS

Stiochiometry and positioning of α subunits influence the biophysical and pharmacological profiles of K_v1.1- and 1.2-containing channels

4.1 Overview

In K_v1 channels susceptible to blockade by TEA, all four subunits make an energetic contribution to binding a single TEA molecule at the extracellular mouth, where an aromatic residue in the pore-forming region is required for high sensitivity (MacKinnon and Yellen, 1990; Kavanaugh et al., 1991; Heginbotham and MacKinnon, 1992; Kavanaugh et al., 1992). TEA sensitivity is mainly due to the presence in K_v1.1 of the critical residue (Y379, Kavanaugh et al., 1991), whereas K_v1.2 homo-tetrameric channel that has valine (V381) at the equivalent location (Fig. 4.1) is only feebly inhibited by TEA. Even though the TEA sensitivity of adjacently- and diagonally-positioned K_v1.1 and 1.2 subunits in K_v1 channels is different (Al-Sabi et al., 2010), earlier studies had deduced that only the stoichiometry of these α subunits and not their arrangement influences the susceptibility to TEA (Hurst et al., 1992; Shen et al., 1994). Clarification of this important question was sought herein by establishing if inhibition of K^+ currents by TEA is affected by varying the number and position of sensitive K_v1 subunits tandem-linked within tetramers. This strategy allows pre-determination of not just the combinations of α subunits but, also, their actual arrangements in the channels trafficked to the plasmalemma (Al-Sabi

et al., 2010). As a major aim of this investigation was to establish the optional positioning within tetrameric channels of residues that contribute to TEA sensitivity, the tyrosine known to be essential in $K_v1.1$ was substituted initially into $K_v1.2$ at position 381 and/or together with a R354A mutation to make it more like the highly susceptible $K_v1.1$ subunit (Fig. 4.1). In the first instance, $K_v1.1$ and 1.2 homomeric channels were used for this purpose because concatenation has been shown not to alter their blockade by TEA (Al-Sabi et al., 2010). Further mutation(s) in selected pore-aligned residue(s) of the first $K_v1.2$ α subunit in $K_v1.2$-1.2-1.1-1.2 were introduced to evaluate their effects on the channels' biophysical and pharmacological profiles.

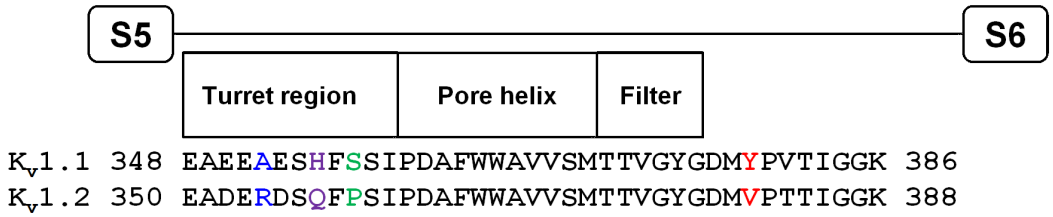

Fig. 4.1 Amino acid sequence alignment of turret, pore helix and filter regions of $K_v1.1$ and 1.2. Colour highlighted amino acids in $K_v1.2$ mutated to the highlighted sequence in $K_v1.1$.

4.2 Pre-defined $K_v1.1$ and 1.2 α gene cassettes assembled into pIRES2-EGFP plasmid in position-specific arrangements

Concatenation of K_v1 genes in a single open reading frame (ORF) was carried out to facilitate their expression as functional channels on the surface of HEK-293 for examination of their biophysical and pharmacological properties. Tetrameric constructs encoding $K_v1.1$-1.2-1.1-1.1, $K_v1.2$-1.2-1.1-1.1 and $K_v1.2$-1.2-1.1-1.2 (Fig. 4.2A and B) were engineered, using an inter-subunit linker derived from the *Xenopus* β-globin gene and paired restriction sites (Al-Sabi et al., 2010). $K_v1.1$-1.2-1.1-1.1 channel is expected to be TEA sensitive, as $K_v1.1$ subunits at position I and III should form a diagonal arrangement

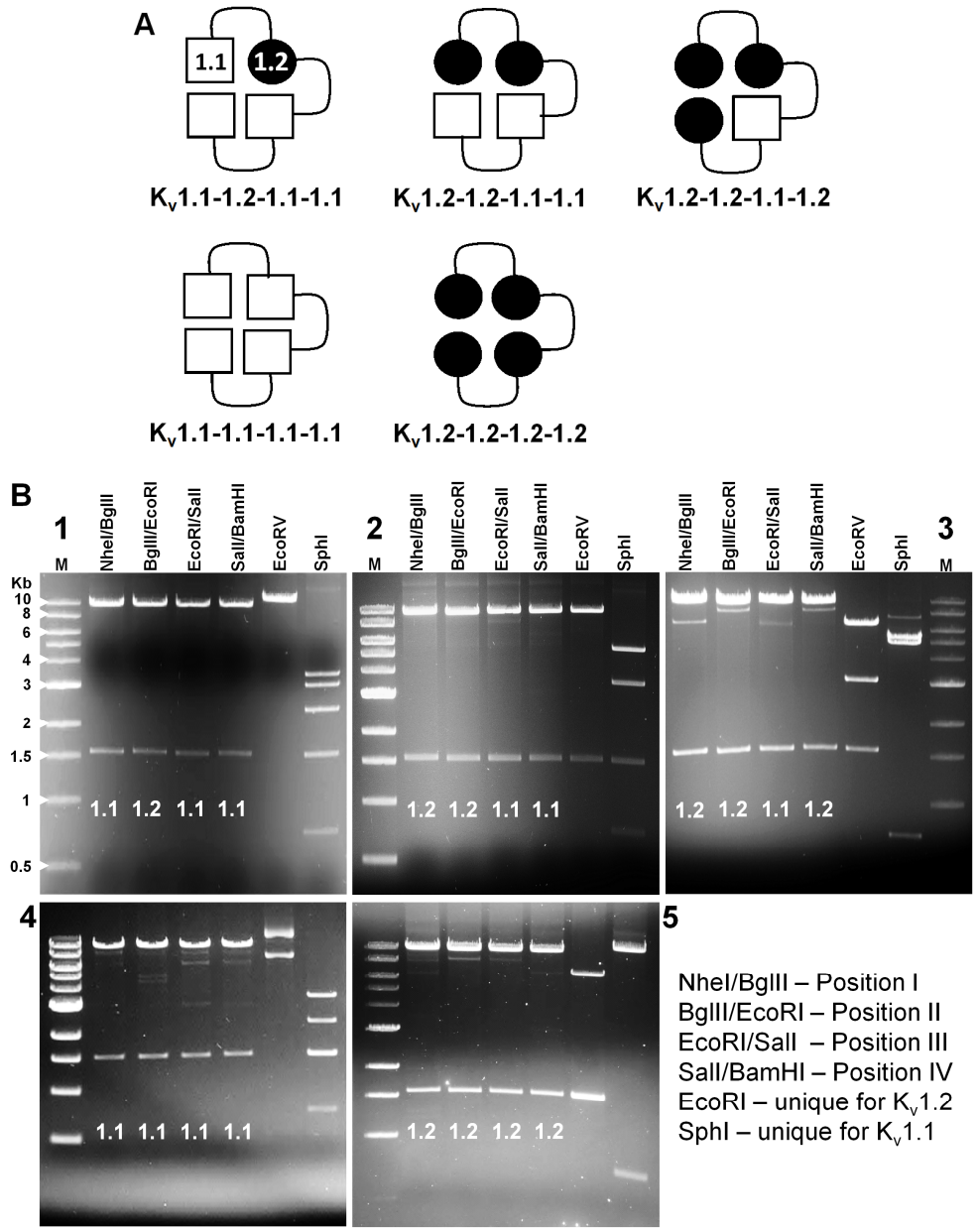

Fig. 4.2 Overview of K_v1.1 and 1.2 concatenated tetrameric constructs used in this study, and sequential release of constituents from representative K_v1.X tetramers.

(A) Concatenated constructs of Kv1 subunit genes in pre-defined positions predicted for the expressed proteins. (B) Tetrameric DNA constructs K_v1.1-1.2-1.1-1.1 (B1), K_v1.2-1.2-1.1-1.1 (B2), K_v1.2-1.2-1.1-1.2 (B3), K_v1.1-1.1-1.1-1.1 (B4) and K_v1.2-1.2-1.2-1.2 (B5) digested with position-specific enzymes (NheI/BglII, BglII/EcoRI, EcoRI/SalI and SalI/BamHI) released K_v1.1 or K_v1.2 subunits (~1.5 Kb), along with the half-linkers and restriction enzyme sites (RES) as seen in the agarose (0.85%) gel electrophoretograms. EcoRV and SphI are unique RES in K_v1.2 or K_v1.1 subunits, respectively and, thus, used to verify the presence of either K_v1.2 or K_v1.1 in tetrameric constructs. M, 1 Kb DNA ladder.

postulated to be preferential for high affinity TEA binding (Al-Sabi et al., 2010), with an additional K_v1.1 subunit in the fourth position. Addition of K_v1.2 to position I resulted in K_v1.2-1.2-1.1-1.1, a channel less sensitive to TEA as equal copies of K_v1.1 and 1.2 were placed adjacently (Al-Sabi et al., 2010). On the other hand, K_v1.2-1.2-1.1-1.2 channel (Fig. 4.2A and B) was chosen because it shares with the latter identical subunits in the second and third positions, but having three copies of K_v1.2 that would be expected to make this channel relatively insensitive to TEA. Homo-tetrameric K_v1.1 and 1.2 channels were utilized as positive and negative controls, respectively.

Desired position-specific alignment and orientation of K_v1 subunit gene(s) in all the constructs built herein were confirmed by restriction digestion with position-specific (NheI/BglII, BglII/EcoRI, EcoRI/SalI and SalI/BamHI) and gene-specific (EcoRV and SphI) restriction enzymes (Fig. 4.2B), respectively. In addition, correct nucleotide sequences of the constructs used in this study were confirmed by DNA sequencing.

4.3 Characteristics of concatenated gene constructs expressed in HEK-293 cells

HEK-293 cells were transiently-transfected with homo- or hetero-tetramers (K_v1.1-1.1-1.1-1.1, K_v1.1-1.2-1.1-1.1 and K_v1.2-1.2-1.2-1.2), and surface biotinylated (c.f. Fig. 2.3; see Material and Methods) to establish that the channels were expressed and delivered to the plasma membrane as concatenated intact protein. The analysis of cell lysates by SDS-PAGE and Western blotting with subunit-specific antibodies K_v1.1 or 1.2 visualised proteins with Mr of ~240 K (Fig. 4.3). This confirms that the concatenated strategy recombinantly built single chain homomeric or heteromeric channels as desired.

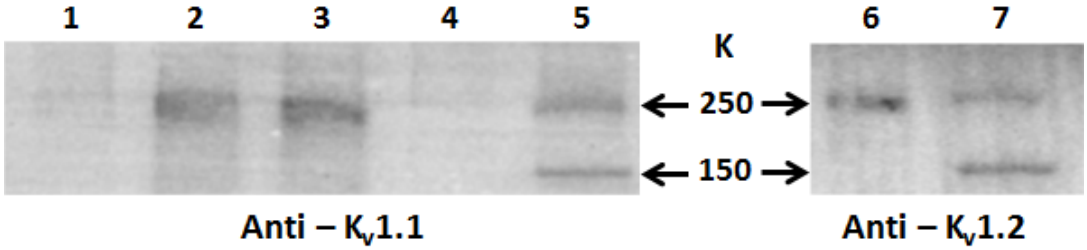

Fig. 4.3 Surface biotinylation of mammalian cells transfected with concatenated K_v1 channel α genes demonstrated expression on the cells surface of intact proteins with the expected size of tetramers.
Transiently-transfected HEK-293 cells were surface biotinylated before being solubilized with 1% Triton X-100. Surface proteins were isolated from these lysates with streptavidin-agarose beads and run on SDS-PAGE (12%) acrylamide gel before being analyzed by Western blotting, using specific antibodies for Kv1.1 (lanes 1-4), or $K_v1.2$ (lane 6). Lanes: (1) non-transfected cells, (2) $K_v1.1$-1.1-1.1-1.1 (3) $K_v1.1$-1.2-1.1-1.1, (4 and 6) $K_v1.2$-1.2-1.2-1.2. Protein markers are indicated in lanes 5 and 7.

4.4 Homomeric $K_v1.2$ channel is made susceptible to TEA by the V381Y mutation, yet a $K_v1.1$ tetramer is more sensitive to TEA

Homomeric K_v1 channels comprising four copies of either $K_v1.1$, 1.2 or mutated forms of $K_v1.2$ subunits were evaluated for their TEA sensitivities compared with heteromeric channels made of different combination of these subunits. The homomeric $K_v1.1$ channel proved >300-fold more sensitive to TEA than its $K_v1.2$ counterpart, as shown by the dose-response curves obtained by Qpatch recordings (Fig. 4.4) and corresponding IC_{50} values (Table 4.1). The latter accord with those reported for $K_v1.1$ and 1.2 homomers expressed in *Xenopus* and mammalian cells (Kavanaugh et al., 1991; Grissmer et al., 1994; Gutman et al., 2005).

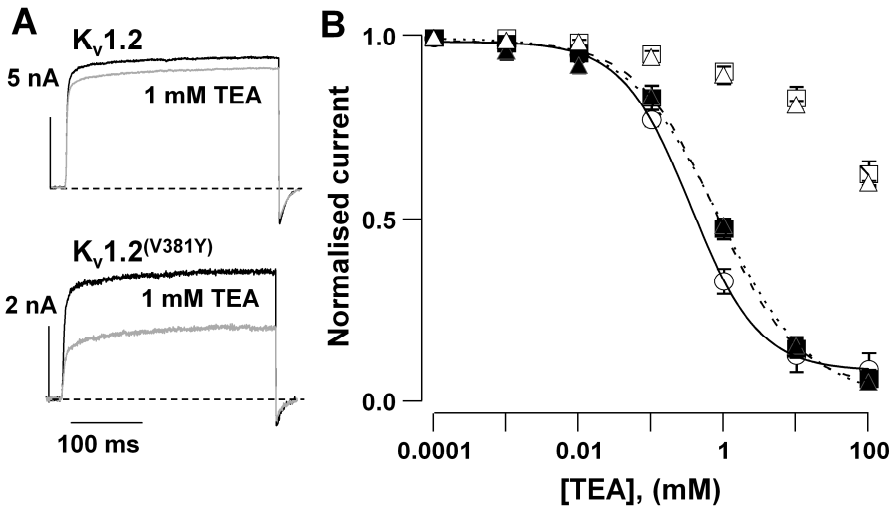

Fig. 4.4 Delayed rectifier channel currents of wild-type and mutated monomeric $K_v1.2$.

(A) Representative current traces from $K_v1.2$ homomeric channel and mutated form $K_v1.2$(V381Y) in the absence (black traces) and presence (grey traces) of 1 mM TEA. (B) Dose-response curves for the $K_v1.2$ homomeric (□) and $K_v1.2$(R354A) (△) channels display little inhibition whereas $K_v1.2$(V381Y) (■), $K_v1.2$(V381Y/R354A) (▲) and $K_v1.1$ homomer (○) show increasing susceptibility to TEA. Some of the error bars fall within the data points. (n = 4-7).

TEA susceptibility of the $K_v1.2$ channel was enhanced greatly when valine 381 is replaced by tyrosine [($K_v1.2^{(V381Y)}$); for position of the mutation, see Fig.4.5, and Fig. 4.6] as revealed in representative current traces (Fig. 4.4A) and TEA dose-response curves (Fig. 4.4B), with the difference in sensitivity being reduced to 2-fold compared to $K_v1.1$ (Table 4.1).

Table 4.1 IC_{50} values for TEA inhibition of wild-type and mutated forms of homomeric $K_v1.1$ and 1.2 channels expressed in HEK-293 cells

Channel	$K_v1.1$	$K_v1.2$ (V381Y)	$K_v1.2$ (R354A/V381Y)	$K_v1.2$ (R354A)	$K_v1.2$
IC_{50} [mM]	0.35 ± 0.02 (5)	*0.8 ± 0.04 (6)	*0.87 ± 0.16 (4)	>100 (4)	>100 (7)

Results are means ± S.E.M., *n* replicates are in parenthesis. * P < 0.01 values are significant compared to $K_v1.1$ (unpaired Student's *t*-test).

As the TEA sensitivity of $K_v1.2^{(V381Y)}$ channel does not exactly match that of $K_v1.1$ homomer (Table 4.1, $P < 0.01$ unpaired *t*-test), this might be due to the effect of other pore residues that differ between $K_v1.1$ and 1.2. Nevertheless, $K_v1.2^{(R354A)}$ channel showed unaltered insensitivity, comparable to that of $K_v1.2$ (Fig. 4.4, Table 4.1); moreover, when that mutation was combined with V381Y [$K_v1.2^{(R354A/V381Y)}$], it gave a TEA value similar to that of the $K_v1.2^{(V381Y)}$ channel (Table 4.1); thus, $K_v1.2^{(R354A)}$ mutation alone was excluded from further study herein, though it should be noted that this residue affects the binding of peptide toxin blockers (Visan et al., 2004).

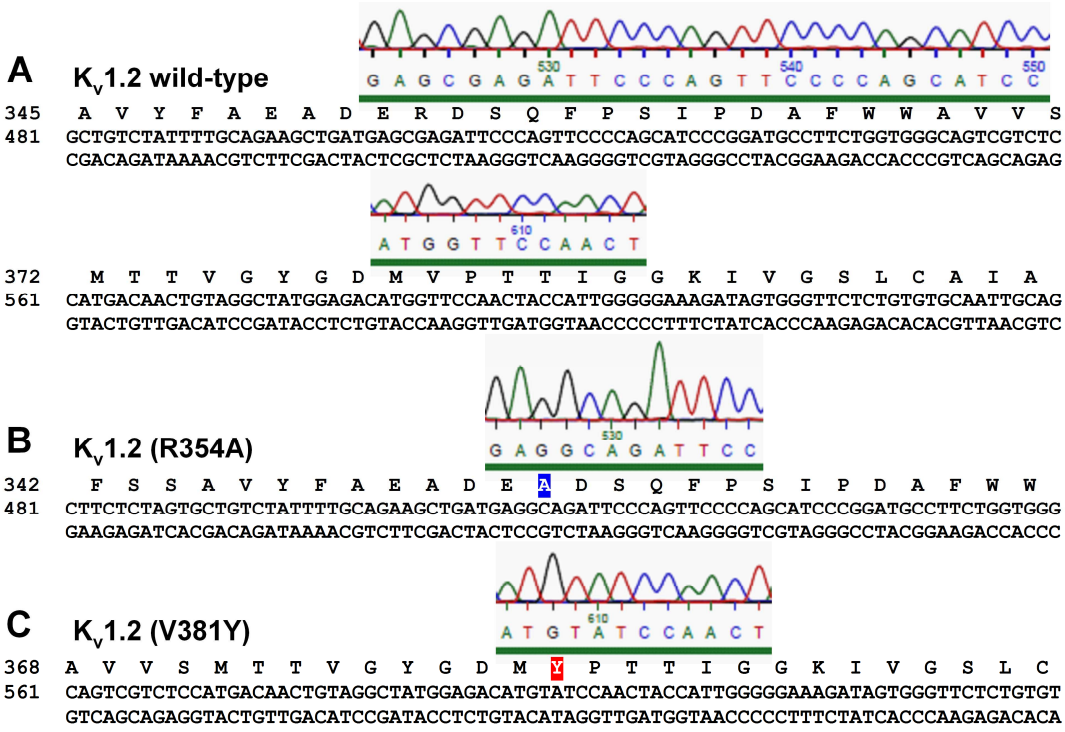

Fig. 4.5 Nucleotide sequencing shows the expected change of encoded amino acids resulting from mutations introduced in $K_v1.2$ gene.

Wild type monomeric $K_v1.2$ subunit (A) was mutated in the pore-region using site-directed mutagenesis and cloned into expression vector (pIRES2-EGFP) to generate mutated $K_v1.2$ channel subunits - (valine 381 to tyrosine - $K_v1.2$(V381Y) (B) and arginine 354 to alanine - $K_v1.2$(R354A) (C). Position I specific $K_v1.2$ subunit carrying mutation (V381Y) was incorporated into tetrameric constructs containing $K_v1.1/1.2$ subunits (Fig. 4.6). Sequences: Top line is amino acid sequence (numbering was given according to the published mRNA sequence). Middle (sense strand) and bottom (anti-sense strand) lines are of nucleotide sequences (numbering was generated by the

sequencer during sequencing). A distinct colour was assigned to each nucleotide to identify their representative traces during sequencing.

The information acquired at this stage provided a logical basis for using the K_v1.1 and 1.2 genes to build the hetero-tetramers of different combinations and to introduce selected mutants of K_v1.2 at the first position in some variants, with the purpose of ascertaining the effects of positioning of these subunits and mutants on the channels' overall sensitivity to TEA.

4.5 Different compositions of K_v1.1/1.2-containing heteromers give I_K with distinct voltage-dependence of activation kinetics

K_v1 heteromers were generated and their voltage-dependencies of activation were examined by conventional whole-cell patch-clamp recordings, after HEK-293 cells had been transfected separately with concatenated constructs built from different combinations of K_v1.1 and 1.2 subunits. As sequence alignment of the pore regions shows these monomers to be highly conserved, except in particular locations at the turret region and nearby the selectivity filter (see Fig. 4.1), selected mutation(s) (Fig. 4.6) were introduced at the first position of K_v1.2-1.2-1.1-1.2 channel and their influences on conductance-voltage relationship (g_K-V) examined (Fig. 4.7). All these K_v1 concatemers showed delayed rectifying outward K_v currents (I_K) when subjected to a depolarizing voltage step; representatives are displayed in Fig. 4.7A. The g_K-V profile of each concatenated hetero-tetrameric channel could be well fitted by a single Boltzmann function (Fig. 4.7B).

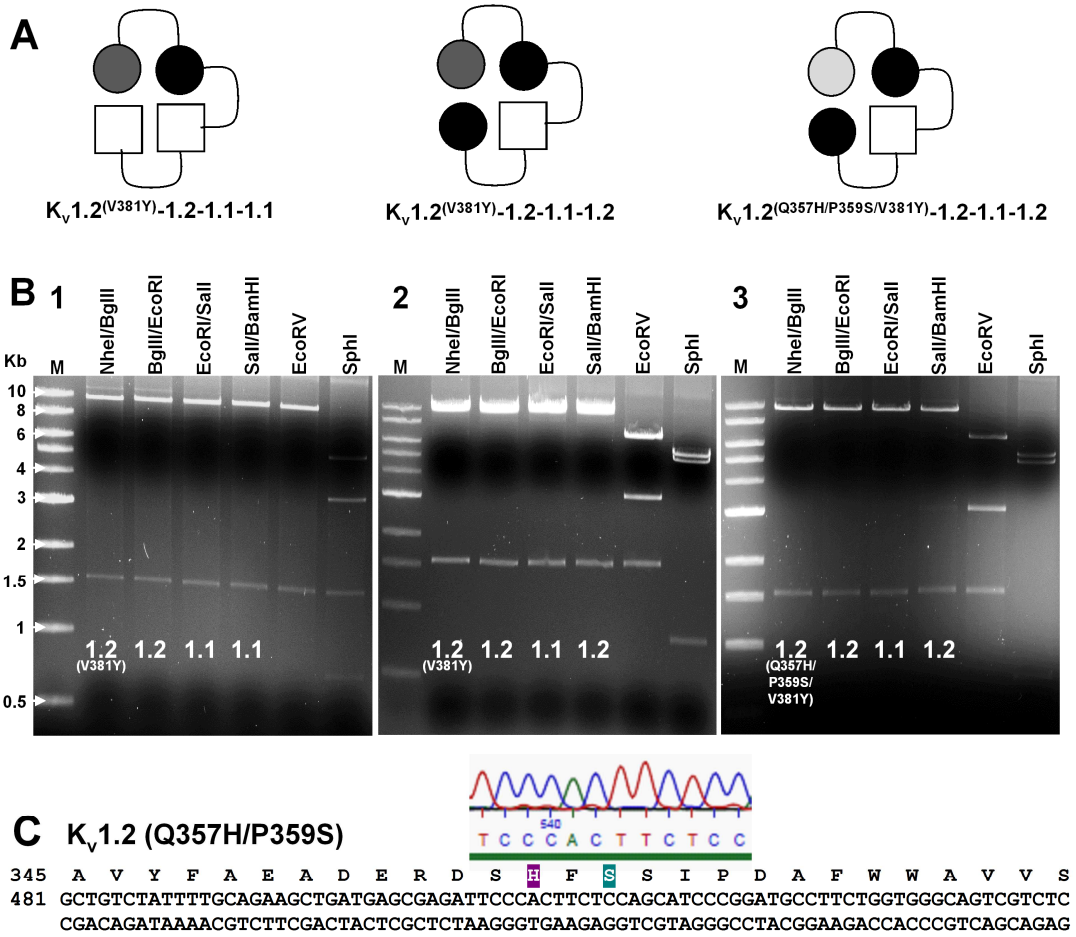

Fig. 4.6 Created $K_v1.1/1.2$-containing channels varying in stoichiometry carried mutation (s) in $K_v1.2$ cloned at first position of a tetramer.

(A) Schematic of predicted expressed proteins with mutant $K_v1.2$ subunit in a tetramer (B) NheI/BglII, BglII/EcoRI, EcoRI/SalI and SalI/BamHI digested $K_v1.1/1.2$ constructs containing $K_v1.2$ mutant subunit: $K_v1.2$(V381Y)-1.2-1.1-1.1 (B1), $K_v1.2$(V381Y)-1.2-1.1-1.2 (B2) and $K_v1.2$(Q357H/P359S/V381Y)-1.2-1.1-1.2 (B3) released position-specific subunits. $K_v1.1$ and 1.2 subunits were verified by gene-specific enzymes SphI and EcoRV, respectively. As seen in agarose (0.85%) gel electrophoretogram, a band at ~1.5 Kb represents the $K_v1.1$ or 1.2 gene along with half-linkers and restriction enzyme sites. M, 1 Kb DNA ladder. (C) DNA sequencing confirmed the mutation of turret region amino acids, glutamine 357 and proline 359 of $K_v1.2$ to histidine and serine, respectively. Sequences: Top line is amino acid sequence (numbering was given according to the published mRNA sequence). Middle (sense strand) and bottom (anti-sense strand) lines are of nucleotide sequences (numbering was generated by the sequencer). A distinct colour was assigned to each nucleotide to aid their identification.

As predicted, concatenated homo-tetrameric $K_v1.1$ channel yielded a I_K current with the most negative $V_{1/2}$ value (Table 4.2), which is indistinguishable from its non-concatenated counterpart ($V_{1/2}$ = -30 ± 1, n = 13; Al-Sabi et al., 2010). On the other hand, concatenated $K_v1.2$ channel activated at more depolarised potentials and revealed, as expected, the most positive $V_{1/2}$ value (Table 4.2), similar to the value for homomeric $K_v1.2$ channel ($V_{1/2}$ = -2 ± 1, n = 7). This indicates that the concatenation did not affect the voltage-dependence of activation of the tetrameric channels tested, for homo-tetramers at least. Previously, heteromeric channels with similar composition but different subunit positioning ($K_v1.2$-1.2-1.1-1.1 and $K_v1.1$-1.2-1.1-1.2) were found to have similar biophysical characteristics (Al-Sabi et al., 2010), albeit different $V_{1/2}$ values (Table 4.2).

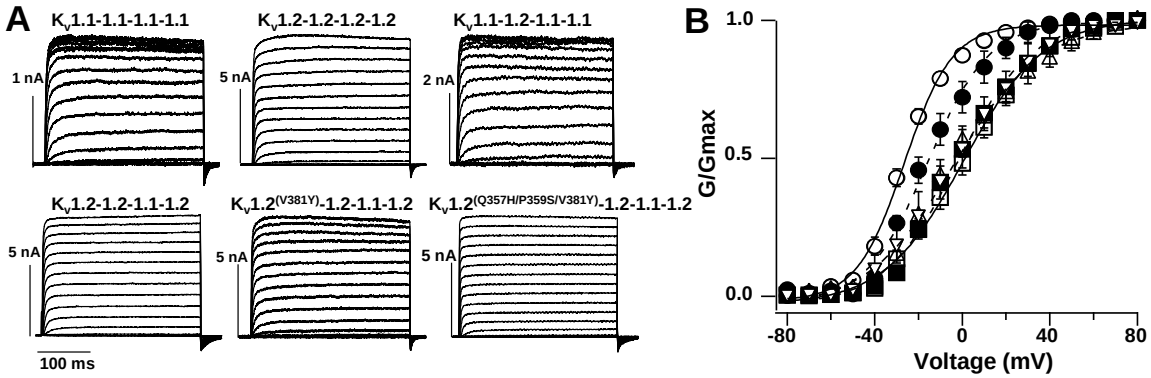

Fig. 4.7 Biophysical profiles of tetramers distinct in their subunit composition.

(A) Representative current traces recorded from transfected HEK-293 cells by conventional patch-clamp, in response to depolarising steps from -80 to 80 mV in 10 mV increments. (B) Conductance-voltage relationship of the steady state currents calculated from -82 mV reversal potential after 200 ms at indicated voltages; Boltzmann fits of the data for concatenated homomeric Kv1.1 (○) and Kv1.2 (□), Kv1.1-1.2-1.1-1.1 (●), Kv1.2-1.2-1.1-1.2 (■), Kv1.2(V381Y)1.2-1.1-1.2 (△) and Kv1.2 (Q357H/P359S/V381Y)-1.2-1.1-1.2 (▽) channels. Some of the error bars fall within the data points. (n = 4-7).

The 3 copies of $K_v1.1$ subunits in $K_v1.1$-1.2-1.1-1.1 shifted the channel's $V_{1/2}$ toward less negative potentials than $K_v1.1$ channel (Fig. 4.7B, Table 4.2); likewise even one copy of $K_v1.2$ in $K_v1.1$-1.2-1.1-1.1 is enough to exert such a shift in $V_{1/2}$ from that of $K_v1.1$-1.1-1.1-1.1 concatemer ($P < 0.001$, Mann-Whitney *U* test, Table 4.2).

However, $K_v1.2$-1.2-1.1-1.1 with 2 copies of each subunit showed a further but not significant shift in $V_{1/2}$ value compared to $K_v1.1$-1.2-1.1-1.1. Three $K_v1.2$ subunits in $K_v1.2$-1.2-1.1-1.2 channel produced a I_K current with a $V_{1/2}$ close to the value of tandem-linked $K_v1.2$-1.2-1.2-1.2 (Fig. 4.7B, Table 4.2); hence, one copy of $K_v1.1$ in the tetramer causes just a minor shift in $V_{1/2}$ from that of $K_v1.2$-1.2-1.2-1.2. Hence, the shifts in $V_{1/2}$ values observed are directly influenced by the number of identical subunits in the tetramers.

Table 4.2 Votage-dependace of activation of K_v1 concatanated heteromers and mutants compared with their tandem-linked parental homomers

Parameter	$K_v(1.1)_4$	$K_v1.1$-1.2-1.1-1.1	$K_v1.1$-1.2-1.1-1.2	$K_v1.2$-1.2-1.1-1.1	$K_v1.2$-1.2-1.1-1.2	$K_v1.2^{(V351Y)}$-1.2-1.1-1.2	$K_v1.2^{(Q357H/P359S/V351Y)}$-1.2-1.1-1.2	$K_v(1.2)_4$
$V_{1/2}$	-32 ± 1	*-20 ± 1	†*-22 ± 1	†*-18 ± 1	*-2 ± 1	*-4 ± 2	*-3 ± 1	*-1 ± 1
k (mV)	12 ± 1 (5)	16 ± 1 (4)	11 ± 1 (7)	12 ± 1 (14)	17 ± 1 (4)	20 ± 2 (5)	21 ± 1 (5)	19 ± 1 (5)

Results are represented as means ± S.E.M., *n* replicates are in parenthesis. *$P < 0.001$ values are significant compared to $K_v(1.1)_4$ (Mann-Whitney *U* test). † Data taken from Al-Sabi et al., 2010.

In contrast, tetramers having the same subunit compositions and positioning ($K_v1.2$-1.2-1.1-1.2) but with a selected pore mutation ($K_v1.2^{(V381Y)}$-1.2-1.1-1.2) (Fig. 4.6A and B) gave a similar $V_{1/2}$, close to that for homomeric $K_v1.2$-1.2-1.2-1.2 channel (Fig. 4.7A and B). Additional mutations at the turret region of that channel arrangement

($K_v1.2^{(Q357H/P359S/V381Y)}$-1.2-1.1-1.2) (Table 4.2) failed to significantly shift the $V_{1/2}$ compared to that of the wild-type, apparently because these mutations are not involved in the gating of this K_v1 channel.

Clearly, these results indicated that subunit composition of these concatenated channels affects their biophysical properties, namely the voltage-dependence of activation.

4.6 TEA sensitivities of K_v1 concatemeric channels are affected by altering their subunit composition or introducing a selective pore mutation

While tandem-linked homo-tetrameric $K_v1.1$ channel showed similar TEA sensitivity to their homomeric counterparts (Fig. 4.8A, Table 4.1 and 4.3), replacing one of its subunits with an insensitive $K_v1.2$ constituent to produce $K_v1.1$-1.2-1.1-1.1 resulted in a significant 3-fold drop in TEA sensitivity (IC_{50}) compared to that of $K_v1.1$-1.1-1.1-1.1 (Fig. 4.8A and B, Table 4.3, $P < 0.01$, un-paired *t*-test).

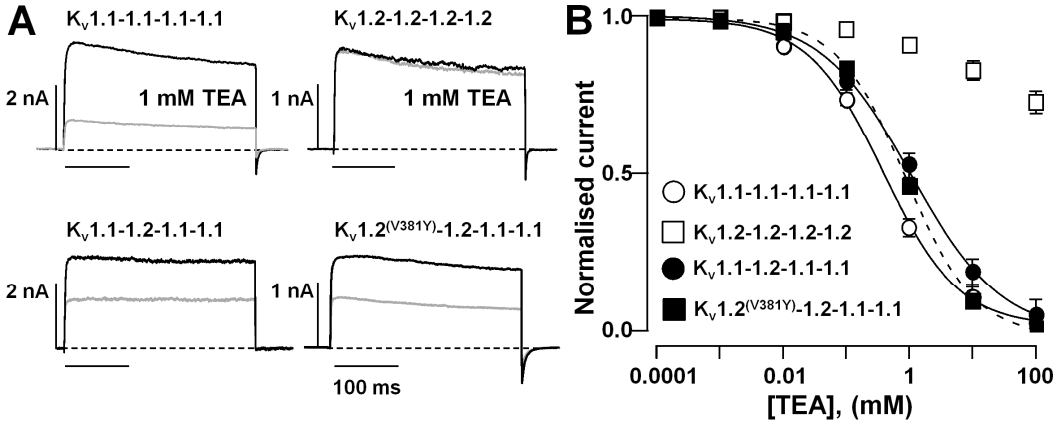

Fig. 4.8 Current traces of $K_v1.1/1.2$-containing hetero-tetrameric channels in the absence or presence of TEA.

(A) Representative current traces from QPatch recordings in the absence (black traces) and presence (grey traces) of 1 mM TEA. (B) Dose-response curves for $K_v1.2$-1.2-1.2-1.2 (□), $K_v1.1$-1.2-1.1-1.1 (●), $K_v1.2$(V381Y)-1.2-1.1-1.1 (■) and $K_v1.1$-1.1-1.1-1.1(○) in order of increase susceptibility to TEA. Some of the error bars fall within the data points. (n = 5-8).

A similar shift in TEA susceptibility could be achieved by mutating the first insensitive subunit, $K_v1.2^{(V381Y)}$-1.2-1.1-1.1 (Fig. 4.8A and B, Table 4.3), with an IC_{50} of ~1 mM. Furthermore, K_v1.2-1.2-1.1-1.2, with a single K_v1.1 subunit at the third position gave a I_K current insensitive to TEA (Fig. 4.10A); its IC_{50} was indistinguishable from that of K_v1.2-1.2-1.2-1.2 channel (Fig. 4.8, Table 4.3), indicating that one copy of K_v1.1 subunit is insufficient for TEA co-operative binding.

Table 4.3 IC_{50} values for inhibition by TEA of wild-type and mutated forms of K_v1 concatenated tetramers

Channel	**IC_{50} [mM]**
K_v1.1-1.1-1.1-1.1	0.39 ± 0.1 (8)
K_v1.1-1.2-1.1-1.1	*1.1 ± 0.1 (6)
§K_v1.1-1.2-1.1-1.2	*0.9 ± 0.1 (8)
§K_v1.2-1.2-1.1-1.1	8 ± 1 (4)
K_v1.2-1.2-1.1-1.2	> 100 (4)
K_v1.2-1.2-1.2-1.2	> 100 (7)
$K_v1.2^{(V381Y)}$-1.2-1.1-1.1	*0.9 ± 0.1 (5)
$K_v1.2^{(V381Y)}$-1.2-1.1-1.2	> 100 (4)
$K_v1.2^{(V381Y)}$-1.2-1.2-1.1	9 ± 1 (6)
$K_v1.2^{(Q357H/V381Y)}$-1.2-1.1-1.2	> 100 (4)
$K_v1.2^{(Q357H/P359S/V381Y)}$-1.2-1.1-1.2	> 100 (5)

Results are represented as means ± S.E.M., *n* replicates are in parenthesis. * ($P < 0.01$) values are significant compared to K_v1.1-1.1-1.1-1.1, (unpaired Student's *t*-test); § data are taken from (Al-Sabi et al., 2010) for comparison.

Collectively, these results indicate that the pharmacological profile of K_v1 tetramers can be altered by changing the stoichiometry of subunits (e.g. by increasing the number of TEA

sensitive subunits) or by selected mutation of $K_v1.2$ in the first position of certain heteromers.

4.7 Mutating a $K_v1.2$ in its pore region does not induce TEA sensitivity into $K_v1.2$-1.2-1.1-1.2 unless the $K_v1.1$ is arranged adjacently to the mutated $K_v1.2$

In the next experiments, the stoichiometry of the subunits was kept equal with the first subunit mutated to $K_v1.2^{(V381Y)}$ in the expectation of increasing the channel's susceptiblity to TEA [i.e. to that of the diagonally-arranged ($K_v1.1$-1.2-1.1-1.2) channel reported previously (Al-Sabi et al., 2010) (see Table 4.3)]. Surprisingly, the I_K produced by $K_v1.2^{(V381Y)}$-1.2-1.1-1.2 channel proved to be TEA-insensitive (IC_{50} > 100) and, therefore, remained similar to its wild-type (Fig. 4.10A and B, Table 4.3).

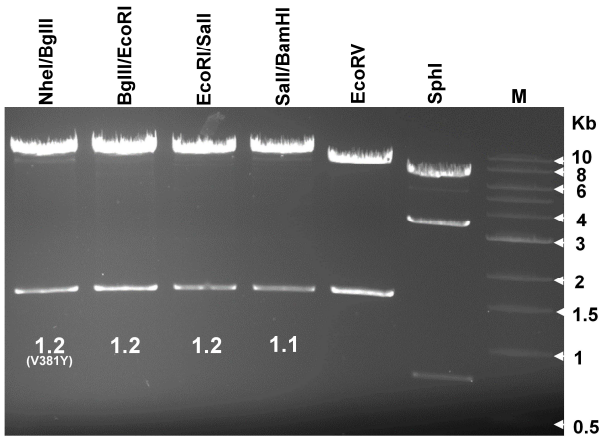

Fig. 4.9 Restriction digestions showing the subunits released from the mutated hetero-tetrameric DNA construct.

$K_v1.2$(V381Y)-1.2-1.2-1.1 gene construct was made by positioning $K_v1.1$ gene adjacent to $K_v1.2$(V381Y) nucleotide sequence. Positioning of $K_v1.1$ and 1.2 genes in the concatemer were confirmed by position-specific and gene-specific enzyme digestion followed by agarose gel electrophoresis. A band at ~1.5 Kb represents the $K_v1.1$ or $K_v1.2$ gene along with half-linkers and restriction enzyme sites. M, 1 Kb DNA ladder.

This unexpected observation was further investigated by inserting additional mutations, resembling their equivalents in $K_v1.1$ subunit at the turret region (see Fig. 4.1), $K_v1.2^{(Q357H/V381Y)}$-1.2-1.1-1.2 and $K_v1.2^{(Q357H/P359S/V381Y)}$-1.2-1.1-1.2, but these also gave I_K currents resistant to TEA (Table 4.2).

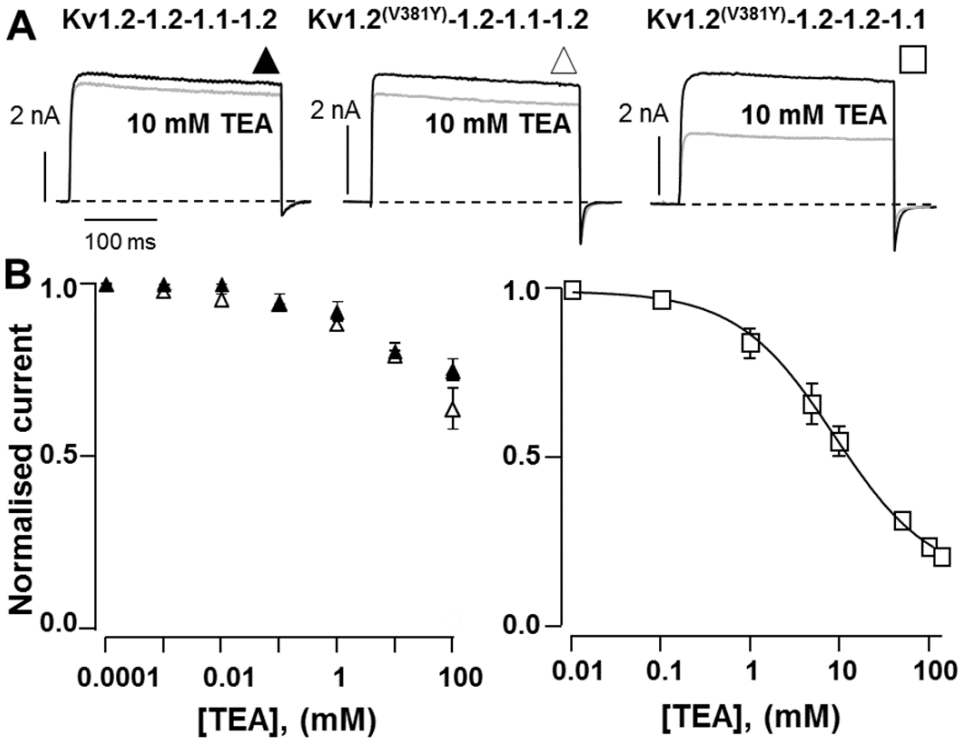

Fig. 4.10 Variation in sensitivity to TEA is revealed from the K^+ currents observed for mutated $K_v1.2$ channels.

(A) Current traces recorded using QPatch from the wild-type and variant channels in the absence (black traces) and presence (grey traces) of 10 mM TEA. (B) Dose-response curves for the $K_v1.2$-1.2-1.1-1.2 (▲) and its mutant $K_v1.2$(V381Y)-1.2-1.1-1.2 (△) channel show similar TEA insensitivity (IC_{50} > 100; B, left panel). Dose-inhibition plot for the additional mutated form $K_v1.2$(V381Y)-1.2-1.2-1.1 (□) (B, right panel reveals increased susceptibility; IC_{50} = 9+1). Some of the error bars fall within the data points. (n = 4-6).

However, a TEA-sensitive I_K current resulted (Fig. 4.10A) from swapping $K_v1.1$ and 1.2 subunit in the third and fourth position of $K_v1.2^{(V381Y)}$-1.2-1.1-1.2 channel to produce a

channel retaining the same stoichiometry but with a $K_v1.1$ subunit in close proximity or adjacent (when assembled) to the mutated-sensitive $K_v1.2$ [$K_v1.2^{(V381Y)}$-1.2-1.2-1.1 channel (Fig. 4.9)]. Its IC_{50} approximated to the channel having two copies of sensitive subunit in an adjacent arrangement [i.e. $K_v1.2$-1.2-1.1-1.1 channel] (Table 4.3). Hence, with the channels' subunit stoichiometries maintained, the positioning of sensitive subunits modulates the extent of their susceptibility to inhibition of their I_K by TEA.

4.8 $K_v1.1$ subunits lower the activation threshold and speed-up activation kinetics of K_v1 channels recombinantly expressed in mammalian cells

To examine how demyelination-associated enrichment of K_v1 channels with $K_v1.1$ subunit could affect their functional properties, biophysical profiles of the currents mediated by concatenated homo-$K_v(1.1)_4$ or $K_v(1.2)_4$ and hetero-tetramers ($K_v1.1$-1.2-1.1-1.1, $K_v1.1$-1.1-1.2-1.2) were analyzed. Each mediated voltage-activated non-inactivating K^+ currents, which were consistently larger in cells expressing $K_v1.2$ homo-tetramers or those containing this subunit together with $K_v1.1$ (Fig. 4.11 C1-E1). Most importantly, $K_v1.1$ homo-tetrameric channels activated at less depolarized thresholds than the currents resulting from the others (Bagachi et al., 2014). This feature is reflected clearly in conductance-voltage (gK-V) plot of the K^+ currents, with $K_v(1.1)_4$ activating from significantly more hyperpolarized potentials (close to -60 mV) compared to the $K_v1.1$-1.2-1.1-1.1, $K_v1.1$-1.1-1.2-1.2 and $K_v(1.2)_4$ channels (Fig. 4.11 C2-E2, Table 4.4). In all cells, the gK-V relationships of the K^+ currents were fitted well with a Boltzmann function with half-maximal values of activation ($V_{1/2}$) for $K_v(1.1)_4$ being most negative followed by intermediate potentials for the currents mediated by $K_v1.1$-1.2-1.1-1.1 or $K_v1.1$-1.1-1.2-1.2, and the most depolarized values observed with $K_v(1.2)_4$ channels (Table 4.4).

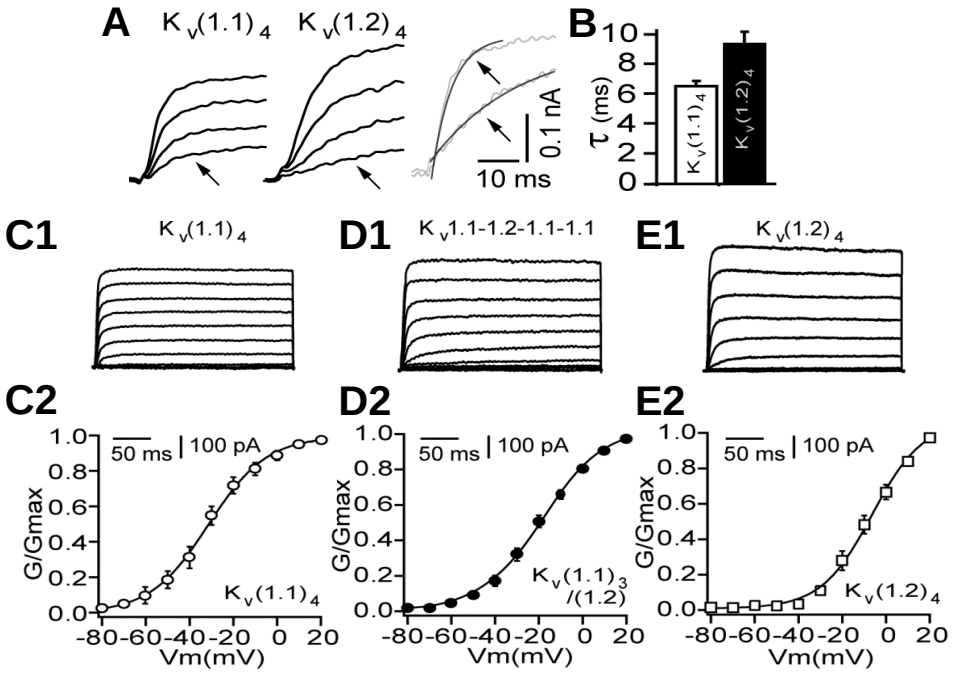

Fig. 4.11 Functional characterization of recombinant $K_v1.1$ homo-tetramers reveals distinctive biophysical profiles from those of $K_v1.1/1.2$ hetero-tetramers.

(A, C1–E1) Representative recordings of macroscopic currents (300 ms pulse) from HEK-293 cells transfected with the individual recombinant channels. (A, B) Activation rate of the voltage-dependent K^+ currents mediated by $K_v(1.1)_4$ (left) and $K_v(1.2)_4$ (middle) channels (within the range of 10–30% of max. current) at 5 mV from indicated voltages (below) with super-imposed (right) representative traces from. A notable difference between the rates of activation of $K_v(1.1)_4$ and $K_v(1.2)_4$ is revealed by fitting the data with a single exponential (see B). (C2–E2) Conductance-voltage relations of macroscopic currents measured, based on the K^+ current of the last 100 ms for each channel. Conductance at various command potentials were normalized and fitted with a single Boltzmann function. The difference in conductance values of $K_v(1.1)_4$ and $K_v(1.2)_4$ channel were statistically significant from 255 mV (P, 0.05, Mann-Whitney *U* test, see Table 4.4 for summary of the biophysical data). (n = 6-10).

Interestingly, significant differences were also observed between activation rates of these currents at near-threshold potentials, with $K_v(1.1)_4$ channel displaying a faster activation rate than the others (Fig. 4.11 A and B, C; Table 4.4).

Table 4.4 $V_{1/2}$ for activation and onset rate of currents mediated by the different recombinant channels expressed in HEK-293 cells

Parameters	$K_v(1.1)_4$	K_v1.1-1.2-1.1-1.1	K_v1.1-1.2-1.2-1.2	$K_v(1.2)_4$
$V_{1/2}$ (mV)	-35 ± 1 (6)	**-20 ± 1 (10)	#**-17 ± 1 (9)	**-7 ± 1 (8)
$tau_{1/2}$ (ms)	13 ± 2 (6)	*18 ± 1 (8)	**24 ± 1 (8)	**29 ± 2 (8)

Results are represented as means ± S.E.M. (*n*-values); * ($P < 0.05$) and ** ($P < 0.005$) numbers are significant compared to those from $K_v(1.1)_4$, (Mann Whitney *U* test); # data are taken from Al-Sabi et al., 2010.

4.9 K_v1.1- and K_v1.2-containing channels can be distinguished by selective blockers

HEK-293 cells expressing channels composed of homo-tetrameric $K_v(1.1)_4$, $(1.2)_4$ or hetero-tetrameric combinations of both subunits [K_v1.1-1.2-1.1-1.1 and [$K_v(1.1)_2$-$K_v(1.2)_2$] were used to mimic those possibly present in demyelinated optic nerve (ON) axons. DTX_K potently and selectively inhibited only the K_v1.1 homo-tetrameric channels, with sub-nanomolar IC_{50} (Table 4.5); introduction of a single K_v1.2 subunit into the tetramer (K_v1.1-1.2-1.1-1.1) lowered its susceptibility to blockade by DTX_K. Having two copies of K_v1.2 and K_v1.1 subunits in the concatamer (K_v1.1-1.1-1.2-1.2), resulted in an even lower sensitivity to DTX_K (IC_{50} > 100 nM). On the other hand, $K_v(1.2)_4$ channel was blocked by TsTX-Kα but apparently insensitive to DTX_K (Table 4.5). The K^+ current elicited by a heteromeric channel with equal numbers of K_v1.1 and 1.2 subunits proved, 6 -fold less sensitive to TsTX-Kα than $K_v(1.2)_4$. Furthermore, TsTX-Kα blockade was insignificant on K_v1 channels containing 3 or 4 copies of K_v1.1 subunits. Collectively, these results showed that DTX_K and TsTX-Kα are potent inhibitors of K_v1 channels that contain at least three copies of K_v1.1 and two copies of 1.2 subunits, respectively.

Table 4.5 Differential inhibition of concatenated K_v1 channels expressed in HEK-293 cells by DTX_K and TsTX-Kα

K_v1 channels	IC50 (nM)	
	DTX_K	TsTX-Kα
$K_v(1.1)_4$	0.27 ± 0.07 (5)	>100 (3)#
$K_v1.1$-1.2-1.1-1.1	*4 ± 0.1 (4)	>100 (3)
$K_v1.1$-1.2-1.2-1.2	>100 (4)	15 ± 2 (4)#
$K_v(1.2)_4$	>100 (3)	2.6 ± 0.2 (3)#

Results are represented as means ± S.E.M.; *n*-values are in brackets; * ($P < 0.05$) numbers are significant compared to $K_v(1.1)_4$ (t-test), # data were taken from Al-Sabi et al., 2010.

4.9 Discussion

4.9.1 Tetrameric K_v1 channels composed of pre-determined subunit combinations exhibit distinct functional characteristics

An innovative cloning platform was employed herein that affords expression of four α subunits as a single protein, with pre-determined compositions and positions of subunits as functional channels on the plasmalemma. This technology confines channel assembly to a proscribed order and paved the way for studying K_v1 heteromers of defined stoichiometry. Studies focused on $K_v1.1$-1.2-1.1-1.1 and $K_v1.2$-1.2-1.1-1.2 or variants thereof. These two heteromeric channels showed distinct g_K-V plots fitted well by single-Boltzmann distribution, predictable profiles toward TEA reflective of their different subunit compositions; importantly, such distinctive characteristics are indicative of uniform single-type channel populations. In addition, concatenated homo-oligomers of $K_v1.1$ or 1.2 were

made as control channels; importantly, these proved indistinguishable from their respective homomeric counterparts, demonstrating that tandem linkage does not alter their properties, in accord with other earlier findings (Sokolov et al., 2007; Al-Sabi et al., 2010). Notably, gradual changes were observed in both the biophysical properties (e.g.: g_K-V relationship) and TEA sensitivity upon altering the ratio of $K_v1.1$ to $K_v1.2$ subunits in tetramers indicating that hybrid channels containing mixtures of $K_v1.1$ and 1.2 exhibit intermediate phenotypes being a blend of those of the parental channels.

4.9.2 Positioning of α subunits and those possessing a key tyrosine profoundly affects TEA inhibition of the K^+ currents

As predicted, mutating $K_v1.2$ in the first position in $K_v1.2^{(V381Y)}$-1.2-1.1-1.1 construct yielded a channel having ~ 9-fold higher TEA sensitivity, similar to that of $K_v1.1$-1.2-1.1-1.1 (Table 4.3). This improved TEA susceptibility is presumably due to the presence of 2 copies of $K_v1.1$ subunits that cooperatively interact with TEA in addition to the contribution of another sensitive subunit, $K_v1.2^{(V381Y)}$ mutant, at the first position, while $K_v1.2$ occupied the second position in both channels. However, replacing the first position of the other standard concatemers, $K_v1.2$-1-2.1.1-1.2 with $K_v1.2^{(V381Y)}$, $K_v1.2^{(Q357H/V381Y)}$ or $K_v1.2^{(Q357H/P359S/V381Y)}$ did not improve inhibition of their K^+ currents by TEA (Table 4.3). One explanation could be attributed to a repulsive effect from the two adjacent $K_v1.2$ subunits (in the second and fourth positions) which might prevent interaction of $K_v1.2^{(V381Y)}$ subunit with TEA, and that turret region mutations added to the latter do not alter the channel's overall sensitivity. The postulated repulsion was absent when $K_v1.2$ subunit at the fourth position was replaced with $K_v1.1$; this channel ($K_v1.2^{(V381Y)}$-1.2-1.1-1.1) displayed a 100-fold enhanced TEA sensitivity (Table 4.3). A more modest change

could be achieved by keeping the same composition of the channel ($K_v1.2^{(V381Y)}$-1-2.1.1-1.2) but repositioning the sensitive $K_v1.1$ to be adjacent to the mutated sensitive subunit, as in $K_v1.2^{(V381Y)}$-1.2-1.2-1.1 channel (Table 4.3).

It seems that the higher affinity binding of the TEA (in case of homomeric $K_v1.1$ or its concatenated form) is achieved by simultaneously binding four aromatic side chains, one from each subunit through cation-π cooperative interaction (Hurst et al., 1992; Kavanaugh et al., 1992; Ahern et al., 2009). The insensitivity of $K_v1.2^{(V381Y)}$-1.2-1.1-1.2 channel might arise from the binding of TEA being perturbed by valine 381 from the two wild-type $K_v1.2$ subunits, and/or its three threonine 383 residues that differ from $K_v1.1$ and reside very close to the essential tyrosine 379. Accordingly, Kavanaugh et al. (Kavanaugh et al., 1992) showed that $K_v1.1^{(Y379V)}$ homomer was 30-fold less sensitive to TEA than wild-type and became completely insensitive when an additional mutation was introduced ($K_v1.1^{(Y379V/V381T)}$). These observations can be related to the difference in TEA sensitivities observed herein between concatemers of $K_v1.1$ and $K_v1.2^{(V381Y)}$; threonine 383 in $K_v1.2^{(V381Y)}$ could be responsible for the ~2-fold lower sensitivity compared to that of $K_v1.1$ homomer. Likewise, $K_v1.1$ subunit at the third position in $K_v1.2^{(V381Y)}$-1.2-1.1-1.2 channel likely failed to endow TEA sensitivity because 3 copies of non-permissive threonine 383 and 2 of valine 381 are provided by the surrounding $K_v1.2$ subunits. However, in $K_v1.2^{(V381Y)}$-1.2-1.2-1.1 channel, the $K_v1.1$ subunit at the fourth position was, apparently, free to bind TEA without the negative effect of threonine 383-containing subunits along with the adjacent $K_v1.2^{(V381Y)}$, thereby, giving moderate TEA sensitivity (IC_{50} = 9 mM) similar to $K_v1.2$-1.2-1.1-1.1 channel.

4.9.3 Pharmacological research prospective for K_v1 channel concatemers

Although K_v1 channels are expressed broadly throughout many regions of the CNS, their differential expression facilitates the appropriate modulation of neurotransmission. $K_v1.1$ and 1.2 are localized along axons, as dense clusters in juxta-paranodal regions of myelinated nerves, and other subcellular compartments. They form hetero-tetramers of varying composition to support fast axonal repolarization and rapid conduction of high frequency AP (Wang et al., 1993; Rhodes et al., 1995; Wang et al., 1995). Hence, $K_v1.1$- and 1.2-containing channels in these axons modulate AP propagation and dampen unwanted repetitive firing (Wang et al., 1994; Ogawa et al., 2010). This might be achieved by formation of oligomeric subtypes of channels with different heteromeric combinations of subunits to achieve biophysical properties best tailored for particular functions. In this context, Robbins and Tempel (2012) have suggested that heteromeric assembly of $K_v1.1$ and 1.2 subunits that varies between cell types and locations in CNS could be a reason why $K_v1.1$ or 1.2 null mice display spontaneous seizures though with distinct phenotypes. Recent observation in $K_v1.1^{+/+}$ mice revealed that K^+ channels composed of $K_v1.1$ in juxta-paranodal regions dampen excitability in motor nerves during fatigue or ischemic insult (Brunetti et al., 2012). These collective findings highlight that recombinant forms of heteromeric $K_v1.1$ and 1.2 could provide relevant targets for drug research and development. Accordingly, $K_v1.1$-1.2-1.2-1.2 channel was used recently as a target for high-throughput screening of selective inhibitors (Wacker et al., 2012). This promising venture should impact on searches for potent and selective blockers of neuronal K_v1 heteromers.

4.9.4 Implications for MS and other demyelinating disorders of the central nervous system

A well-established molecular mechanism for stabilizing the membrane potential of demyelinated axons is provided by Na^+/K^+ ATPase which, due to its electrogenic nature, provides a persistent hyperpolarizing drive during sustained activity, moving the axonal membrane potential away from the firing threshold (Bostock and Grafe, 1985). An over-expression of K^+ channels enriched with $K_v1.1$ subunits in the ON axons from cuprizone-fed mice provides another, perhaps, equally powerful means for stabilizing the membrane potential at sub-threshold voltages. Unlike genetic knock-down of $K_v1.2$ subunit (the main partner of $K_v1.1$) associated with reduced excitability of central neurons (Brew et al., 2007), $K_v1.1$ null mutants exhibit hyper-excitability and augmented axonal conductivity (Smart et al., 1998; Brew et al., 2003), suggesting a powerful dampening influence of $K_v1.1$-concatenating channels on neuronal responsiveness. Assessment of the K^+ current mediated by recombinant $(K_v1.1)_4$ homo-trameric channels in HEK-293 cells revealed a lower activation threshold and faster kinetics than those recorded for $(K_v1.2)_4$ homo-tetramers or $K_v1.2$ subunit-containing hetero-tetramers. Indeed, the faster activation from more negative potentials of the K^+ current mediated by $K_v1.1$ subunit-dominated channels in HEK-293 cells could restrain and stabilize the axonal membrane at sub-threshold potentials. Considering the selective increase and ectopic expression of $K_v1.1$ subunit in axons of demyelinated ON in relation to restoration of conductivity by DTX_K point to this being a potential target for ameliorative interventions. The sparse information available on specific molecular alterations responsible for impaired conductivity of demyelinated axons along with the poor selectivity of small K_v channel blockers with their considerable adverse effects have greatly hampered the development of effective restorative means. Interference

of 4-AP, one of the most promising candidates, with remyelination and regeneration of impaired oligodendrocytes (Bacia et al., 2004) renders its clinical use for rescuing axonal conductivity problematic; this stresses the urgent need for identification and evaluation of novel drug candidates. Hence, the recognition herein of novel K_v1 channels enriched with $K_v1.1$ subunit represent a significant step forward towards the development of a specific extra-cellular blocker of such channels with potential for recovering the conductivity of demyelinated axons.

CHAPTER 5

RESULTS

Screening of various dipyromethanes compounds using recombinantly expressed K_v1.X channels, identified a novel and selective inhibitor for K_v1.1 channels

5.1 Overview

K_v1 channels, exposed upon demyelination of axons in patients suffering from MS, contribute to abnormal propagation of nerve signals and resultant debilitating muscle weakness. Although aminopyridines can inhibit the K_v1 channels, such therapy is only beneficial in the short-term; also, their blockade of other K^+ channel types results in serious off-target effects, including seizures (Judge and Bever Jr., 2006). The observation of K_v1.1-containing channels being expressed ectopically in ON demyelinated axons from mice fed cuprizone (Bagchi et al., 2014), mimicking changes in MS, has given an indication of the responsible subtypes; furthermore, the abnormal conductivity induced could be near-normalised by attenuating the K_v1.1-mediated currents with DTX_K, a selective blocker (Robertson et al., 1996). Thus, K_v1.1 is a promising target for extracellular inhibitors to potentially ameliorate such symptoms in demyelinated conditions like MS. In search of low molecular weight blockers, K_v1.1- and 1.2-containing concatenated tetramers, recombinantly built with a designed platform (Al-Sabi et al., 2010; Chapter 4) were utilized to screen small molecule inhibitors for their selectivity to block the K_v1 channels.

5.2 Rational design of a new selective inhibitor of K_v1.1 channels

For designing selective blockers, their size and phobicity are vital criteria because if made too small, they would enter deep into the inner pore region of the K^+ channel and, similar to 4-aminopyridine, selectivity would be lost. We recently reported the activity of various substituted porphyrin derivatives as potent and selective blockers of neuronal K_v1 channels (Daly et al., 2015). Unfortunately, due to their phototoxicity and high molecular weights, the porphyrins are non-ideal candidates for the treatment of neuronal diseases. However, by using results from their structure-activity analysis, in combination with molecular modelling performed by Dr. G. K. Kinsella (Dublin Institute of Technology, Ireland), valuable pharmacophore information was realised that can be applied to develop a more suitable lead structure. To aid their design, a homology model of rat K_v1.1 tetramer was developed for molecular docking, based on the crystallographic structure of the mammalian closely-related K_v1.2 (Long et al., 2005). In this regard, it is noteworthy that symmetrically-substituted porphyrins bearing alkyl amino groups (cationic-charged at physiological pH) can tightly bind a KcsA-K_v1.3 channel (Ader et al., 2008, Gradl et al., 2003). The goal was to rationally design an inhibitor which is 1) large enough to avoid entering the deep inner pore region of the K_v channels, 2) target the essential amino acid residues in the vicinity of the selectivity filter/inner turret region of the channels and 3) and lack photo-toxicity .

In coordination with Dr. Kieran Nolan's group, the scaffold of the dipyrromethane (***DPM***) derivatives, outlined in the Scheme 1, was modelled using the same homology structure of K_v1.1 as for the porphyrins. The geometric quality of the backbone conformations and energy profiles of the modelled structures fall well within the restrictions established for reliable structures (Bowie et al., 1991; Colovos and Yeates, 1993; Laskowski et al., 1996).

For refining the side chain of amino acids in the pore region of $K_v1.1$ channel, flexible docking was performed with the Autodock protocol (Morris et al., 2009). The first interesting feature revealed was that these molecules have Cdocker energy scores almost double that of any of the porphyrin molecules reported previously. ***DPM I – III*** gave the highest scores of the series evaluated. Modelling showed that the docked molecules interact with the outer region of the channel mimicking that of DTX_K, a renowned high affinity and absolutely specific inhibitor of $K_v1.1$ (Robertson et al., 1996). This mechanism of binding does not possess the same characteristics as 4-aminopyridine but can participate in hydrogen bonding and π-π stacking interactions. These advantageous features highlight that the dipyrromethane scaffold has promise as the basis for a new lead target molecule.

The predicted interactions of ***DPM I*** with the $K_v1.1$ channel model (Fig. 5.1A) via hydrogen bonds (HB) are: Glu353 (two chains); Asp361 (one chain); Tyr375 (one chain); Gly376 (one chain); Tyr379 (two chains); Pro 380 (one chain) and Val381 (one chain). Hydrophobic contacts include: Met378 (one chain) and Tyr379 (one chain). Similar channel interactions were observed with ***DPM II*** (Fig. 5.1B) i.e. HB with: Glu353 (one chain); Gly374 (all chains); Tyr375 (two chains); Gly376 (two chains); Asp377 (two chains); Tyr379 (one chain); Pro 380 (one chain) and Val381 (one chain). Again, hydrophobic contacts involved Tyr379 (two chains). Hence, both compounds were predicted to contact Glu353 of the outer turret and a range of residues in the inner turret. However, the arm of ***DPM II*** was expected to be positioned slightly deeper into the inner turret (e.g. making contact with Gly374 of all chains) than ***DPM I***. Predicted interactions of ***DPM III*** with Kv1.1 channel (Fig. 5.2A) involve HB with: Val373 (two chains) Gly374 (three chains); Tyr375 (three chains); Gly376 (two chains) Tyr379 (two chains). Note that these residues reside in the pore, with pi stacking interactions with Tyr379 of $K_v1.1$ being

important. Guided by the outcomes from these modelling studies, this new generation of dipyrromethanes, ***DPM I – III*** were prepared with various substitutions, bearing alkylammonium side-chains, and screened against recombinantly-generated K_v1 channels of known subunit structures.

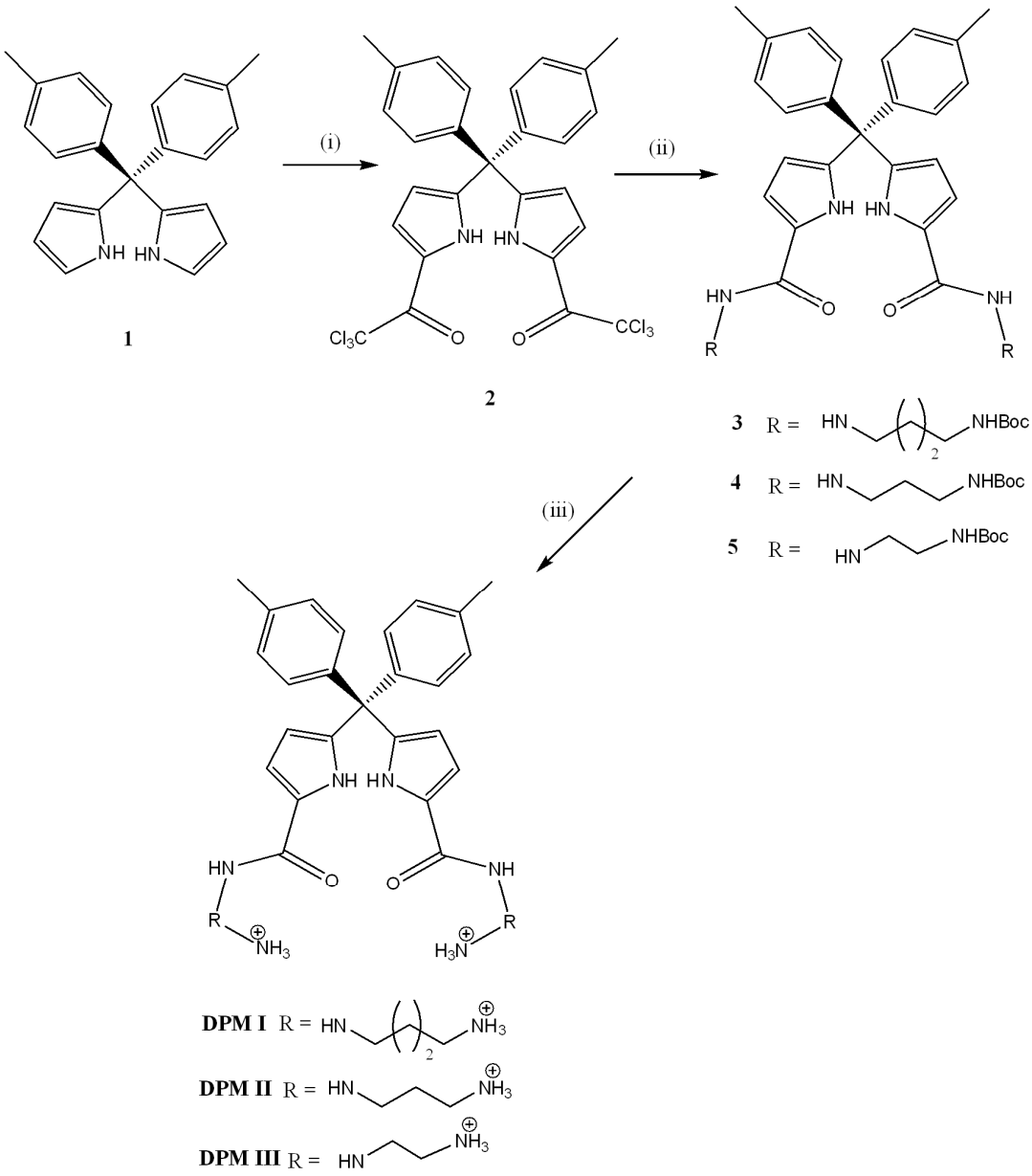

Scheme 1. Synthetic route employed to prepare the dipyrromethane-based K^+ channel inhibitors.
Three steps were used to build the compounds from the dipyrromethane scaffold 1 (i) DMAP, trichloroacetic acid, DCM; (ii) N-boc protected diamine, TEA, DCM room temperature; (iii) 4M HCl dioxane, DCM.

5.3 Structural characteristics of synthesised and purified *DPM I - III*

Their synthesis (Scheme 1) first involved preparing a dipyrromethane scaffold by condensation of pyrrole and 4,4-dimethylbenzophenone in the presence of boron trifluorodietherate [BF3(OEt)2] to yield compound **1** in 50% yield. Introduction of the required carboxyl groups into compound **1** at the 2 position of pyrrole was achieved in quantitative yields by electrophilic di-substitution of 1 with trichloroacetic anhydride (TClAA) in the presence of a catalyst 4-dimethyl-aminopyridine (DMAP) to generate compound **2**. The latter was converted to the N-Boc protected precursor **3-5**, by stirring **2** with the appropriate mono N-Boc protected alkyl diamine and TEA at room temperature overnight, to give compounds **3-5** in quantitative yield without need for further purification. Deprotection of compound **3-5** was achieved using 4M HCl in dioxane to give protonated derivatives ***DPM I – III***, in quantitative yields. The identity and purity of ***DPM I-III*** were confirmed by high-resolution spectrometry and NMR.

All the synthesis and characterization of above compounds was performed by Dr. Kieran Nolan's group.

5.4 *DPM III* preferentially inhibits $K_v1.1$ currents, slows activation and elevates the threshold potential

To measure the reactivity of ***DPM I-III*** with K_v1 channels, K^+ current generated by those containing the major α subunits found in mammalian brain (Shamotienko et al., 1997; Coleman et al., 1999) K^+ currents were recorded electrophysiologically, using whole-cell voltage patch-clamp. Representative K^+ current traces, in the absence or presence of 10 μM ***DPM I***, revealed some (albeit limited) inhibition of $K_v1.1$ (Fig. 5.1A) and $K_v1.3$ (Fig. 5.1C), with negligible effects on $K_v1.2$, 1.4 or 1.6 channels (Fig. 5.1C). Candidate ***DPM II***,

which possesses a shorter alkyl chain compared to ***DPM I***, gave much more inhibition of $K_v1.1$ at 10 µM (35 ± 3 %, n = 3) and to a lesser extent for $K_v1.3$ (16 ± 6 %, n = 3) channels whilst being ineffective towards $K_v1.2$ or 1.6 homomers (Fig. 5.1B, C). Unexpectedly, the $K_v1.4$-mediated current was also considerably reduced by 10 µM ***DPM II*** (32 ± 2 %, n = 3) (Fig. 5.1C).

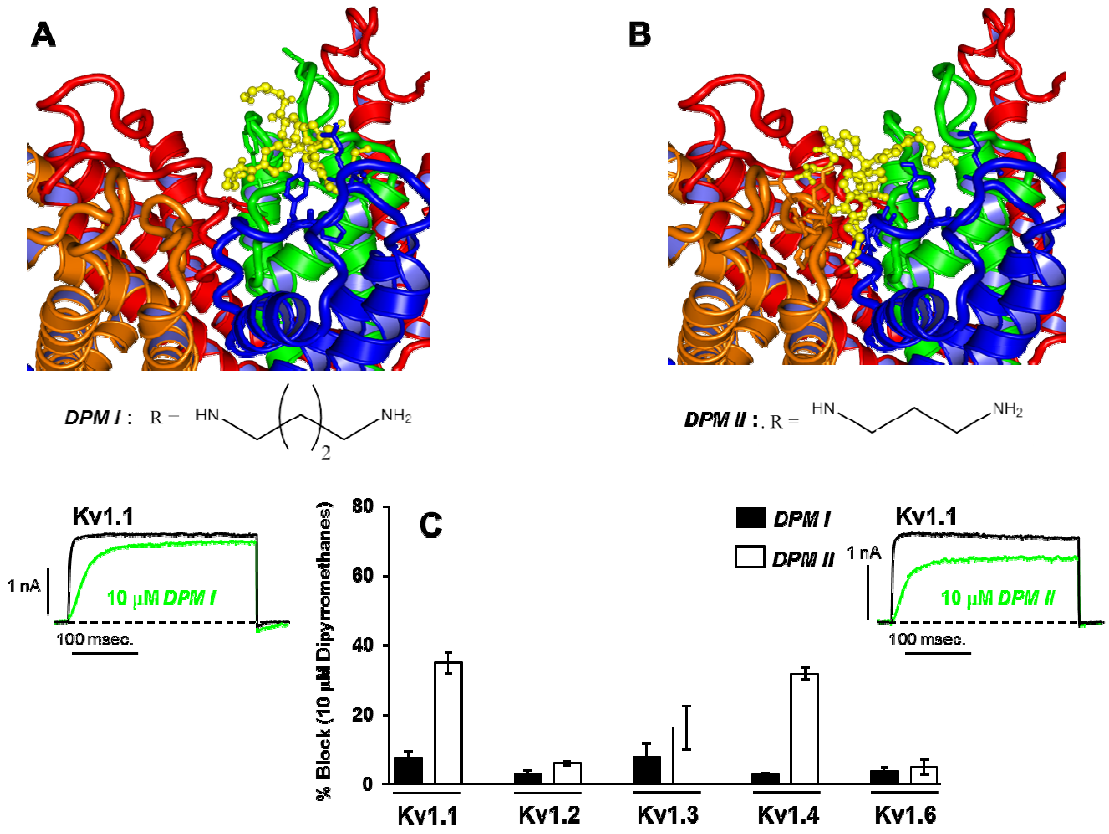

Fig. 5.1 A docking model of $K_v1.1$ channel with two *DPMs (I and II)* and homomeric $K_v1.X$ channel and current traces showing the pharmacological activity of two *DPMs*.

Side views of the docking of ***I*** (A) and ***II*** (B) to the extracellular pore region of $K_v1.1$ channel. Notice that the former interacts with the outer turret region slightly off-centre of the pore, while the latter interacts more centrally, protruding deep enough to reach the selectivity filter of $K_v1.1$. Representative electrophysiologically-recorded current traces (lower panels) reveal that ***DPM I*** produced limited inhibition of $K_v1.1$ and 1.3 current amplitude with even lower reductions of $K_v1.2$, 1.4 and 1.6 currents. More extensive blockade of $K_v1.1$, 1.4 and 1.3 was caused by ***DPM II***, with minimal decreases in $K_v1.2$ and 1.6. (C) The $K_v1.1$ channel recordings show greater inhibition by ***DPM II*** than ***I***. (n = 3-5).

The final candidate, ***DPM III***, which has the shortest chain, caused a preferential block (40 ± 3 %, n = 9) of K_v1.1 homomeric channel which could be reversed upon washing (Fig. 5.2B, D). Its selectivity was highlighted by a lack of effect on K_v1.2, 1.4 or 1.6, though some inhibition (~20%) of K_v1.3 was apparent (Fig. 5.2C, D).

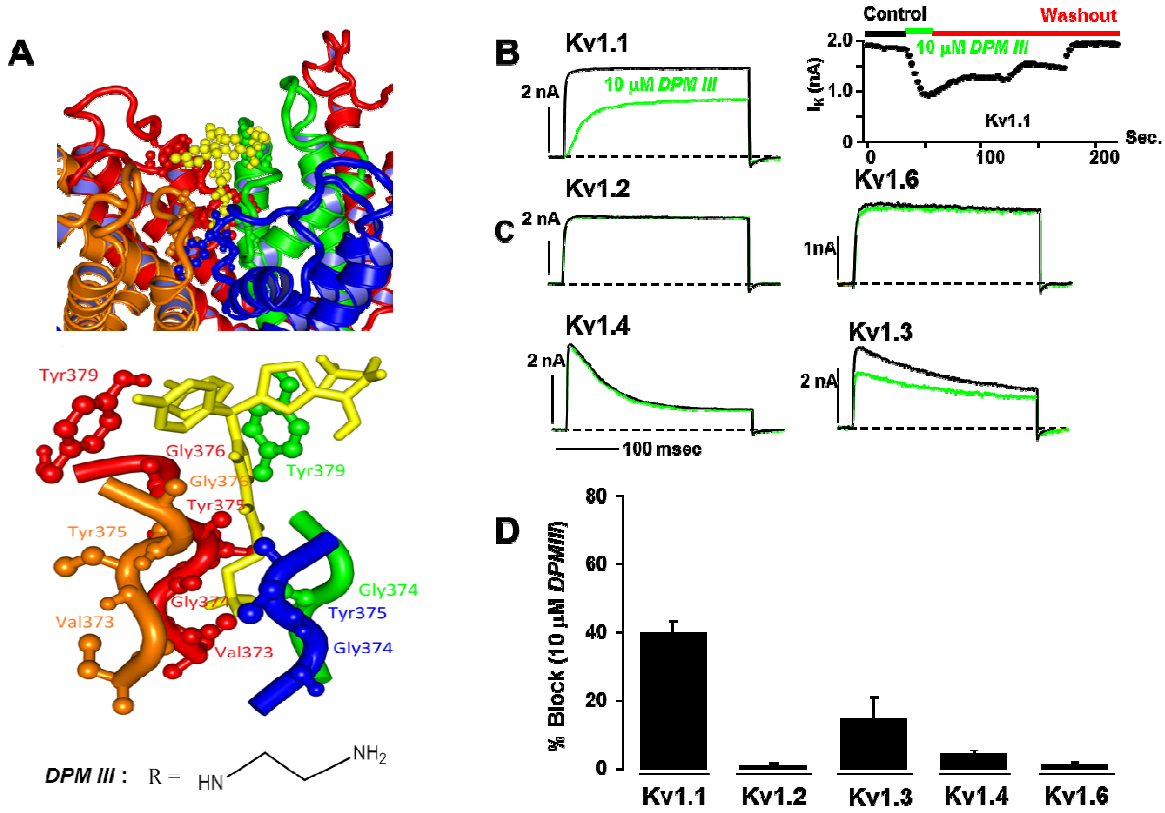

Fig. 5.2 *DPM III* showed preferential selectivity for K_v1.1 channel.

(A) Illustrates modelling of the docking of ***DPM III*** with the α subunit of monomeric K_v1.1 channel. The interacting residues of each α subunits of the channel are represented in orange, red, blue and green colors. Notice the interaction of side chains of ***DPM III*** with the inner turret lining via residues from 4 subunits of K_v1.1 channel; however, the interactions are mainly with two subunits. Images were generated using Pymol (De Lano, 2002). (B) Representative current traces from K_v1.1 channel in the absence (black) and presence (green) of 10 µM of ***DPM III*** showing inhibition which was relieved on washing. Currents were evoked at 20 mV voltage steps from -90 mV holding potential. (C) Recordings demonstrate a lack of effect of 10 µM ***DPM III*** on K_v1.2, 1.4 and 1.6 but some inhibition of K_v1.3. (D) Histogram confirms the preferential inhibition by ***DPM III*** of K_v1.1 over other channels tested. (n = 3-9).

Analysis of different hetero-tetramers of tandem-linked K_v1.1 and 1.2 stably expressed in HEK-293 cells yielded varying susceptibilities to the blocker.

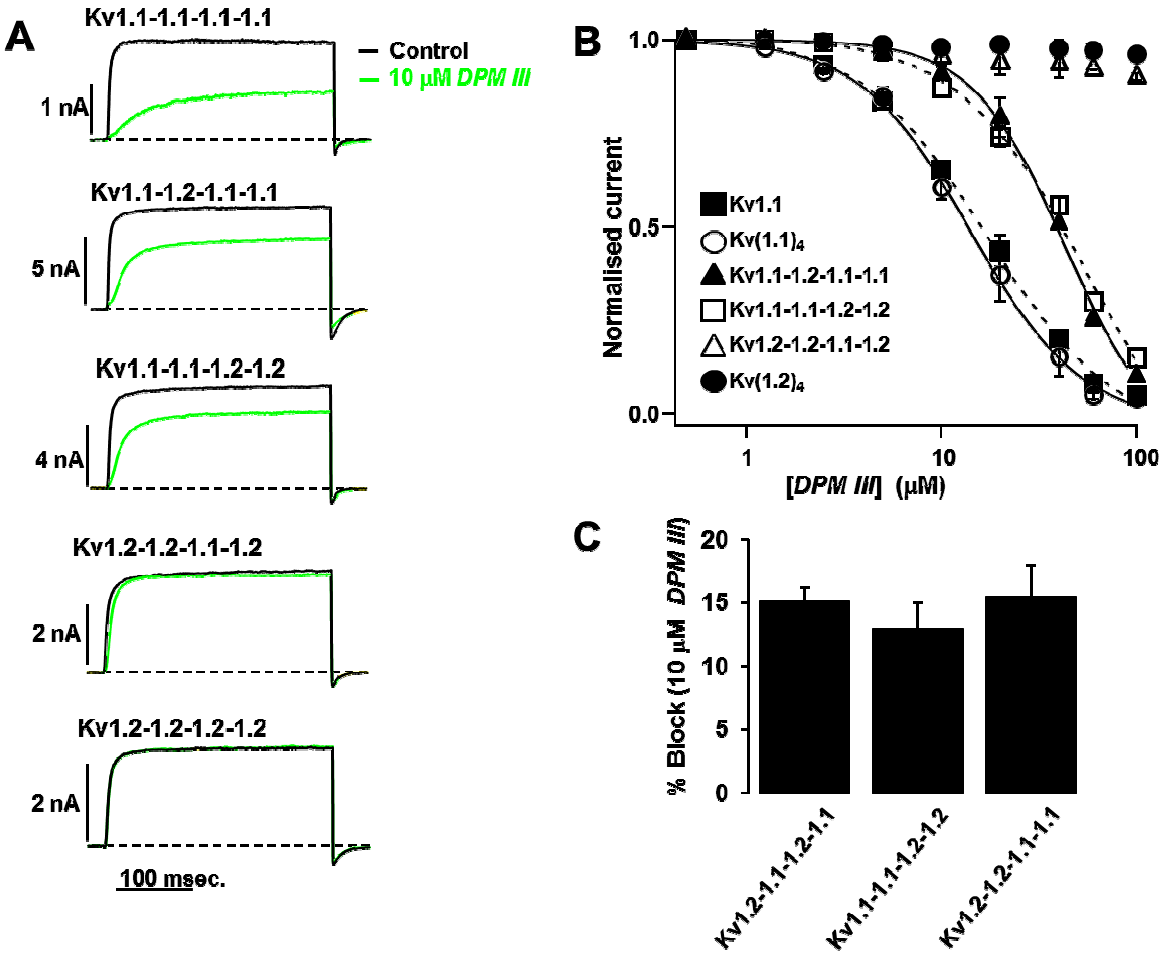

Fig. 5.3 Concatenated K_v1.1/1.2-containing channels displayed different sensitivities to *DPM III*.

(A) Representative current traces from K_v1.1/1.2-containing tetrameric channel in the absence (black) and presence (green) of 10 µM ***DPM III***. It partially inhibited channels containing two, three or four copies of K_v1.1 subunits, while proving ineffective against K_v1.2 homo-tetramer or K_v1.2-1.2-1.1-1.2 channels. (B) Dose-response curves for $K_v(1.1)_4$ (○) and K_v1.1 (■) demonstrate similar sensitivity, followed by K_v1.1-1.2-1.1-1.1 (▲) and K_v1.1-1.1-1.2-1.2 (□), while K_v1.2-1.2-1.1-1.2 (△) and $K_v(1.2)_4$ (●) were non-susceptible. Some of the error bars fall within the data points. The IC_{50} values are summarized in Table 5.1. (C) Summary of equal inhibition by ***DPM III*** of tetrameric channels containing two copies of K_v1.1 in different positioning within the concatemers. (n = 4-8).

Decreasing the copy number of $K_v1.1$ in those concatemers lowered the extent of inhibition by 10 μM ***DPM III*** (Fig. 5.3A); $K_v(1.1)_4 > K_v(1.1)_3 1.2 > K_v(1.1)_2(1.2)_2$ with $K_v(1.1)(1.2)_3$ and $K_v(1.2)_4$ being insensitive. The dose-dependencies for blockade revealed that the IC_{50} values decreased from 14 μM for $K_v(1.1)_4$ to 54 and 57 μM upon introducing 1 and 2 copies of $K_v1.2$, respectively (Table 5.1). Notably, altering the positions of $K_v1.1$ and 1.2 within the concatemers did not influence their blockade by 10 μM ***DPM III*** (Fig. 5.3C).

Table 5.1 IC_{50} values for inhibition by *DPM III* of $K_v1.1$ homomer compared to various K_v1 concatenated tetramers

K_v1 channel	**IC_{50} [μM]**	**Hill slope**	**n**
$K_v1.1$	16 ± 1	1.4 ± 0.2	8
$K_v(1.1)_4$	14 ± 1	1.5 ± 0.2	8
$K_v(1.1)_3$-1.2	§54 ± 7	1.5 ± 0.1	7
$K_v(1.1)_2$-$(1.2)_2$	§57 ± 15	1.3 ± 0.2	5
$K_v1.1$-$(1.2)_3$	>100	---	6
$K_v(1.2)_4$	>100	---	4

Results are represented as means ± S.E.M. §values are significant compared to $K_v(1.1)_4$, $P < 0.05$, unpaired Student's *t*-test. (n=4-8)

Interestingly, inhibition of $K_v1.1$ channels by ***DPM III*** was associated with significant slowing (~10-fold) of activation (Fig. 5.3A, 5.4A). The time constants ($\tau_{activation}$) for activation of $K_v1.1$ currents were slowed from 1.9 (± 0.15 ms, n = 4) to 20.3 (± 3.3 ms, n = 4), $p < 0.005$ (Fig. 5.4A) for the homomer and 2.2 (± 0.1 ms, n = 5) to 19.5 (± 3.4 ms, n = 4), $p < 0.001$ for the concatemer. Likewise, $\tau_{activation}$ values for the heteromeric channels were increased by 10 μM ***DPM III*** for channels in which the number of $K_v1.1$ subunits was raised to 2 in $K_v(1.1)_2$-$(1.2)_2$ [from 2.8 ± 0.4 ms, n = 6 to 18 ± 2 ms, n = 5] and 3 in

$K_v(1.1)_3$-1.2 [from 3.1 ± 0.2 ms, n = 5 to 14 ± 2 ms, n = 5], derived from the representative current traces shown (Fig. 5.3A). Moreover, the g_k-V relationship of $K_v1.1$ channel was altered by 10 µM ***DPM III*** from a half-maximal value for activation ($V_{1/2}$) of -27 (± 1 mV, n = 7) to +11 (± 1 mV, n = 4) (Fig. 5.4B), a significant shift of ~40 mV towards positive potentials.

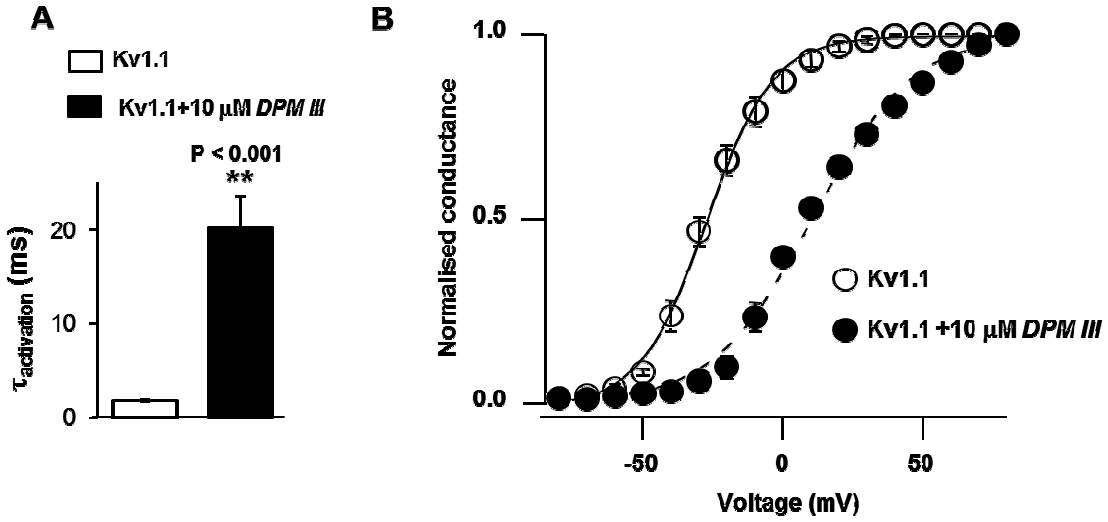

Fig. 5.4 The activation kinetics of the K^+ current mediated by $K_v1.1$ channel are slowed by *DMP III* and the threshold potential raised by.

(A) Time constants of activation (activation) for homomeric $K_v1.1$ before (empty bar) and after application of 10 µM ***DPM III*** (filled bar), determined by fitting the current traces with a mono-exponential function. Notice a significant slowing in the time-course of activation ($P < 0.001$). (B) Conductance-voltage relationship of the steady-state currents calculated from -82 mV reversal potential after 200 ms at indicated voltages. Boltzmann fits of the data for homomeric $K_v1.1$ (○) showing a shift towards more positive potentials induced by ***DPM III*** (●). Some of the error bars fall within the data points. (n = 4-5).

Collectively, these findings unveil notable inhibition by ***DPM III*** of K_v1-containing K^+ channels and compounded modulation of the biophysical properties of $K_v1.1$. This dual action of ***DPM III*** in selectively inhibiting K^+ currents which would be expected to reduce

the hyperpolarization caused by homomeric $K_v1.1$ and $K_v1.1$-containing channels such as those that are found to be enriched after demyelination of ON axons (Bagchi et al., 2014).

5.5 Discussion

The pharmacological properties of ***DPM III***, measured electrophysiologically, confirmed those predicted from *in silico* analysis. This compound is devoid of reactivity with $K_v1.2$, 1.4 or 1.6 channels, and preferentially inhibits $K_v1.1$ over 1.3 channels. Evaluation of this promising molecule on $K_v1.1/1.2$-heteromeric channels was possible by utilizing a cloning platform that afforded expression of four α subunits as single-chain proteins on the plasmalemma, with the stochiometry and positions of their subunits pre-determined (Al-Sabi et al., 2010; also see Chapter 4). Tetrameric combinations that should correspond to those predicted to occur in brain (Shamotienko et al., 1997; Coleman et al., 1999) were selected for investigation, including those $K_v1.1$-enriched channels observed in demyelinated axons (Bagchi et al., 2014). Selectivity and potency of ***DPM III*** inhibiting $K_v1.1$ channel arises from acting extracellularly, in large part, with the inner turret regions of $K_v1.1$ before occluding the channel deep in its vestibule. Its limited cross reactivity with $K_v1.3$, may be due to the latter's accessible serines closely resembling those lining the turret of $K_v1.1$ (Daly et al., 2015). On the other hand, $K_v1.1$ and 1.2 channels share similar susceptibility to 4-AP due to their conserved inner vestibule region where this molecule interacts (Stuhmer et al., 1989; McCormack et al., 1991). The selective inhibition and slowing of activation kinetics of the $K_v1.1$ channel highlights the dual advantages of ***DPM III***. Bagchi et al. (2014) demonstrated that in demyelinated axons of mouse ON an increase in ectopic expression of $K_v1.1$ subunit contributes to abnormal compound APs (CAPs). These K^+ channels decrease the voltage threshold (i.e. they activate at more negative

potentials) and accelerate the activation kinetics, thereby, perturb the axonal propagation of electrical signals. It was found that this dysfunction can be partially overcome by the $K_v1.1$-selective inhibitor, DTX_K (Bagchi et al. 2014). Although such an avid toxin cannot be considered as a potential neurotherapeutic, its beneficial effects observed *in vitro* warrant the development of more suitable smaller inhibitors. It is encouraging that ***DPM III*** offers a double advantage in preferentially inhibiting $K_v1.1$-dependent currents, including slowing their activation and shifting the conductance-voltage relationship of $K_v1.1$ to more positive potentials. Such a beneficial modulatory action could further help normalize the CAPs in demyelinated axons, a discovery of relevance to patho-physiology of MS. Its effect on the activation kinetics could be explained by interaction deep in the pore region of $K_v1.1$ channels. Furthermore, ***DPM III*** is impermeable to intact cell membranes and can distinguish between $K_v1.1$ and the much more prevalent 1.2 channels. In contrast, the internal blocker, 4-AP, is readily membrane permeable, interacts with both $K_v1.1$ and 1.2 channels with similar potency and can cross the blood-brain barrier.

Unlike 4-AP, ***DPM III*** was found to be a more specific and potent blocker of recombinant $K_v1.1$, and devoid of effect on $K_v1.2$. In this regard, evidence exists for the involvement of $K_v1.2$ in peripheral nerve hyper-excitability in patients suffering from type II diabetes or amyotrophic lateral sclerosis (Shibuya et al., 2011, Zenker et al., 2012), an undesirable situation that could possibly be avoided by using ***DPM III.*** As the inflammatory component in MS pathophysiology is of prime importance, the noted inhibition of $K_v1.3$ by ***DPM III*** might have an additional beneficial effect because this channel is known to activate T cells and is highly expressed on the inflammatory infiltrates in MS; moreover, $K_v1.3$ is a functional marker of activated effector memory T cells in experimental allergic

encephalomyelitis and in myelin-specific T cells derived from the peripheral blood of MS patients. So ***DPM III*** not only presents potential therapeutic properties that could be useful to restore conduction in demyelinated fibers but might also modulate the inflammatory events which occur in MS.

CHAPTER 6

GENERAL DISCUSSION

The key experimental observations of this research were discussed in the respective chapters covering the different objectives (see Section 1.12).

The focus on characterization of neuronal K^+ channels, particularly K_vs, is ongoing work in Prof. Dolly's lab since the identification of voltage-sensitive K^+ (K_v1) channel proteins isolated using α DTX (Dolly et al., 1984; Mehraban et al., 1984). This polypeptide from the green mamba *Dendroaspis angusticeps*, had been shown by electrophysiological recording to selectively inhibit A-type K^+ currents (Halliwell et al., 1986) or slow inactivating variants (Stansfeld et al., 1987). Complementary genetic approaches revealed that mammalian K_v channels consist of four α subunits forming a central pore as tetramers, each containing six transmembrane α-helical segments S1–S6 and a membrane-reentering P-loop (P), which are arranged circumferentially around the central pore region as see in Fig. 6.1 (Tempel et al., 1987; Kamb et al., 1988; Pongs et al., 1988; MacKinnon, 1991). Four subunits are assembled, probably in the endoplasmic reticulum and targeted to the plasma membrane to form a functional channel, with both their N- and C-termini in the cytoplasm. Many studies have been performed on the monomeric channels which were assumed to have formed functional tetramers. However, such investigations on these channels are still considered limited; re-creating a channel with four individual α-subunit genes to form a single protein would be very advantageous for assessing their properties in order to mimic

the native neuronal K_v1 homo- and hetero-tetrameric channels observed in brain (Shamotienko et al., 1997; Coleman et al., 1999). Thus, the present work reported an improved method for gaining insights into the functional and biophysical characteristics of K_v1 channels, using a concatenated strategy that has been developed in our Centre (Dolly and Shamotineko, Patent, 2011).

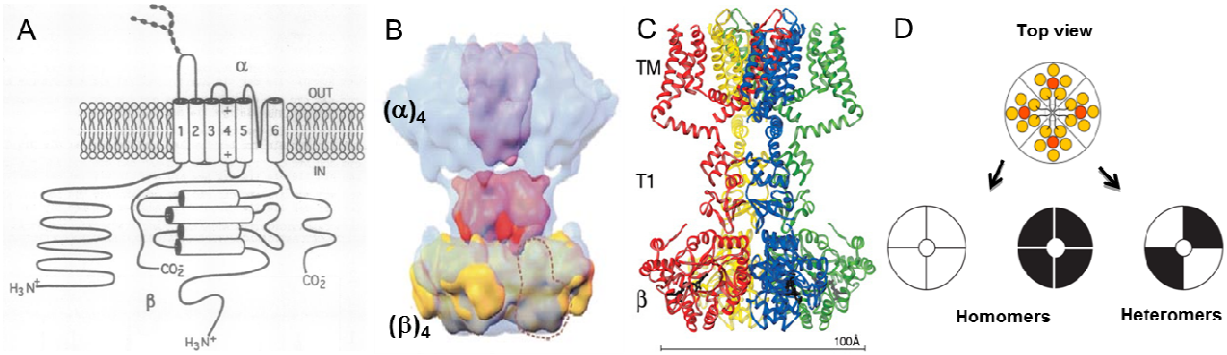

Fig. 6.1 Neuronal K_v1 are $(\alpha)_4(\beta)_4$ proteins - complete structures solved. (A) Membrane topography of K_v1 α and β subunits. Membrane topography shows that K_v1 channels contain 6-TM and 1-P domain, which has a cytoplasmic N and C-terminal associated with β-subunit. (adapted from Scott et al., 1994). (B, C) 3D structure of brain K_v1 channels (adapted from Orlova et al., 2003) and X-ray structure of a $K_v(1.2)_4$ $(\beta_2)_4$ (adapted from Long et al., 2005), respectively, revealed the assembly of 4 α and 4 β subunits. (D) Predicted arrangement of α subunits. Various subtypes of K_v1 α subunits occur in neurons, which can possibly form homomers and heteromers.

Development and use of concatenation for mimicking the possible K_v1 subunit combinations of neuronal tetrameric channels

Previous studies used co-expression of different ratios of various K_v channel monomeric subunits or concatenated dimers in the hope of obtaining functional channels. Though they succeeded in producing linked tetramers (Heginbotham and MacKinnon, 1992; Hurst et al., 1992; Kavanaugh et al., 1992; Liman et al., 1992), it proved cumbersome to demonstrate that uniform populations of heteromeric channels were expressed in the plasmalemma.

Using our much better strategy, concatenated tetramers composed of K_v1.1, 1.2, 1.4 and 1.6 α subunits representative of their neuronal counterparts were obtained, using versatile methodology for generating constructs encoding controlled combinations and spatial arrangements of subunits; these resulted in multimeric tetrameric proteins after expression in mammalian cells. Unique restriction sites were identified where enzymes do not cut within the actual genes of interest but allow cloning of subunit genes into cassettes at pre-selected positions. This requires careful design of concatenated constructs that are physically connected by linkers of the appropriate size; otherwise, adverse effects could arise in terms of alterations in the conformational states of some subunits (McCormack et al., 1992). Also, the sequences chosen must be devoid of selected unique restriction sites. This was facilitated by a half-linker strategy which we invented to join appropriately-selected pairs of restriction enzyme sites NheI/BglII, BglII/EcoRI, EcoRI/SalI and SalI/BamHI (see Sections 2.3.1 and 2.3.3, Chapter 2). Such a process is accomplished by a single PCR, using specific primers for 4 pairs of enzymes and the 2 halves of the link on either sides of the gene. This novel concept permitted the simultaneous and easy creation of a bank of intermediate cassettes, which were utilized to produce a large number of hetero-tetramers. Advantageously, the concept of having position-specific enzyme sites with half-linkers permits the insertion of any particular gene into a given position. Likewise, the ease of the whole process involving few steps minimizes errors, time and cost which made it much more advantageous than the concatenation methods attempted by others (Liman et al., 1992; Akhtar et al, 2002).

Restriction enzyme digestion and DNA sequencing of extracted DNA from *E. coli* transformed with the concatenated genes established that the tetramers had the correct

integrity and composition. There was no indication of a position-dependent over-representation of any subunit or channels that assembled with distorted symmetry, problems noted with K_v1 concatemers made by a less stringent method and expressed in *Xenopus* oocytes (McCormack et al., 1992; Hurst et al., 1995).

Pre-defined arrangement of concatenated α subunits was confirmed by the observed abolishment of $K_v1.4$ NIB function when placed adjacent to the NIP domain of $K_v1.6$

Hetero-polymerization has been reported to occur only among members of the same subfamily of K_v channels (Covarrubias et al. 1991; Salkoff et al., 1992). Heteromeric channels using $K_v1.4$, 1.6, 1.2 or 1.1 have been localized in several structures within the nervous system (Wang et al., 1993, 1994; Scott et al., 1994a; Shamotienko et al., 1997; D'Adamo et al., 1999). However, the relative order of subunits within the channel may be different. The reliability of our concatenation in expressing functional tetrameric channel with pre-defined positioning of α subunits, was verified by producing different types of inactivation profiles, exploiting the functionalities of NIB and NIP domains present in $K_v1.4$ and 1.6, respectively (Hoshi et al., 1990; Zagotta et al., 1990; Tseng-Crank et al., 1990). After transfecting HEK-293 cells with genes encoding various α subunits ($K_v1.4$-, 1.6- and 1.2-α subunits), having distinct pharmacological and/or biophysical characteristics, the resultant concatenated tetramers exhibited the expected findings without evidence of any proteolysis of linked subunits possible during their expression (Baumann, et al., 2003) and, also, one can expect that large constructs may exhibit decreased expression and reduced delivery to the cell surface membrane (Ji et al., 2008). Such difficulties were circumvented as our cell surface biotinylation and Western blotting experiments confirmed the plasmalemmal expression of intact tetrameric channel without evidence of any

proteolysis (see Section 3.3, Chapter 3), which was not performed by others previously (McCormack et al., 1992; Hurst et al., 1995). The system validated in the present study for creating heteromers which exhibit fast inactivation provided scope for evaluating a biochemical basis for their distinct biophysical properties. Placing K_v1.4 and 1.6 subunits distant in hetero-tetramers (K_v1.4–1.2–1.6–1.2 and K_v1.4–1.2–1.2–1.2) gave fast-inactivating channels. When they were placed in adjacent positions (K_v1.4–1.6–1.2–1.2 and K_v1.4–1.2–1.2–1.6) the channels showed slow inactivation with variable τ_{1inact} but not τ_{2inact} values. Moreover, significant shift in $V_{1/2}$ of the K_v1.4–1.6–1.2–1.2 and K_v1.4–1.2–1.2–1.6 channels towards more depolarized potentials correlates with the slow inactivation due to predicted adjacent positioning of the NIP to NIB, contrasting with that for the fast-inactivating K_v1.4–1.2–1.6–1.2 channels. K_v1 channels with mutations in the NIP domain of K_v1.6 (K_v1.4–1.2–1.6$^{(E27/30/32A)}$–1.2) and (K_v1.4–1.6$^{(E27/30/32A)}$–1.2–1.2) showed inactivation profiles similar to K_v1.4–1.2–1.6–1.2, suggesting NIP domain in K_v1.6 prevents fast inactivation and also highlights that presence of a mutant subunit did not affect the concatenation and function of the tetramer.

Role of subunit stoichiometry and positioning in determining the biophysical and pharmacological properties of K_v1.1/1.2-containing tetrameric channels

K_v1.2 has been found to be the predominant isoform in αDTX-sensitive acceptors from several regions of mammalian brain (Scott et al., 1994a). However, the function of a particular K^+ channel subunit cannot be dictated only by its subcellular location, but also by the other subunit types with which it combines. For example, K_v1.1 prevents the axonal localization of K_v1.4-complexed channels, but not K_v1.2-containing heteromultimers (Jenkins et al., 2011). Both K_v1.1 and 1.2 were localized at juxta-paranodal regions of

myelinated axons and synaptic terminals in mouse (Wang et al., 1993 and 1994) and rat brain (McNamara et al, 1993 and 1996; Sheng et al., 1994; Wang et al., 1999). This localization suggests that both the channels may influence AP propagation, repolarization, and conduction as well as regulate neurotransmittter release. Though both are of same subfamily and co-express at identical subcellular locations and have similar implications in epilepsy and ataxia, loss of function of one or other exhibits a difference in seizure phenotypes (Robbins and Tempel, 2012). Likewise, their pharmacological profiles are distinct; K_v1.1 channel is sensitive to TEA and 1.2 insensitive (MacKinnon and Yellen, 1990; Kavanaugh et al., 1991). Since they are abundantly co-localized, it becomes important to know how they act when they form hetero-tetramers with different stoichiometry and positioning. Co-expression studies indicated that stoichiometry is the key component that influences the susceptibility to TEA (Hurst et al., 1992; Shen et al., 1994), but did not address the influence of positioning, due to lack of an ideal concatenation strategy. Though earlier published data suggests that TEA sensitivity of adjacently- and diagonally-positioned K_v1.1 and 1.2 subunits in K_v1 channels is different when using equal copies of both subunits (Al-Sabi et al., 2010), the data herein establishes that both stoichiometry and positioning affects TEA binding to sensitive K_v1 subunits in concatenated tetramers. Homo-tetrameric K_v1.1 and 1.2 channels both yielded a I_K current with the most negative $V_{1/2}$ value and most positive $V_{1/2}$ value, respectively, similar to their non-concatenated counterparts; this indicates that concatenation does not affect the biophysical characteristics. With increase in the number of identical subunits in K_v1.1/1.2 hetero-tetramers the $V_{1/2}$ values shifted towards their homomeric channels, showing the direct influence of subunit stoichiometry on their biophysical criteria. In addition, replacing one of K_v1.1 subunit with an insensitive K_v1.2 constituent to produce K_v1.1-1.2-1.1-1.1,

made the channel significantly less sensitive than $K_v1.1$ homo-tetramer. Raising the ratio of $K_v1.2$ to $K_v1.1$ in $K_v1.1$-1.1-1.1-1.1 reduced the sensitivity of the tetrameric channel to TEA proving that the number of insensitive subunits affects TEA binding.

Mutations of the pore region of $K_v1.2$ in tetrameric $K_v1.1/1.2$-containing channels that increases TEA binding

Due to the lack of TEA sensitivity related to $K_v1.2$ channels some critical amino acid residues were examined. When the key amino acid valine 381 in the pore region of $K_v1.2$ channel was mutated to tyrosine ($K_v1.2^{(V381Y)}$), the TEA binding increased greatly. Also, similar sensitivity was recorded with a double mutation $K_v1.2^{(R354A/V381Y)}$ of non-concatenated homomer; however, these values still differ significantly from that for $K_v1.1$ homomer. Concatenated tetramer with pore mutation ($K_v1.2^{(V381Y)}$-1.2-1.1-1.1) behaved similarly as $K_v1.1$-1.2-1.1-1.1 channel and proved ~10 times more TEA sensitive compared to its previously reported wild-type (Table 4.3, Al-Sabi et al., 2010). This showed that the $K_v1.2^{(V381Y)}$ subunit in this tetramer is behaving similarly to $K_v1.1$. In contrast, the channel possessing one more $K_v1.2$ subunit ($K_v1.2^{(V381Y)}$-1.2-1.1-1.2) did not behave close to $K_v1.1$-1.2-1.1-1.2, but displayed sensitivity similar to $K_v1.2$-1.2-1.1-1.2. Using the same stoichiometry but with positioning $K_v1.1$ adjacent to mutated subunit ($K_v1.2^{(V381Y)}$-1.2-1.2-1.1) made the channel significantly sensitive to TEA, similar to that of $K_v1.2$-1.2-1.1-1.1. It is notable that increasing one insensitive copy of $K_v1.2$ in $K_v1.2^{(V381Y)}$-1.2-1.1-1.1 did yield different sensitivity than expected, and further changing the position of $K_v1.1$ with same stoichiometry showed a 10-fold difference between their sensitivities. Overall, our results showed that both stoichiometry and positioning influence the biophysical and pharmacological properties of $K_v1.1/1.2$-containing channels. Since the mutation in turret

region of $K_v1.2$ is behaving close to that of $K_v1.1$ raising sensitivity to TEA, $K_v1.1$ is an ideal target for blockers or inhibitors. As TEA and 4-AP are considered as non-selective blockers (Lin et al., 1993), used in millimolar range which could cause severe toxicity in clinical applications, it is desirable to develop a new selective blocker for $K_v1.1$, which is a prime target in treating MS (Judge and Bever Jr., 2006).

Development and screening of K_v1 channel selective blockers (dipyromethane compounds) using monomeric and concatenated tetrameric $K_v1.X$ channels

Recent findings from our lab demonstrated that $K_v1.1$-containing channels are expressed ectopically and contribute to abnormal CAP in demyelinated axons from ON of mice fed with cuprizone (Bagchi et al., 2014). In collaboration with a group led by Dr. Kieran Nolan in Chemistry Department, DCU, we utilized the monomeric and concatenated K_v1 channels subunits as representative targets for the development of new, small and selective inhibitors of $K_v1.1$. The observations from the experimental data to date look promising; out of three compounds (***DPM I – III***) tested, ***DPM III*** was found to be selective and effective as a blocker of $K_v1.1$ in micromolar range. Selectivity of ***DPM III***, a dipyrromethane molecule bearing two C2-alkylammonium side chains, is assumed to be achieved mainly by interaction with residue Tyr379 in the inner turret region of $K_v1.1$, distinct from 4-AP, which interacts with conserved inner vestibule region similar in $K_v1.1$ and 1.2 channels (Stuhmer et al., 1989; McCormack et al., 1991). Molecular modelling studies revealed that ***DPM III*** binds to the outer region of the $K_v1.1$ channel while inserting its reactive groups into the channel pore, mimicking the action of DTX_K (Stansfeld et al., 1987). This limits its cross reactivity with $K_v1.3$, which has similar residues lining the turret region of $K_v1.1$), while discriminating other K_v1 channels ($K_v1.2$, 1.4 and 1.6). Highly

significant inhibition of $K_v1.1$ channel by 10 μM ***DPM III*** compared to $K_v1.2$, 1.4 and 1.6, proves the potency and selectivity of ***DPM III*** for $K_v1.1$.

$K_v1.1/1.2$-containing channels were used to assess the activity of ***DPM III*** on concatenated heteromeric channels. The dose-dependencies for blockade revealed that the IC_{50} of concatenated $K_v(1.1)_4$ is 14 μM. Substituting the copy number of $K_v1.1$ with 1.2 in the concatemers reduced the percentage of inhibition by 10 μM ***DPM III***, as channels become insensitive. Though the stoichiometry of $K_v1.1$ to 1.2 influenced the blocking of heteromeric channels by ***DPM III***, the change in the $K_v1.1$ subunit positioning within the concatemers did not influence their blockade ***DPM III***. Since the $K_v1.2$ mutation in turret region, as stated above, affected the binding of TEA for $K_v1.1/1.2$-containing channels with difference in stoichiometry and positioning of wild-type $K_v1.1$, similarly, it is interesting to find the effect of ***DPM III*** on $K_v1.1$ and 1.2 tetramers containing mutated $K_v1.2$.

Future directions

More research is still needed before we can understand how exactly the K_v1 channels behave in an octomeric complex (with both α and β subunits) in mammalian cells and cultured neurons. Coleman et al. was the first to report the α-subunit composition of $(\alpha)_4(\beta)_4$ oligomers and their association with β-subunits in human CNS, using cerebral grey and white matter, plus spinal cord from autopsy samples. Sequential immuno-precipitation identified the abundance of $K_v1.1$, 1.2, and 1.4 in all the tissues (Coleman et al., 1999). Future co-expression of concatenated pre-defined individual α and β subunit homo- and

hetero-tetramers, could give more valuable information on the function of the individual subunit and thereby, further elucidate the complexity.

With availability of the successful expression system in mammalian cells and fully defined cloned K_v1 genes, it would be advantageous to proceed to validate the characteristics of recombinant K_v1 channels by expressing them in cultured neurons. To assess the validity of the biophysical and pharmacological characteristics obtained in HEK-293 cells it seems highly desirable to express K_v1 in neurons so covalent modifications would be more authentic provided a developmental stage can be selected before expression of endogenous channels. This could be attempted in hippocampal neurons. Little or no expression of K_v1 channels have been reported for hippocampus at an embryonic stage of Wistar rat (Ficker and Heinemann, 1992), Spargue-dawley rat (Maletic-Savatic et al., 1995) and mouse (Grosse et al., 2000, Sánchez-Ponce et al., 2012). Preliminary experiments in our hands showed that cultured neurons from embryonic18 (E18) hippocampus of Spargue-dawley rats did not express $K_v1.1$ and 1.2 channels in day 7 cultures *in vitro*. Search for the existence of other K_v channels is being continued. Hence, selection of early stage hippocampal culture (within 7 days *in vitro*) as an ideal platform for viral expression of monomeric and tetrameric $K_v1.X$ channels in neuronal cells, followed by confirmation of their expression using biochemical methods; allows determination of their biophysical and pharmacological properties electrophysiologically. Since other proteins such as CAMs and MAGUKs associate with K_v1 channels in neurons (Ogawa et al., 2008), it is expected that these channels will behave differently, both in biochemical and biophysical terms than those HEK-293 cells. Such new information could provide a more reliable basis for molecular modeling and design of specific inhibitors as drugs (see Chapter 4). Also, further

studies involving co-expression of recombinant β subunits (β1.1 or β2.1) with K_v1.1 or 1.2 in the hippocampal neuronal platform, mimicking the native K^+ channel expression, and assessing their membrane distribution, biophysical and pharmacological properties, should provide more functional data to foster a deeper understanding of the control of neuronal excitability.

BIBLIOGRAPHY

Ahern, C. A., Eastwood, A. L., Dougherty, D. A. & Horn, R. (2009) An electrostatic interaction between TEA and an introduced pore aromatic drives spring-in-the-door inactivation in Shaker potassium channels. *J Gen Physiol*. 134**,** 461-9.

Aiyar, J., Withka, J. M., Rizzi, J. P., Singleton, D. H., Andrews, G. C., Lin, W., Boyd, J., Hanson, D. C., Simon, M., Dethlefs, B. & et al. (1995) Topology of the pore-region of a K^+ channel revealed by the NMR-derived structures of scorpion toxins. *Neuron*. 15**,** 1169-81.

Akhtar, S., Shamotienko, O., Papakosta, M., Ali, F. & Dolly, J. O. (2002) Characteristics of brain K_v1 channels tailored to mimic native counterparts by tandem linkage of alpha subunits: implications for K^+ channelopathies. *J Biol Chem*. 277**,** 16376-82.

Al-Sabi, A., Shamotienko, O., Dhochartaigh, S. N., Muniyappa, N., Le Berre, M., Shaban, H., Wang, J., Sack, J. T. & Dolly, J. O. (2010) Arrangement of K_v1 alpha subunits dictates sensitivity to tetraethylammonium. *J Gen Physiol*. 136**,** 273-82.

Bagchi, B., Al-Sabi, A., Kaza, S., Scholz, D., O'Leary, V. B., Dolly, J. O. & Ovsepian, S. V. (2014) Disruption of myelin leads to ectopic expression of $K_v1.1$ channels with abnormal conductivity of optic nerve axons in a cuprizone-induced model of demyelination. *PLoS One*. 9**,** e87736.

Bardou, O., Trinh, N. T. & Brochiero, E. (2009) Molecular diversity and function of K^+ channels in airway and alveolar epithelial cells. *Am J Physiol Lung Cell Mol Physiol*. 296**,** L145-55.

Barros, F., Dominguez, P. & de la Pena, P. (2012) Cytoplasmic domains and voltage-dependent potassium channel gating. *Front Pharmacol*. 3**,** 49.

Baumann, A., Grupe, A., Ackermann, A. & Pongs, O. (1988) Structure of the voltage-dependent potassium channel is highly conserved from Drosophila to vertebrate central nervous systems. *EMBO J*. 7**,** 2457-63.

Baumann, S. W., Baur, R. & Sigel, E. (2003) Individual properties of the two functional agonist sites in GABA(A) receptors. *J Neurosci*. 23**,** 11158-66.

Beeton, C., Barbaria, J., Giraud, P., Devaux, J., Benoliel, A. M., Gola, M., Sabatier, J. M., Bernard, D., Crest, M. & Beraud, E. (2001) Selective blocking of voltage-gated K^+

channels improves experimental autoimmune encephalomyelitis and inhibits T cell activation. *J Immunol*. 166**,** 936-44.

Beeton, C., Wulff, H., Singh, S., Botsko, S., Crossley, G., Gutman, G. A., Cahalan, M. D., Pennington, M. & Chandy, K. G. (2003) A novel fluorescent toxin to detect and investigate K_v1.3 channel up-regulation in chronically activated T lymphocytes. *J Biol Chem*. 278**,** 9928-37.

Bever, C. T., Jr. (1994) The current status of studies of aminopyridines in patients with multiple sclerosis. *Ann Neurol*. 36 Suppl**,** S118-21.

Bezanilla, F. (2008) Ion channels: from conductance to structure. *Neuron*. 60**,** 456-68.

Bowie, J. U., Luthy, R. & Eisenberg, D. (1991) A method to identify protein sequences that fold into a known three-dimensional structure. *Science*. 253**,** 164-70.

Breeze, A. L. & Dolly, J. O. (1989) Interactions between discrete neuronal membrane binding sites for the putative K^+-channel ligands beta-bungarotoxin, dendrotoxin and mast-cell-degranulating peptide. *Eur J Biochem*. 178**,** 771-8.

Brew, H. M., Gittelman, J. X., Silverstein, R. S., Hanks, T. D., Demas, V. P., Robinson, L. C., Robbins, C. A., McKee-Johnson, J., Chiu, S. Y., Messing, A. & Tempel, B. L. (2007) Seizures and reduced life-span in mice lacking the potassium channel subunit Kv1.2, but hypoexcitability and enlarged K_v1 currents in auditory neurons. *J Neurophysiol*. 98**,** 1501-25.

Brew, H. M., Hallows, J. L. & Tempel, B. L. (2003) Hyperexcitability and reduced low threshold potassium currents in auditory neurons of mice lacking the channel subunit K_v1.1. *J Physiol*. 548**,** 1-20.

Brunetti, O., Imbrici, P., Botti, F. M., Pettorossi, V. E., D'Adamo, M. C., Valentino, M., Zammit, C., Mora, M., Gibertini, S., Di Giovanni, G., Muscat, R. & Pessia, M. (2012) Kv1.1 knock-in ataxic mice exhibit spontaneous myokymic activity exacerbated by fatigue, ischemia and low temperature. *Neurobiol Dis*. 47**,** 310-21.

Buckingham, S. D., Kidd, J. F., Law, R. J., Franks, C. J. & Sattelle, D. B. (2005) Structure and function of two-pore-domain K^+ channels: contributions from genetic model organisms. *Trends Pharmacol Sci*. 26**,** 361-7.

Christie, M. J., Adelman, J. P., Douglass, J. & North, R. A. (1989) Expression of a cloned rat brain potassium channel in Xenopus oocytes. *Science*. 244**,** 221-4.

Chung, Y. H., Joo, K. M., Nam, R. H., Kim, Y. S., Lee, W. B. & Cha, C. I. (2005) Immunohistochemical study on the distribution of the voltage-gated potassium channels in the gerbil cerebellum. *Neurosci Lett*. 374**,** 58-62.

Coleman, S. K., Newcombe, J., Pryke, J. & Dolly, J. O. (1999) Subunit composition of K_v1 channels in human CNS. *J Neurochem*. 73**,** 849-58.

Colovos, C. & Yeates, T. O. (1993) Verification of protein structures: patterns of nonbonded atomic interactions. *Protein Sci*. 2**,** 1511-9.

Covarrubias, M., Wei, A. A. & Salkoff, L. (1991) Shaker, Shal, Shab, and Shaw express independent K^+ current systems. *Neuron*. 7**,** 763-73.

D'Adamo, M. C., Imbrici, P., Sponcichetti, F. & Pessia, M. (1999) Mutations in the KCNA1 gene associated with episodic ataxia type-1 syndrome impair heteromeric voltage-gated K^+ channel function. *FASEB J*. 13**,** 1335-45.

da Silva, B. J., de Melo, R. P., Falco-Filho, E. L. & de Araujo, C. B. (1997) Potassium source for ion-exchange glass waveguide fabrication. *Appl Opt*. 36**,** 5949-50.

Daly, D., Al-Sabi, A., Kinsella, G. K., Nolan, K. & Dolly, J. O. (2015) Porphyrin derivatives as potent and selective blockers of neuronal K_v1 channels. *Chem Commun (Camb)*. 51**,** 1066-9.

Devaux, J., Gola, M., Jacquet, G. & Crest, M. (2002) Effects of K^+ channel blockers on developing rat myelinated CNS axons: identification of four types of K^+ channels. *J Neurophysiol*. 87**,** 1376-85.

Dolly, J. O., Halliwell, J. V., Black, J. D., Williams, R. S., Pelchen-Matthews, A., Breeze, A. L., Mehraban, F., Othman, I. B. & Black, A. R. (1984) Botulinum neurotoxin and dendrotoxin as probes for studies on transmitter release. *J Physiol (Paris)*. 79**,** 280-303.

Doyle, D. A., Morais Cabral, J., Pfuetzner, R. A., Kuo, A., Gulbis, J. M., Cohen, S. L., Chait, B. T. & MacKinnon, R. (1998) The structure of the potassium channel: molecular basis of K^+ conduction and selectivity. *Science*. 280**,** 69-77.

Edwards, L., Nashmi, R., Jones, O., Backx, P., Ackerley, C., Becker, L. & Fehlings, M. G. (2002) Upregulation of $K_v1.4$ protein and gene expression after chronic spinal cord injury. *J Comp Neurol*. 443**,** 154-67.

England, S. K., Uebele, V. N., Shear, H., Kodali, J., Bennett, P. B. & Tamkun, M. M. (1995) Characterization of a voltage-gated K^+ channel beta subunit expressed in human heart. *Proc Natl Acad Sci U S A*. 92**,** 6309-13.

Eunson, L. H., Rea, R., Zuberi, S. M., Youroukos, S., Panayiotopoulos, C. P., Liguori, R., Avoni, P., McWilliam, R. C., Stephenson, J. B., Hanna, M. G., Kullmann, D. M. & Spauschus, A. (2000) Clinical, genetic, and expression studies of mutations in the potassium channel gene KCNA1 reveal new phenotypic variability. *Ann Neurol*. 48**,** 647-56.

Ficker, E. & Heinemann, U. (1992) Slow and fast transient potassium currents in cultured rat hippocampal cells. *J Physiol*. 445**,** 431-55.

Gagnon, D. G. & Bezanilla, F. (2009) A single charged voltage sensor is capable of gating the Shaker K^+ channel. *J Gen Physiol*. 133**,** 467-83.

Glaudemans, B., van der Wijst, J., Scola, R. H., Lorenzoni, P. J., Heister, A., van der Kemp, A. W., Knoers, N. V., Hoenderop, J. G. & Bindels, R. J. (2009) A missense mutation in the Kv1.1 voltage-gated potassium channel-encoding gene KCNA1 is linked to human autosomal dominant hypomagnesemia. *J Clin Invest*. 119**,** 936-42.

Goldberg, E. M., Clark, B. D., Zagha, E., Nahmani, M., Erisir, A. & Rudy, B. (2008) K^+ channels at the axon initial segment dampen near-threshold excitability of neocortical fast-spiking GABAergic interneurons. *Neuron*. 58**,** 387-400.

Grissmer, S., Nguyen, A. N., Aiyar, J., Hanson, D. C., Mather, R. J., Gutman, G. A., Karmilowicz, M. J., Auperin, D. D. & Chandy, K. G. (1994) Pharmacological characterization of five cloned voltage-gated K^+ channels, types Kv1.1, 1.2, 1.3, 1.5, and 3.1, stably expressed in mammalian cell lines. *Mol Pharmacol*. 45**,** 1227-34.

Grosse, G., Draguhn, A., Hohne, L., Tapp, R., Veh, R. W. & Ahnert-Hilger, G. (2000) Expression of K_v1 potassium channels in mouse hippocampal primary cultures: development and activity-dependent regulation. *J Neurosci*. 20**,** 1869-82.

Grupe, A., Schroter, K. H., Ruppersberg, J. P., Stocker, M., Drewes, T., Beckh, S. & Pongs, O. (1990) Cloning and expression of a human voltage-gated potassium channel. A novel member of the RCK potassium channel family. *EMBO J*. 9**,** 1749-56.

Gutman, G. A., Chandy, K. G., Adelman, J. P., Aiyar, J., Bayliss, D. A., Clapham, D. E., Covarriubias, M., Desir, G. V., Furuichi, K., Ganetzky, B., Garcia, M. L., Grissmer, S., Jan, L. Y., Karschin, A., Kim, D., Kuperschmidt, S., Kurachi, Y., Lazdunski, M.,

Lesage, F., Lester, H. A., McKinnon, D., Nichols, C. G., O'Kelly, I., Robbins, J., Robertson, G. A., Rudy, B., Sanguinetti, M., Seino, S., Stuehmer, W., Tamkun, M. M., Vandenberg, C. A., Wei, A., Wulff, H., Wymore, R. S. & International Union of Pharmacology. (2003) International Union of Pharmacology. XLI. Compendium of voltage-gated ion channels: potassium channels. *Pharmacol Rev*. 55**,** 583-6.

Gutman, G. A., Chandy, K. G., Grissmer, S., Lazdunski, M., McKinnon, D., Pardo, L. A., Robertson, G. A., Rudy, B., Sanguinetti, M. C., Stuhmer, W. & Wang, X. (2005) International Union of Pharmacology. LIII. Nomenclature and molecular relationships of voltage-gated potassium channels. *Pharmacol Rev*. 57**,** 473-508.

Halliwell, J. V., Othman, I. B., Pelchen-Matthews, A. & Dolly, J. O. (1986) Central action of dendrotoxin: selective reduction of a transient K^+ conductance in hippocampus and binding to localized acceptors. *Proc Natl Acad Sci U S A*. 83**,** 493-7.

Hebert, S. C., Desir, G., Giebisch, G. & Wang, W. (2005) Molecular diversity and regulation of renal potassium channels. *Physiol Rev*. 85**,** 319-71.

Heginbotham, L. & MacKinnon, R. (1992) The aromatic binding site for tetraethylammonium ion on potassium channels. *Neuron*. 8**,** 483-91.

Heginbotham, L., Abramson, T. & MacKinnon, R. (1992) A functional connection between the pores of distantly related ion channels as revealed by mutant K^+ channels. *Science*. 258**,** 1152-5.

Heginbotham, L., Lu, Z., Abramson, T. & MacKinnon, R. (1994) Mutations in the K^+ channel signature sequence. *Biophys J*. 66**,** 1061-7.

Heinemann, S. H., Rettig, J., Wunder, F. & Pongs, O. (1995) Molecular and functional characterization of a rat brain $K_v\beta3$ potassium channel subunit. *FEBS Lett*. 377**,** 383-9.

Heinemann, S. H., Rettig, J., Graack, H. R. & Pongs, O. (1996) Functional characterization of K_v channel beta-subunits from rat brain. *J Physiol*. 493 (Pt 3)**,** 625-33.

Heitzmann, D. & Warth, R. (2008) Physiology and pathophysiology of potassium channels in gastrointestinal epithelia. *Physiol Rev*. 88**,** 1119-82.

Hille, B. (2001) Ion Channels of Excitable Membranes. 3rd Edition, MA, Sunderland : Sinauer Associates.

Horresh, I., Poliak, S., Grant, S., Bredt, D., Rasband, M. N. & Peles, E. (2008) Multiple molecular interactions determine the clustering of Caspr2 and Kv1 channels in myelinated axons. *J Neurosci*. 28**,** 14213-22.

Hoshi, T., Zagotta, W. N. & Aldrich, R. W. (1990) Biophysical and molecular mechanisms of Shaker potassium channel inactivation. *Science*. 250**,** 533-8.

Hurst, R. S., Kavanaugh, M. P., Yakel, J., Adelman, J. P. & North, R. A. (1992) Cooperative interactions among subunits of a voltage-dependent potassium channel. Evidence from expression of concatenated cDNAs. *J Biol Chem*. 267**,** 23742-5.

Hurst, R. S., North, R. A. & Adelman, J. P. (1995) Potassium channel assembly from concatenated subunits: effects of proline substitutions in S4 segments. *Receptors Channels*. 3**,** 263-72.

Iverson, L. E., Tanouye, M. A., Lester, H. A., Davidson, N. & Rudy, B. (1988) A-type potassium channels expressed from Shaker locus cDNA. *Proc Natl Acad Sci U S A*. 85**,** 5723-7.

Jan, L. Y. & Jan, Y. N. (1990) How might the diversity of potassium channels be generated? *Trends Neurosci*. 13**,** 415-9.

Jan, L. Y. & Jan, Y. N. (1997) Cloned potassium channels from eukaryotes and prokaryotes. *Annu Rev Neurosci*. 20**,** 91-123.

Jenkins, P. M., McIntyre, J. C., Zhang, L., Anantharam, A., Vesely, E. D., Arendt, K. L., Carruthers, C. J., Kerppola, T. K., Iniguez-Lluhi, J. A., Holz, R. W., Sutton, M. A. & Martens, J. R. (2011) Subunit-dependent axonal trafficking of distinct alpha heteromeric potassium channel complexes. *J Neurosci*. 31**,** 13224-35.

Ji, W., Xu, P., Li, Z., Lu, J., Liu, L., Zhan, Y., Chen, Y., Hille, B., Xu, T. & Chen, L. (2008) Functional stoichiometry of the unitary calcium-release-activated calcium channel. *Proc Natl Acad Sci U S A*. 105**,** 13668-73.

Judge, S. I. & Bever, C. T., Jr. (2006) Potassium channel blockers in multiple sclerosis: neuronal K_v channels and effects of symptomatic treatment. *Pharmacol Ther*. 111**,** 224-59.

Kalman, K., Nguyen, A., Tseng-Crank, J., Dukes, I. D., Chandy, G., Hustad, C. M., Copeland, N. G., Jenkins, N. A., Mohrenweiser, H., Brandriff, B., Cahalan, M., Gutman, G. A. & Chandy, K. G. (1998) Genomic organization, chromosomal localization, tissue distribution, and biophysical characterization of a novel

mammalian Shaker-related voltage-gated potassium channel, K_v1.7. *J Biol Chem*. 273**,** 5851-7.

Kamb, A., Iverson, L. E. & Tanouye, M. A. (1987) Molecular characterization of Shaker, a Drosophila gene that encodes a potassium channel. *Cell*. 50**,** 405-13.

Kamb, A., Tseng-Crank, J. & Tanouye, M. A. (1988) Multiple products of the Drosophila Shaker gene may contribute to potassium channel diversity. *Neuron*. 1**,** 421-30.

Kauferstein, S., Huys, I., Lamthanh, H., Stocklin, R., Sotto, F., Menez, A., Tytgat, J. & Mebs, D. (2003) A novel conotoxin inhibiting vertebrate voltage-sensitive potassium channels. *Toxicon*. 42**,** 43-52.

Kavanaugh, M. P., Hurst, R. S., Yakel, J., Varnum, M. D., Adelman, J. P. & North, R. A. (1992) Multiple subunits of a voltage-dependent potassium channel contribute to the binding site for tetraethylammonium. *Neuron*. 8**,** 493-7.

Kavanaugh, M. P., Varnum, M. D., Osborne, P. B., Christie, M. J., Busch, A. E., Adelman, J. P. & North, R. A. (1991) Interaction between tetraethylammonium and amino acid residues in the pore of cloned voltage-dependent potassium channels. *J Biol Chem*. 266**,** 7583-7.

Kim, D. S., Kim, J. E., Kwak, S. E., Won, M. H. & Kang, T. C. (2007) Seizure activity affects neuroglial K_v1 channel immunoreactivities in the gerbil hippocampus. *Brain Res*. 1151**,** 172-87.

Kirsch, G. E., Taglialatela, M. & Brown, A. M. (1991) Internal and external TEA block in single cloned K^+ channels. *Am J Physiol*. 261**,** C583-90.

Kiss, L. & Korn, S. J. (1998) Modulation of C-type inactivation by K^+ at the potassium channel selectivity filter. *Biophys J*. 74**,** 1840-9.

Klassen, T., Davis, C., Goldman, A., Burgess, D., Chen, T., Wheeler, D., McPherson, J., Bourquin, T., Lewis, L., Villasana, D., Morgan, M., Muzny, D., Gibbs, R. & Noebels, J. (2011) *Cell*. 145**,** 1036-48.

Kole, M. H., Letzkus, J. J. & Stuart, G. J. (2007) Axon initial segment Kv1 channels control axonal action potential waveform and synaptic efficacy. *Neuron*. 55**,** 633-47.

Kubo, Y., Reuveny, E., Slesinger, P. A., Jan, Y. N. & Jan, L. Y. (1993) Primary structure and functional expression of a rat G-protein-coupled muscarinic potassium channel. *Nature*. 364**,** 802-6.

Kullmann, D. M. (2002) The neuronal channelopathies. *Brain*. 125**,** 1177-95.

Kuo, M. M., Haynes, W. J., Loukin, S. H., Kung, C. & Saimi, Y. (2005) Prokaryotic K(+) channels: from crystal structures to diversity. *FEMS Microbiol Rev*. 29**,** 961-85.

Labro, A. J. & Snyders, D. J. (2012) Being flexible: the voltage-controllable activation gate of K_v channels. *Front Pharmacol*. 3**,** 168.

Laskowski, R. A., Rullmannn, J. A., MacArthur, M. W., Kaptein, R. & Thornton, J. M. (1996) AQUA and PROCHECK-NMR: programs for checking the quality of protein structures solved by NMR. *J Biomol NMR*. 8**,** 477-86.

Lee, H., Wang, H., Jen, J. C., Sabatti, C., Baloh, R. W. & Nelson, S. F. (2004) A novel mutation in KCNA1 causes episodic ataxia without myokymia. *Hum Mutat*. 24**,** 536.

Lee, S. M., Kim, J. E., Sohn, J. H., Choi, H. C., Lee, J. S., Kim, S. H., Kim, M. J., Choi, I. G. & Kang, T. C. (2009) Down-regulation of delayed rectifier K^+ channels in the hippocampus of seizure sensitive gerbils. *Brain Res Bull*. 80**,** 433-42.

Legros, C., Pollmann, V., Knaus, H. G., Farrell, A. M., Darbon, H., Bougis, P. E., Martin-Eauclaire, M. F. & Pongs, O. (2000) Generating a high affinity scorpion toxin receptor in KcsA-K_v1.3 chimeric potassium channels. *J Biol Chem*. 275**,** 16918-24.

Li, M., Jan, Y. N. & Jan, L. Y. (1992) Specification of subunit assembly by the hydrophilic amino-terminal domain of the Shaker potassium channel. *Science*. 257**,** 1225-30.

Liman, E. R., Tytgat, J. & Hess, P. (1992) Subunit stoichiometry of a mammalian K^+ channel determined by construction of multimeric cDNAs. *Neuron*. 9**,** 861-71.

Lin, C. S., Boltz, R. C., Blake, J. T., Nguyen, M., Talento, A., Fischer, P. A., Springer, M. S., Sigal, N. H., Slaughter, R. S., Garcia, M. L. & et al. (1993) Voltage-gated potassium channels regulate calcium-dependent pathways involved in human T lymphocyte activation. *J Exp Med*. 177**,** 637-45.

Liu, Y., Jurman, M. E. & Yellen, G. (1996) Dynamic rearrangement of the outer mouth of a K^+ channel during gating. *Neuron*. 16**,** 859-67.

Lockery, S. R. & Goodman, M. B. (2009) The quest for action potentials in *C. elegans* neurons hits a plateau. *Nat Neurosci.* 12**,** 377-8.

Long, S. B., Campbell, E. B. & Mackinnon, R. (2005) Crystal structure of a mammalian voltage-dependent Shaker family K^+ channel. *Science*. 309**,** 897-903.

MacKinnon, R. (1991) New insights into the structure and function of potassium channels. *Curr Opin Neurobiol*. 1**,** 14-9.

MacKinnon, R. (2004) Nobel Lecture. Potassium channels and the atomic basis of selective ion conduction. *Biosci Rep*. 24**,** 75-100.

MacKinnon, R. & Yellen, G. (1990) Mutations affecting TEA blockade and ion permeation in voltage-activated K^+ channels. *Science*. 250**,** 276-9.

Majumder, K., De Biasi, M., Wang, Z. & Wible, B. A. (1995) Molecular cloning and functional expression of a novel potassium channel beta-subunit from human atrium. *FEBS Lett*. 361**,** 13-6.

Maletic-Savatic, M., Lenn, N. J. & Trimmer, J. S. (1995) Differential spatiotemporal expression of K^+ channel polypeptides in rat hippocampal neurons developing in situ and in vitro. *J Neurosci*. 15**,** 3840-51.

Manganas, L. N., Akhtar, S., Antonucci, D. E., Campomanes, C. R., Dolly, J. O. & Trimmer, J. S. (2001a) Episodic ataxia type-1 mutations in the $K_v1.1$ potassium channel display distinct folding and intracellular trafficking properties. *J Biol Chem*. 276**,** 49427-34.

Manganas, L. N., Wang, Q., Scannevin, R. H., Antonucci, D. E., Rhodes, K. J. & Trimmer, J. S. (2001b) Identification of a trafficking determinant localized to the Kv1 potassium channel pore. *Proc Natl Acad Sci U S A*. 98**,** 14055-9.

McCormack, K., Tanouye, M. A., Iverson, L. E., Lin, J. W., Ramaswami, M., McCormack, T., Campanelli, J. T., Mathew, M. K. & Rudy, B. (1991) A role for hydrophobic residues in the voltage-dependent gating of Shaker K^+ channels. *Proc Natl Acad Sci U S A*. 88**,** 2931-5.

McCormack, K., Lin, L., Iverson, L. E., Tanouye, M. A. & Sigworth, F. J. (1992) Tandem linkage of Shaker K^+ channel subunits does not ensure the stoichiometry of expressed channels. *Biophys J*. 63**,** 1406-11.

McNamara, N. M., Muniz, Z. M., Wilkin, G. P. & Dolly, J. O. (1993) Prominent location of a K^+ channel containing the alpha subunit Kv 1.2 in the basket cell nerve terminals of rat cerebellum. *Neuroscience*. 57**,** 1039-45.

McNamara, N. M., Averill, S., Wilkin, G. P., Dolly, J. O. & Priestley, J. V. (1996) Ultrastructural localization of a voltage-gated K^+ channel alpha subunit ($K_v1.2$) in the rat cerebellum. *Eur J Neurosci*. 8**,** 688-99.

Mehraban, F., Breeze, A. L. & Dolly, J. O. (1984) Identification by cross-linking of a neuronal acceptor protein for dendrotoxin, a convulsant polypeptide. *FEBS Lett*. 174**,** 116-22.

Milkman, R. (1994) An *Escherichia coli* homologue of eukaryotic potassium channel proteins. *Proc Natl Acad Sci U S A*. 91**,** 3510-4.

Miller, C. (2000) An overview of the potassium channel family. *Genome Biol*. 1**,** REVIEWS0004.

Milo, R. & Kahana, E. (2010) Multiple sclerosis: geoepidemiology, genetics and the environment. *Autoimmun Rev*. 9**,** A387-94.

Morales, M. J., Castellino, R. C., Crews, A. L., Rasmusson, R. L. & Strauss, H. C. (1995) A novel beta subunit increases rate of inactivation of specific voltage-gated potassium channel alpha subunits. *J Biol Chem*. 270**,** 6272-7.

Morales, M. J., Wee, J. O., Wang, S., Strauss, H. C. & Rasmusson, R. L. (1996) The N-terminal domain of a K^+ channel beta subunit increases the rate of C-type inactivation from the cytoplasmic side of the channel. *Proc Natl Acad Sci U S A*. 93**,** 15119-23.

Mourre, C., Lazdunski, M. & Jarrard, L. E. (1997) Behaviors and neurodegeneration induced by two blockers of K^+ channels, the mast cell degranulating peptide and Dendrotoxin I. *Brain Res*. 762**,** 223-7.

Nagaya, N. & Papazian, D. M. (1997) Potassium channel alpha and beta subunits assemble in the endoplasmic reticulum. *J Biol Chem*. 272**,** 3022-7.

Nashmi, R., Jones, O. T. & Fehlings, M. G. (2000) Abnormal axonal physiology is associated with altered expression and distribution of $K_v1.1$ and $K_v1.2$ K^+ channels after chronic spinal cord injury. *Eur J Neurosci*. 12**,** 491-506.

Newsom-Davis, J. & Mills, K. R. (1993) Immunological associations of acquired neuromyotonia (Isaacs' syndrome). Report of five cases and literature review. *Brain*. 116 (Pt 2)**,** 453-69.

O'Grady, S. M. & Lee, S. Y. (2005) Molecular diversity and function of voltage-gated (Kv) potassium channels in epithelial cells. *Int J Biochem Cell Biol*. 37**,** 1578-94.

Ogawa, Y., Horresh, I., Trimmer, J. S., Bredt, D. S., Peles, E. & Rasband, M. N. (2008) Postsynaptic density-93 clusters K_v1 channels at axon initial segments independently of Caspr2. *J Neurosci*. 28**,** 5731-9.

Ogawa, Y., Oses-Prieto, J., Kim, M. Y., Horresh, I., Peles, E., Burlingame, A. L., Trimmer, J. S., Meijer, D. & Rasband, M. N. (2010) ADAM22, a Kv1 channel-interacting protein, recruits membrane-associated guanylate kinases to juxtaparanodes of myelinated axons. *J Neurosci*. 30**,** 1038-48.

Orlova, E. V., Papakosta, M., Booy, F. P., van Heel, M. & Dolly, J. O. (2003) Voltage-gated K^+ channel from mammalian brain: 3D structure at 18A of the complete (alpha)4(beta)4 complex. *J Mol Biol*. 326**,** 1005-12.

Papazian, D. M., Schwarz, T. L., Tempel, B. L., Jan, Y. N. & Jan, L. Y. (1987) Cloning of genomic and complementary DNA from Shaker, a putative potassium channel gene from Drosophila. *Science*. 237**,** 749-53.

Papazian, D. M., Schwarz, T. L., Tempel, B. L., Timpe, L. C. & Jan, L. Y. (1988) Ion channels in Drosophila. *Annu Rev Physiol*. 50**,** 379-94.

Parcej, D. N. & Dolly, J. O. (1989) Dendrotoxin acceptor from bovine synaptic plasma membranes. Binding properties, purification and subunit composition of a putative constituent of certain voltage-activated K^+ channels. *Biochem J*. 257**,** 899-903.

Parcej, D. N., Scott, V. E. & Dolly, J. O. (1992) Oligomeric properties of alpha-dendrotoxin-sensitive potassium ion channels purified from bovine brain. *Biochemistry*. 31**,** 11084-8.

Pascual, J. M., Shieh, C. C., Kirsch, G. E. & Brown, A. M. (1995) Multiple residues specify external tetraethylammonium blockade in voltage-gated potassium channels. *Biophys J*. 69**,** 428-34.

Pfaffinger, P. J. & DeRubeis, D. (1995) Shaker K^+ channel T1 domain self-tetramerizes to a stable structure. *J Biol Chem*. 270**,** 28595-600.

Poliak, S., Gollan, L., Martinez, R., Custer, A., Einheber, S., Salzer, J. L., Trimmer, J. S., Shrager, P. & Peles, E. (1999) Caspr2, a new member of the neurexin superfamily, is localized at the juxtaparanodes of myelinated axons and associates with K^+ channels. *Neuron*. 24**,** 1037-47.

Poliak, S., Gollan, L., Salomon, D., Berglund, E. O., Ohara, R., Ranscht, B. & Peles, E. (2001) Localization of Caspr2 in myelinated nerves depends on axon-glia interactions and the generation of barriers along the axon. *J Neurosci*. 21**,** 7568-75.

Poliak, S., Salomon, D., Elhanany, H., Sabanay, H., Kiernan, B., Pevny, L., Stewart, C. L., Xu, X., Chiu, S. Y., Shrager, P., Furley, A. J. & Peles, E. (2003) Juxtaparanodal

clustering of Shaker-like K^+ channels in myelinated axons depends on Caspr2 and TAG-1. *J Cell Biol*. 162**,** 1149-60.

Pongs, O. (1992) Molecular biology of voltage-dependent potassium channels. *Physiol Rev*. 72**,** S69-88.

Pongs, O., Kecskemethy, N., Muller, R., Krah-Jentgens, I., Baumann, A., Kiltz, H. H., Canal, I., Llamazares, S. & Ferrus, A. (1988) Shaker encodes a family of putative potassium channel proteins in the nervous system of Drosophila. *EMBO J*. 7**,** 1087-96.

Pongs, O. & Schwarz, J. R. (2010) Ancillary subunits associated with voltage-dependent K^+ channels. *Physiol Rev*. 90**,** 755-96.

Pugliatti, M., Rosati, G., Carton, H., Riise, T., Drulovic, J., Vecsei, L. & Milanov, I. (2006) The epidemiology of multiple sclerosis in Europe. *Eur J Neurol*. 13**,** 700-22.

Rasband, M. N., Trimmer, J. S., Schwarz, T. L., Levinson, S. R., Ellisman, M. H., Schachner, M. & Shrager, P. (1998) Potassium channel distribution, clustering, and function in remyelinating rat axons. *J Neurosci*. 18**,** 36-47.

Rasband, M. N., Park, E. W., Zhen, D., Arbuckle, M. I., Poliak, S., Peles, E., Grant, S. G. & Trimmer, J. S. (2002) Clustering of neuronal potassium channels is independent of their interaction with PSD-95. *J Cell Biol*. 159**,** 663-72.

Rehm, H. & Lazdunski, M. (1988) Existence of different populations of the dendrotoxin I binding protein associated with neuronal K^+ channels. *Biochem Biophys Res Commun*. 153**,** 231-40.

Reid, P. F., Pongs, O. & Dolly, J. O. (1992) Cloning of a bovine voltage-gated K^+ channel gene utilising partial amino acid sequence of a dendrotoxin-binding protein from brain cortex. *FEBS Lett*. 302**,** 31-4.

Rettig, J., Heinemann, S. H., Wunder, F., Lorra, C., Parcej, D. N., Dolly, J. O. & Pongs, O. (1994) Inactivation properties of voltage-gated K^+ channels altered by presence of beta-subunit. *Nature*. 369**,** 289-94.

Rhodes, K. J., Keilbaugh, S. A., Barrezueta, N. X., Lopez, K. L. & Trimmer, J. S. (1995) Association and colocalization of K^+ channel alpha- and beta-subunit polypeptides in rat brain. *J Neurosci*. 15**,** 5360-71.

Robbins, C. A. & Tempel, B. L. (2012) $K_v1.1$ and $K_v1.2$: similar channels, different seizure models. *Epilepsia*. 53 Suppl 1**,** 134-41.

Roeper, J., Sewing, S., Zhang, Y., Sommer, T., Wanner, S. G. & Pongs, O. (1998) NIP domain prevents N-type inactivation in voltage-gated potassium channels. *Nature*. 391**,** 390-3.

Ruppersberg, J. P., Stocker, M., Pongs, O., Heinemann, S. H., Frank, R. & Koenen, M. (1991) Regulation of fast inactivation of cloned mammalian IK(A) channels by cysteine oxidation. *Nature*. 352**,** 711-4.

Salkoff, L., Baker, K., Butler, A., Covarrubias, M., Pak, M. D. & Wei, A. (1992) An essential 'set' of K^+ channels conserved in flies, mice and humans. *Trends Neurosci*. 15**,** 161-6.

Sanchez-Ponce, D., DeFelipe, J., Garrido, J. J. & Munoz, A. (2012) Developmental expression of Kv potassium channels at the axon initial segment of cultured hippocampal neurons. *PLoS One*. 7**,** e48557.

Scott, V. E., Muniz, Z. M., Sewing, S., Lichtinghagen, R., Parcej, D. N., Pongs, O. & Dolly, J. O. (1994a) Antibodies specific for distinct Kv subunits unveil a heterooligomeric basis for subtypes of alpha-dendrotoxin-sensitive K^+ channels in bovine brain. *Biochemistry*. 33**,** 1617-23.

Scott, V. E., Rettig, J., Parcej, D. N., Keen, J. N., Findlay, J. B., Pongs, O. & Dolly, J. O. (1994b) Primary structure of a beta subunit of alpha-dendrotoxin-sensitive K^+ channels from bovine brain. *Proc Natl Acad Sci U S A*. 91**,** 1637-41.

Shamotienko, O. G., Parcej, D. N. & Dolly, J. O. (1997) Subunit combinations defined for K^+ channel Kv1 subtypes in synaptic membranes from bovine brain. *Biochemistry*. 36**,** 8195-201.

Shamotienko, O., Akhtar, S., Sidera, C., Meunier, F. A., Ink, B., Weir, M. & Dolly, J. O. (1999) Recreation of neuronal Kv1 channel oligomers by expression in mammalian cells using Semliki Forest virus. *Biochemistry*. 38**,** 16766-76.

Shen, K. Z., Lagrutta, A., Davies, N. W., Standen, N. B., Adelman, J. P. & North, R. A. (1994) Tetraethylammonium block of Slowpoke calcium-activated potassium channels expressed in Xenopus oocytes: evidence for tetrameric channel formation. *Pflugers Arch*. 426**,** 440-5.

Sheng, M., Liao, Y. J., Jan, Y. N. & Jan, L. Y. (1993) Presynaptic A-current based on heteromultimeric K^+ channels detected *in vivo*. *Nature*. 365**,** 72-5.

Sheng, M., Tsaur, M. L., Jan, Y. N. & Jan, L. Y. (1994) Contrasting subcellular localization of the Kv1.2 K^+ channel subunit in different neurons of rat brain. *J Neurosci*. 14**,** 2408-17.

Shi, G., Nakahira, K., Hammond, S., Rhodes, K. J., Schechter, L. E. & Trimmer, J. S. (1996) Beta subunits promote K^+ channel surface expression through effects early in biosynthesis. *Neuron*. 16**,** 843-52.

Shibuya, K., Misawa, S., Arai, K., Nakata, M., Kanai, K., Yoshiyama, Y., Ito, K., Isose, S., Noto, Y., Nasu, S., Sekiguchi, Y., Fujimaki, Y., Ohmori, S., Kitamura, H., Sato, Y. & Kuwabara, S. (2011) Markedly reduced axonal potassium channel expression in human sporadic amyotrophic lateral sclerosis: an immunohistochemical study. *Exp Neurol*. 232**,** 149-53.

Shieh, C. C., Coghlan, M., Sullivan, J. P. & Gopalakrishnan, M. (2000) Potassium channels: molecular defects, diseases, and therapeutic opportunities. *Pharmacol Rev*. 52**,** 557-94.

Smith, C. H. & Ellison, R. S. (1993) Do cats in New Zealand with renal failure require potassium supplementation? *N Z Vet J*. 41**,** 47-8.

Sokolov, M. V., Shamotienko, O., Dhochartaigh, S. N., Sack, J. T. & Dolly, J. O. (2007) Concatemers of brain K_v1 channel alpha subunits that give similar K^+ currents yield pharmacologically distinguishable heteromers. *Neuropharmacology*. 53**,** 272-82.

Solari, A., Uitdehaag, B., Giuliani, G., Pucci, E. & Taus, C. (2002) Aminopyridines for symptomatic treatment in multiple sclerosis. *Cochrane Database Syst Rev*. CD001330.

Stanfield, P. R. (1983) Tetraethylammonium ions and the potassium permeability of excitable cells. *Rev Physiol Biochem Pharmacol*. 97**,** 1-67.

Stansfeld, C. E., Marsh, S. J., Parcej, D. N., Dolly, J. O. & Brown, D. A. (1987) Mast cell degranulating peptide and dendrotoxin selectively inhibit a fast-activating potassium current and bind to common neuronal proteins. *Neuroscience*. 23**,** 893-902.

Stein, W. D. and Litman, T. (2015) Channels, Carriers, and Pumps, 2nd Edition: An Introduction to Membrane Transport. Academic Press, USA.

Stuhmer, W., Stocker, M., Sakmann, B., Seeburg, P., Baumann, A., Grupe, A. & Pongs, O. (1988) Potassium channels expressed from rat brain cDNA have delayed rectifier properties. *FEBS Lett*. 242**,** 199-206.

Stuhmer, W., Ruppersberg, J. P., Schroter, K. H., Sakmann, B., Stocker, M., Giese, K. P., Perschke, A., Baumann, A. & Pongs, O. (1989) Molecular basis of functional diversity of voltage-gated potassium channels in mammalian brain. *EMBO J.* 8**,** 3235-44.

Swanson, R., Marshall, J., Smith, J. S., Williams, J. B., Boyle, M. B., Folander, K., Luneau, C. J., Antanavage, J., Oliva, C., Buhrow, S. A. & et al. (1990) Cloning and expression of cDNA and genomic clones encoding three delayed rectifier potassium channels in rat brain. *Neuron*. 4**,** 929-39.

Swartz, K. J. & MacKinnon, R. (1995) An inhibitor of the $K_v2.1$ potassium channel isolated from the venom of a Chilean tarantula. *Neuron*. 15**,** 941-9.

Taglialatela, M., Vandongen, A. M., Drewe, J. A., Joho, R. H., Brown, A. M. & Kirsch, G. E. (1991) Patterns of internal and external tetraethylammonium block in four homologous K^+ channels. *Mol Pharmacol*. 40**,** 299-307.

Talley, E. M., Sirois, J. E., Lei, Q. & Bayliss, D. A. (2003) Two-pore-Domain (KCNK) potassium channels: dynamic roles in neuronal function. *Neuroscientist*. 9**,** 46-56.

Tempel, B. L., Papazian, D. M., Schwarz, T. L., Jan, Y. N. & Jan, L. Y. (1987) Sequence of a probable potassium channel component encoded at Shaker locus of *Drosophila*. *Science*. 237**,** 770-5.

Tempel, B. L., Jan, Y. N. & Jan, L. Y. (1988) Cloning of a probable potassium channel gene from mouse brain. *Nature*. 332**,** 837-9.

The Multiple Sclerosis Society of Ireland. http://www.ms-society.ie/pages/research/get-involved-in-research/national-incidence-study. Accessed 03 August 2015.

Thorneloe, K. S. & Nelson, M. T. (2005) Ion channels in smooth muscle: regulators of intracellular calcium and contractility. *Can J Physiol Pharmacol*. 83**,** 215-42.

Timpe, L. C., Schwarz, T. L., Tempel, B. L., Papazian, D. M., Jan, Y. N. & Jan, L. Y. (1988) Expression of functional potassium channels from Shaker cDNA in Xenopus oocytes. *Nature*. 331**,** 143-5.

Traka, M., Dupree, J. L., Popko, B. & Karagogeos, D. (2002) The neuronal adhesion protein TAG-1 is expressed by Schwann cells and oligodendrocytes and is localized to the juxtaparanodal region of myelinated fibers. *J Neurosci*. 22**,** 3016-24.

Traka, M., Goutebroze, L., Denisenko, N., Bessa, M., Nifli, A., Havaki, S., Iwakura, Y., Fukamauchi, F., Watanabe, K., Soliven, B., Girault, J. A. & Karagogeos, D. (2003)

Association of TAG-1 with Caspr2 is essential for the molecular organization of juxtaparanodal regions of myelinated fibers. *J Cell Biol*. 162**,** 1161-72.

Tseng-Crank, J. C., Tseng, G. N., Schwartz, A. & Tanouye, M. A. (1990) Molecular cloning and functional expression of a potassium channel cDNA isolated from a rat cardiac library. *FEBS Lett*. 268**,** 63-8.

Tseng-Crank, J., Yao, J. A., Berman, M. F. & Tseng, G. N. (1993) Functional role of the NH2-terminal cytoplasmic domain of a mammalian A-type K^+ channel. *J Gen Physiol*. 102**,** 1057-83.

Veh, R. W., Lichtinghagen, R., Sewing, S., Wunder, F., Grumbach, I. M. & Pongs, O. (1995) Immunohistochemical localization of five members of the K_v1 channel subunits: contrasting subcellular locations and neuron-specific co-localizations in rat brain. *Eur J Neurosci*. 7**,** 2189-205.

Visan, V., Fajloun, Z., Sabatier, J. M. & Grissmer, S. (2004) Mapping of maurotoxin binding sites on $hK_v1.2$, $hK_v1.3$, and hIKCa1 channels. *Mol Pharmacol*. 66**,** 1103-12.

Wacker, S. J., Jurkowski, W., Simmons, K. J., Fishwick, C. W., Johnson, A. P., Madge, D., Lindahl, E., Rolland, J. F. & de Groot, B. L. (2012) Identification of selective inhibitors of the potassium channel $K_v1.1$-1.2((3)) by high-throughput virtual screening and automated patch clamp. *ChemMedChem*. 7**,** 1775-83.

Wang, F. C., Parcej, D. N. & Dolly, J. O. (1999) alpha subunit compositions of Kv1.1-containing K^+ channel subtypes fractionated from rat brain using dendrotoxins. *Eur J Biochem*. 263**,** 230-7.

Wang, H., Kunkel, D. D., Martin, T. M., Schwartzkroin, P. A. & Tempel, B. L. (1993) Heteromultimeric K^+ channels in terminal and juxtaparanodal regions of neurons. *Nature*. 365**,** 75-9.

Wang, H., Kunkel, D. D., Schwartzkroin, P. A. & Tempel, B. L. (1994) Localization of $K_v1.1$ and $K_v1.2$, two K^+ channel proteins, to synaptic terminals, somata, and dendrites in the mouse brain. *J Neurosci*. 14**,** 4588-99.

Wang, H., Allen, M. L., Grigg, J. J., Noebels, J. L. & Tempel, B. L. (1995) Hypomyelination alters K^+ channel expression in mouse mutants shiverer and Trembler. *Neuron*. 15**,** 1337-47.

Wang, Z., Kiehn, J., Yang, Q., Brown, A. M. & Wible, B. A. (1996) Comparison of binding and block produced by alternatively spliced $K_v\beta1$ subunits. *J Biol Chem*. 271**,** 28311-7.

Watanabe, I., Zhu, J., Recio-Pinto, E. & Thornhill, W. B. (2015) The degree of N-glycosylation affects the trafficking and cell surface expression levels of $K_v1.4$ potassium channels. *J Membr Biol.* 248**,** 187-96.

Waxman, S. G. (1992) Demyelination in spinal cord injury and multiple sclerosis: what can we do to enhance functional recovery? *J Neurotrauma*. 9 Suppl 1**,** S105-17.

Wei, A., Covarrubias, M., Butler, A., Baker, K., Pak, M. & Salkoff, L. (1990) K^+ current diversity is produced by an extended gene family conserved in *Drosophila* and mouse. *Science*. 248**,** 599-603.

Wei, A., Jegla, T. & Salkoff, L. (1996) Eight potassium channel families revealed by the *C. elegans* genome project. *Neuropharmacology*. 35**,** 805-29.

Xu, J., Yu, W., Jan, Y. N., Jan, L. Y. & Li, M. (1995) Assembly of voltage-gated potassium channels. Conserved hydrophilic motifs determine subfamily-specific interactions between the alpha-subunits. *J Biol Chem*. 270**,** 24761-8.

Yellen, G., Jurman, M. E., Abramson, T. & MacKinnon, R. (1991) Mutations affecting internal TEA blockade identify the probable pore-forming region of a K^+ channel. *Science*. 251**,** 939-42.

Yellen, G., Sodickson, D., Chen, T. Y. & Jurman, M. E. (1994) An engineered cysteine in the external mouth of a K^+ channel allows inactivation to be modulated by metal binding. *Biophys J*. 66**,** 1068-75.

Zagotta, W. N., Hoshi, T. & Aldrich, R. W. (1990) Restoration of inactivation in mutants of Shaker potassium channels by a peptide derived from ShB. *Science*. 250**,** 568-71.

Zenker, J., Poirot, O., de Preux Charles, A. S., Arnaud, E., Medard, J. J., Lacroix, C., Kuntzer, T. & Chrast, R. (2012) Altered distribution of juxtaparanodal kv1.2 subunits mediates peripheral nerve hyperexcitability in type 2 diabetes mellitus. *J Neurosci*. 32**,** 7493-8.

Zhou, X., Nakamura, S., Xia, S. L. & Wingo, C. S. (2001) Increased CO_2 stimulates K/Rb reabsorption mediated by H-K-ATPase in CCD of potassium-restricted rabbit. *Am J Physiol Renal Physiol*. 281**,** F366-73.

Zuberi, S. M., Eunson, L. H., Spauschus, A., De Silva, R., Tolmie, J., Wood, N. W., McWilliam, R. C., Stephenson, J. B., Kullmann, D. M. & Hanna, M. G. (1999) A novel mutation in the human voltage-gated potassium channel gene (K_v1.1) associates with episodic ataxia type 1 and sometimes with partial epilepsy. *Brain*. 122 (Pt 5)**,** 817-25.